

The University of Texas at Tyler
College of Engineering and Computer Science
Tyler, TX 75799

Final Design Report
For
Wireless Charger Project

A design project to fulfill the requirements of Senior Design
in the Department of Electrical Engineering
at The University of Texas at Tyler

The individuals whose names and signatures appear below certify that the narrative, diagrams, figures, tables, calculations, and analyses contained within this document are their original work except as otherwise cited.

Flory, David



April 12, 2021

Date

França, Natasha



April 12, 2021

Date

Franulovic, Franci



April 12, 2021

Date

Gibbons, Chad



April 12, 2021

Date

Sosa, Francisco

 FS

April 12, 2021

Date

ACKNOWLEDGMENTS

We as a team wish to thank Indus Instruments and Dr. Sridhar Madala for being the benefactors and sponsors of our Project. Indus Instruments develops and creates electronic devices and software to meet the needs of various industries; for instance, they provide Baylor College of Medicine critical equipment for medical research. Dr. Sridhar Madala has been generous with our time and was critical in the initial planning phase of the project. Dr. Madala's familiarity with FCC and international wireless transmission regulations gave clear constraints and direction to this project. Thus, we especially thank Dr. Sridhar Madala for agreeing to be HEC-2's technical advisor.

EXECUTIVE SUMMARY

The team has designed and is prototyping a managed, 30 watt wireless resonant charger for use with lithium-ion battery packs. It shall be a versatile solution to the problem of powering autonomous mobile devices fitted with moderately sized battery packs of approximately four to six 18650 cells configured for 7.4 to 14.7 volts nominal output. With an estimated cost around \$300, it fills a gap between inexpensive inductive chargers in the 5 watt range and custom 90 watt robotic power systems that have an entry level price of \$2000.

Our charging system is made with two essential components: a transmitter and receiver. The transmitter is supplied by standard line voltage and will be responsible for safely delivering up to 30 watts of resonant power to the receiver when in range and appropriately positioned. It shall communicate status with the receiver over a Bluetooth link and shall enable or disable power transmission when requested.

The receiver shall communicate with the transmitter and to a user GUI over Bluetooth links, and optionally with the user's own application (i.e. a robot microcontroller) over a serial link. It will be capable of delivering requested power transmission and charging status information and beginning or ending the charging process. It shall cease charging on receipt of an error status from the charging circuit and will notify the user to take corrective action. Under normal conditions it will deliver power to the charging control IC, which shall charge the attached battery pack.

The charger may be configured to charge 7.4 to 14.7 nominal Li-Ion battery cells, which must have internal protection circuitry in accordance with UL1642 and IEC61960. Optimal configurations would include a 7.4V pack rated for 3.2A charging, a 11.1V pack rated for 2.2A charging, or a 14.8V pack rated for 1.7A charging.

To best demonstrate the full potential of our project, the team is pursuing optional deliverables that should be completed if time permits once the core project is completed. These stretch goals include a mobile robot capable of charging itself for continuous wireless operation and integration with a smart Li-ion battery for detailed fuel gauge and battery health status.

Contents

I Project Description	1
I.A Software Team's Focus for Project	2
I.B Hardware Team's Focus for Project	3
II Final Design Specifications	4
II.A Feasibility Study	6
II.B Microcontroller	7
II.C Transmitter Coil	7
II.D Transmitter	7
II.E Receiver	8
II.F Thermal Considerations for 3.3V and 5V Voltage Regulators	9
II.G Charging Subsystem	11
II.H Battery Considerations	11
II.I Microcontroller Considerations	13
II.J Firmware Requirements: Transmitter	14
II.K Firmware Requirements: Receiver	14
II.L Software Requirements: GUI	15
II.M Coil Considerations	16
II.N Specification Summary	17
II.O Ethical and Professional Considerations	18
II.1 Public Health	18
II.2 Safety and Welfare	18
II.3 Global Factors	19
II.4 Societal factors	19
II.5 Environmental factors	19
II.6 Economic factors	19
III Design Solution	20
III.A Product Architecture	20
III.B Hardware Subsystems	23
III.1 Transmitter Subsystem	23
III.2 Receiver Subsystem	27
III.3 Planar Coil Inductor	30
III.C Software Architecture	31
III.1 Firmware Architecture	31
III.2 GUI Software Architecture	32
III.D Software Modules	33
III.1 Firmware Modules	33
III.2 GUI Software Modules	34
III.E Hardware Off The Shelf Items	36
III.F Software Off The Shelf Items	37
III.G Schematics / Wiring Diagrams / Technical Drawings	38
III.H Custom Software	38

III.1	Firmware Main Program	38
III.2	GUI Software Main Program	39
IV	Prototype Design and Fabrication	40
IV.A	Transmitter Subsystem Prototype Production	40
IV.1	PCB Manufacturing	40
IV.2	Transmitter Prototype Board Assembly	41
IV.3	Post Assembly Inspection	43
IV.B	Receiver Subsystem Prototype Production	43
IV.1	PCB Manufacturing	43
IV.2	Receiver Prototype Board Assembly	44
IV.3	Post Assembly Inspection	46
IV.C	Coil Production	47
IV.D	Expenditure Report	47
IV.E	Budget	51
IV.F	Current Manufacturing Abilities	52
V	Testing and Validation	53
V.A	Transmitter Power Supply Tests	53
V.B	Transmitter Coil Driver Tests	54
V.C	Transmitter Firmware Tests	57
V.D	Transmitter Firmware Tests	58
V.E	Receiver Power Supply Tests	59
V.F	Receiver Wireless Power Rectifier Tests	60
V.G	Receiver Battery Charger Tests	60
V.H	Receiver Firmware Tests	61
V.I	GUI Software Tests	63
V.J	Coil Test	64
V.K	System Level Firmware Tests	65
V.L	Test Results Summary	66
V.1	Transmitter Evaluations	66
V.2	Receiver Evaluations	68
V.M	Experimental Data Collection Sheets with Results	71
V.1	Transmitter Subsystem Data	71
V.2	Receiver Regulators Subsystem Data	72
V.3	Receiver Rectifier Subsystem Data	72
V.4	Charger Subsystem Data	73
V.5	SMBus Subsystem Test Data	73
V.6	Coil Subsystem Test Data	74
VI	Broader Impacts of the Project	74
VII	Conclusion	76
VIII	References	80

Appendices	80
A Codes, Standards, and Constraints	81
B User's Manual and Instructions	82
C Coursework Related Knowledge and Skills	83
D Receiver PCB Schematics	84
D.1 Receiver Controller	85
D.2 Receiver Battery Charger	86
D.3 RF/DC Converter	87
D.4 DC/DC Converter	88
D.5 Top Copper Layer	89
D.6 Top Silk Layer	90
E Transmitter PCB Schematics	91
E.1 Transmitter Controller	92
E.2 DC/DC Converter	93
E.3 Coil Driver	94
E.4 Top Copper Layer	95
E.5 Top Silk Layer	96
F Receiver BOM	97
G Transmitter BOM	101
H Wireless Power Transfer Module BOM	105
I Dimensional Coil Drawing	106
J GUI Wireframe Diagram	107
K Experimental Data Collection Sheets	108
K.1 Transmitter Subsystem Data	108
K.2 Receiver Regulators Subsystem Data	108
K.3 Receiver Rectifier Subsystem Data	109
K.4 Charger Subsystem Data	109
K.5 SMBus Subsystem Test Data	110
K.6 Coil Subsystem Test Data	110

List of Figures

1	Operation Story Block Diagram	2
2	Power Supply of Transmitter and Receiver Subsystems	3
3	Transmitter and Receiver Block Diagrams	3
4	Thermal Resistance vs. PCB Area [5]	10
5	System Level Block Diagram	21
6	GUI Wireframe Diagram	22
7	Transmitter Subsystem Voltage Regulator	23
8	Transmitter Subsystem Block Diagram	24
9	Coil Driver Subcircuit	25
10	SMPS Subcircuit	26
11	Transmitter Subcircuit	26
12	Receiver Subsystem Block Diagram	27
13	Receiver Coil Subsystem Block Diagram	28
14	Receiver Voltage Regulator	28
15	Rectifier and Power Sensor Subcircuit	29
16	Planar Coil CAD Drawing	30
17	Controller Flow Chart	31
18	High Level GUI Software Architecture Example	32
19	Transmitter Top Silk Layer	42
20	Transmitter Top Copper Layer	42
21	Receiver Top Silk Layer	45
22	Receiver Top Copper Layer	46
23	Transmitter Voltage Regulator Circuits	54
24	Oscillator and Buffer Subcircuit	55
25	Transmission Signal Class E Amplifier Subcircuit	56
26	Received Power vs. Distance Test Setup	57
27	Reference Layout for Part and Pin Numbers	57
28	Receiver Coil Terminal Subcircuit	59
29	Receiver RF-DC Converter Efficiency Test Setup	60
30	Current GUI Visual Components Exposed	63
31	VNA Test Setup	64
32	Class E Amplifier Driver Output	66
33	Q1 Drain Voltage Waveform	67
34	Q1 Drain Voltage Waveform	67
35	VNA TX/RX Coil Impedance Measurement	70
36	Isometric Image of Receiver PCB	84
37	Isometric Image of Transmitter PCB	91
38	Dimensional Coil Drawing	106
39	GUI Wireframe Diagram	107

List of Tables

1	Receiver Specifications	4
2	Transmitter Specifications	5
3	Communication Link Specifications	5
4	GUI Specifications	5
5	Final Design's Charging Subsystem Specifications	13
6	Final Design's Coil Tubing Specifications	16
7	Final Design's Receiver Coil Specifications	16
8	Final Design's Receiver Specifications	17
9	Final Design's Transmitter Specifications	18
10	Final Design's Communication Link Specifications	18
11	Final Design's GUI Specifications	18
12	Ethical and Professional Considerations	20
13	Off The Shelf Items Utilized in Prototype	36
14	Off The Shelf Software Items	37
15	Summary of Expenditures	48
16	Man-Hours Expenditure Report in Development and Prototyping	49
17	Development and Prototyping Summary of Man-Hours	50
18	Development and Prototyping Budget	51
19	Prototype Production Timetable	52
20	Transmitted Power vs. Distance Test	68
21	Received Power (DC) vs Distance Test	68
22	Power Transfer vs Load Test	69
23	Overall Efficiency Test	69
24	Relevant Codes and Standards	81
25	Coursework Related Knowledge and Skills Table	83

I. PROJECT DESCRIPTION

Our team noted a need for users to charge medium power devices via wireless charging. After further investigation we also determined that there is a shortage of cost effective medium power wireless chargers on the market.

Our project is a 30 watts nominal resonant wireless charger prototype for use with 4 to 6 cell lithium ion battery packs. It is managed by a microcontroller. It may be monitored and controlled by a user GUI or directly by the target application. Unlike existing customized and proprietary robotic charging systems, our product will charge a standard battery type and be suitable for both stand-alone operations and integration into the user's own design.

The team has been unable to discover any equivalent products to our own for retail. The most comparable product is Wibotic's Standard High Power System[1], a 90 watt magnetic resonance device that is marketed to businesses designing commercial drones and robotic systems. On the lower end, nearly all unbranded, low-cost wireless chargers that are available from mass online retailers supply no more than 5W via inductive charging. For a single industrial unit, we have received a price quote for approximately \$2000 USD. Individuals and small R&D teams that search for suitable devices through online retailers will find that these low-end transmitters are not modular and are limited to one specific purpose such as charging cell phones or key-fobs.

Our charging system employs magnetic resonance coupling to charge a lithium ion battery pack, delivering between 15 and 30 watts of power. The power transmitter and receiver communicates as a unified system that can provide battery management, protect against overcharging, and provide both diagnostic and telemetric information to the user and to an optional serial connection with the powered application's control circuitry. The charging system may be monitored and controlled by the user either through an attached LCD interface or a GUI from either a Bluetooth connected PC or smartphone.

This wireless charging alternative's intended market consists of hobbyists and prototype designers considering a self-docking direct electrical connection solution. This is the charging method used by the Roomba[2], which engages with a custom dock and charges using metal contacts. While this is a cost-effective solution for a mass-produced product, wireless charging is a superior choice for autonomous mobile devices that might have a wide variety of sizes and shapes. The benefits offered by our product's wireless charging include flexible placement of the charger, a compact charging area, greater tolerance for misalignment between the charger and the target device, and the absence of exposed electrical connections. Additionally, this product would solve the same need for OEM producers who are interested in a "turn-key" wireless charging solution.

To best demonstrate the full potential of our project, the team has specified optional deliverables that include a mobile robot capable of charging itself for continuous wireless operation, fully integrated with a smart Li-ion battery for detailed fuel gauge and battery health status.

The team holds that a moderate power, low cost wireless charger with accessible telemetry is useful to a small but important market of robotics hobbyists and developers, who at present, are not being served by either costly, proprietary business-to-business solutions or the low power and poorly documented inductive chargers available on the hobby market.

Below in Figure 1, the general flow of power from the AC to DC Wall Converter to the end user's device and information from the user is shown.

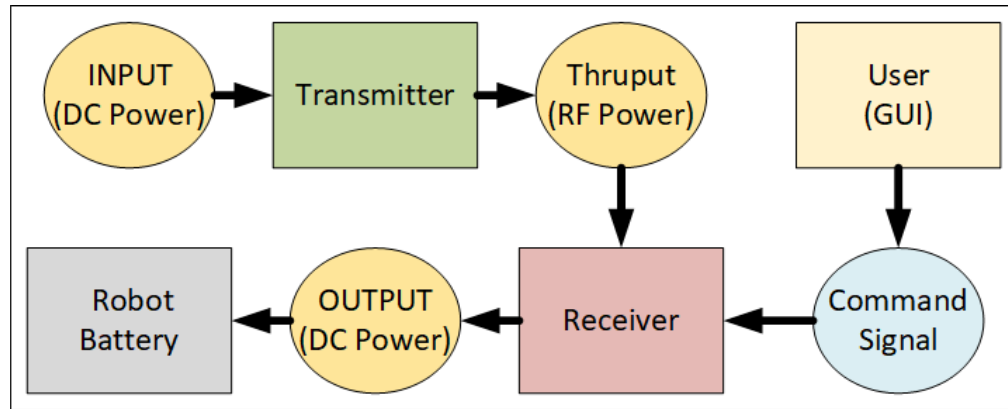


Figure 1: Operation Story Block Diagram

The project is divided between two teams: the hardware team and the software team.

A. Software Team's Focus for Project

The software team is focused on two programs: the microcontrollers' firmware and the graphical user interface (GUI) software application. The firmware operates the transmitter or receiver while the GUI allows for the user to readily monitor and interact throughout the charging process.

B. Hardware Team's Focus for Project

The hardware team is focused on producing three modular components: the receiver PCB, the transmitter PCB, and the coil module. The image below displays how these modules operate together.

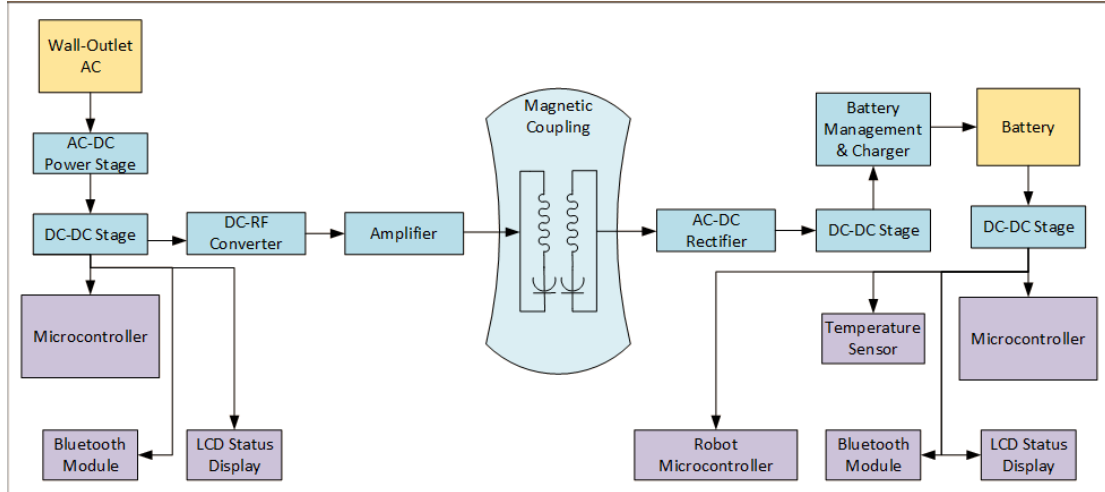


Figure 2: Power Supply of Transmitter and Receiver Subsystems

While the image below explicitly separates out the receiver and transmitter modules. Note that the completed PCB boards have a power transferring coil module affixed to them individually.

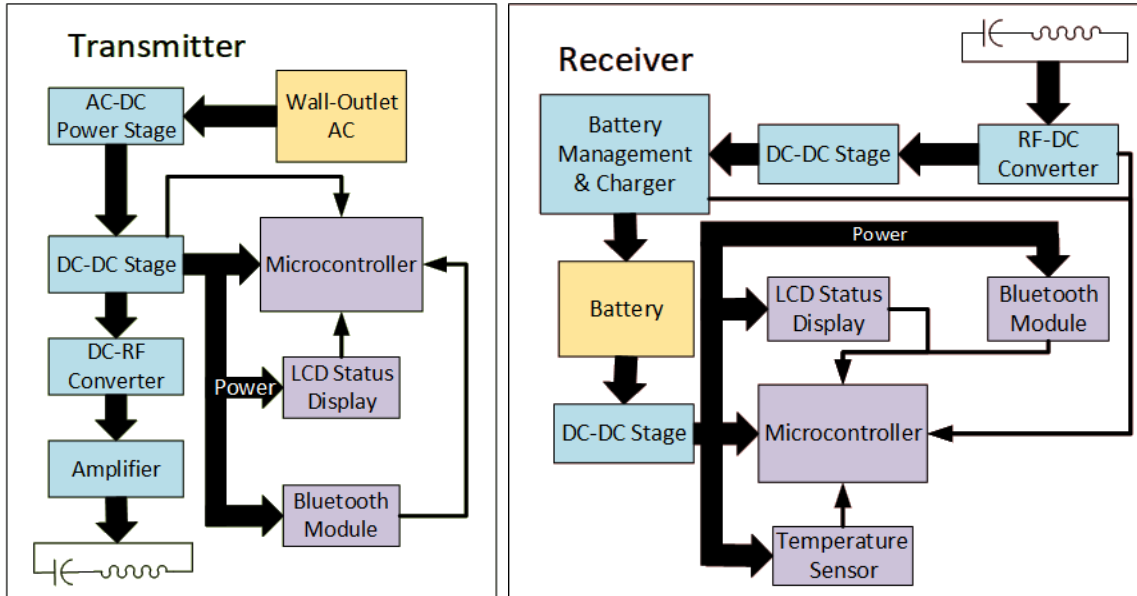


Figure 3: Transmitter and Receiver Block Diagrams

II. FINAL DESIGN SPECIFICATIONS

Table 1 below shows the specs of the receiver subsystem.

Table 1: Receiver Specifications

Charge time (Per 4Ah Battery Packs)	5 Hours Max
Battery pack voltage	14.2 V
Coupling Efficiency Transmitter to Receiver	90%
AC-DC Conversion Efficiency	80%
Charging Controller DC-DC converter	85%
Overall Receiver Conversion Efficiency	61.2%
Maximum Battery Charging Current	1.25 A (14.7 V battery pack)
Charger Subsystem Charge Protocol	Constant Current Constant Voltage (Li-ION Battery)
Battery Type	Lithium-Ion (4 x18650 in Series or 2P4S Configuration)
Power Negotiation	Bluetooth 5 LE
Transmitter Locator Method	RF Localization [Bluetooth]
Deliverable Demo	Self-Moving Device (Robot)
Telemetry	Report State to GUI Device
LCD display	Diagnostic Character String Display

Table 2 below shows the specs of the transmitter subsystem.

Table 2: Transmitter Specifications

Operating frequency	13.56 MHz
RF power output	30 W
Max operating range	5 cm
DC Power supply	48 V 1.25 A max.
Conversion Efficiency DC-AC	80%
Telemetry	Report State to GUI Device

Table 3 below shows the communication specifications.

Table 3: Communication Link Specifications

Communication Medium	Bluetooth 5 LE
Protocol	L2CAP (RFCOMM)

Table 4 below shows the GUI software specifications.

Table 4: GUI Specifications

GUI OS	WinOS, IOS, Linux, & Android
License	LGPL 3.0
Software Architecture	Model-Controller- View (MCV) Architecture
Delivery Model	Open Source (Free App Download)

A. Feasibility Study

The design consists of two subsystems: the transmitter and the receiver. This product is expected to be used by hobbyists and prototype designers for different applications that require contactless charging. There is no similar device available in the price range from \$200 to \$400. The expected cost of the charger system is \$300. There are some commercial chargers available right now and the cost of that system is \$2000. The price of \$300 per system will make wireless charging affordable for hobbyists and freelance hardware developers.

The design tools such as Altium designer and Multisim simulator are available free of charge to all group members using the provided UT Tyler license. Also, parts manufacturers are providing free simulation and evaluation tools for development. In addition to the software evaluation kits may be required for testing certain parts of the system such as the microcontroller, Bluetooth module, and the battery charger controller. Most of those evaluation modules are already purchased and they are available to team members. Evaluation kits are purchased by Indus Instruments.

The system is designed such that it uses standard components that are available at any electronic components store and they can be purchased without restrictions. PCB fabrication will be given to a company located in China that is offering quick turnaround PCB fabrication and fast shipping. Components purchasing and printed circuit board assembly will be done at Indus Instruments. Indus Instruments have all the necessary equipment that can handle surface mount components.

All test equipment required for development and testing will be available. Indus Instruments will provide space and necessary test equipment for the wireless charging system prototype evaluation and testing.

The final product cost is estimated at around \$300 (for small quantities). Most likely for larger quantities, it is possible to decrease the cost even more.

B. Microcontroller

There are four aspects to analyze: economics, technical, legal, and scheduling. A single MSP430FR5994 part costs about \$3 to \$4, while the MSP-EXP430FR5994 LaunchPad kit costs \$16.99. Considering the team only needs two of these microcontrollers (one for the transmitter and one for the receiver), this is an economic and reasonable cost. [3] [4]. On the technical side, this microcontroller's memory, voltage supply limitations, UART and I²C mode specifications, and overall low power consumption makes it the ideal model for our project needs [3]. Some of the most important standards TI's MSP430FR5994 complies with include ANSI, JEDEC, and ESDA [3]. Lastly, the team already has in hands the LaunchPad kit for the microcontroller. The individual microcontrollers are also ready-to-purchase items with delivery times of less than 7 days. More testing will be done once the team has the first PCB design in hands.

C. Transmitter Coil

The circular planar coil was the most inexpensive approach, the copper tubing to make the coils has an approximate value of \$15.99. The design properties also significantly contributed to reducing the complexity of acquiring the main coil parameters. It was important to take this factor into account because of the time constraint of two months. In order to reduce the complexity in our project, the spiral planar design was the best option.

The calculation of the inductance formula in the planar spiral design was easier to acquire than the other two proposed solutions. This was crucial because it significantly gave the project a higher chance of matching the predestined inductance of the circuit requirement of .909 μ H.

The economical and ethical considerations did not affect our decision making as much, due to the fact that there were not many differences. Furthermore, this design was appropriate for our project and the team does have the budget, resources and time to successfully implement this design.

The planar spiral coil design allows the project to more reduces the complexity of the formulas implemented in the calculations.

D. Transmitter

The transmitter class-E amplifier circuit was simulated at an efficiency of 98%. The actual transmitter efficiency would be around 90%. In the simulation, it was determined that the current required to power the class-E amplifier is 0.9 A at 30 V. The power for the transmitter will be supplied by using an external 48 V AC to DC converter followed by a step-down converter in the transmitter subsystem.

The main concern in this subsystem is the immunity of the supporting circuits to the RF electromagnetic field generated by the transmitter coil. The transmitter coil placement must be done such that the electromagnetic field has minimal effects on the electronic circuits in the transmitter. The transmitter sensitive electronic parts may require EMI shields.

During the simulation, the high voltage across the coil was observed. The highest voltage observed was 320 V_{pp} . That voltage poses a serious electric shock hazard. Therefore, the transmitter coil insulation must be capable of withstanding voltages that are in the 500V to 1kV range to provide a safety margin for the design. One way of achieving this is to make a plastic box that would contain the transmitter coil and have insulation that is capable of withstanding voltages in the 500 V to 1000 V range.

Heat dissipation in the Class E amplifier circuit is expected to be around 3W (based on the efficiency of 90%). That dissipation will occur in inductors, capacitors (due to ESR), and the amplifier transistor. The transistor will have a proper heatsink to prevent overheating. Since the dissipation in the transistor is very small (on-resistance is $50 \text{ m}\Omega$) the proper thermal management will be achieved on the printed circuit board. Coils used in the transmitter will be designed such that the coil resistance is minimized which also will decrease the heat dissipation in the transmitter circuit.

E. Receiver

There is a possibility that the receiver RF to DC stage performs with higher losses than the losses that were determined in the simulation. According to the simulation data, the RF to DC conversion will be 81% efficient. In the system specification, the conversion efficiency is set to 80%. It is important to keep efficiency above 80% to prevent excessive heat generation. If received power is 25W and efficiency is 80% then power dissipation is 5 W.

The excessive heat may have adverse effects on battery life and the speed of charging [5]. A higher temperature environment requires lower charging currents to prevent further temperature rise and damage to the battery cells. Also, excessive heat generation must be minimized to avoid the use of fans and large heat-sinks. Heat-sinks and fans would increase the cost and the size of our product. If during the prototype test phase efficiency drops below 80% the circuit must be redesigned to achieve the target specification efficiency.

One problem that is likely to occur is the interference in the battery charging and communication link circuits caused by a strong electromagnetic field generated by the transmitter coil. Even though all good practices will be followed for the circuit board design the electromagnetic interference still may not be prevented. Charging circuit disruption can cause battery failure due to overcharging or overheating. If this problem occurs the additional EMI shielding will be required. The shielding includes placing metal boxes over sensitive electronic subcircuits and placing additional filters in series with DC power supplies for sensitive parts such as a microcontroller, Bluetooth module, and charger controller.

F. Thermal Considerations for 3.3V and 5V Voltage Regulators

According to the simulation data both parts have small power dissipation. The largest power dissipation is 0.18 W (5.0V regulator).

The graph below provides thermal resistance junction to ambient as a function of the printed circuit board. The equation below can be used to find the required thermal resistance junction to ambient (Θ_{JA}). The estimated ambient temperature in the transmitter is 45°C.

$$\Theta_{JA} = \frac{125^{\circ}C - T_{A(max)}}{P_{D(max)}} \left[\frac{{}^{\circ}C}{W} \right] \quad (1)$$

$$\Theta_{JA} = \frac{125-45}{0.18} = 444.44 \left[\frac{{}^{\circ}C}{W} \right]$$

The estimated transmitter PCB area will be around 100cm². Given the board size and thermal resistance vs. board size, those regulators will have a proper heatsink.

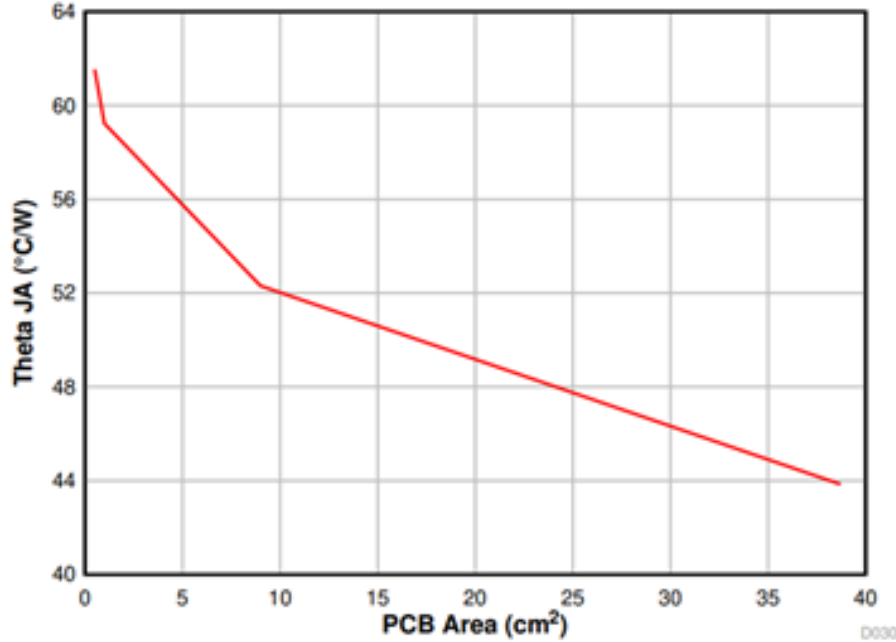


Figure 35. θ_{JA} versus PCB Area

Figure 4: Thermal Resistance vs. PCB Area [5]

Thermal considerations (for class E amplifier voltage regulator (30V, 1.0A buck converter)

$$T_{A(max)} = T_{J(max)} - R_{TH} \cdot P_{TOT} \quad (2)$$

- P_{TOT} is the total device power dissipation in [W]
- T_A is the ambient temperature in [°C]
- T_J is the junction temperature in [°C]
- R_{TH} is the thermal resistance of the package $\left[\frac{^{\circ}C}{W} \right]$
- $T_{A(max)}$ is the maximum ambient temperature in [°C]
- $T_{J(max)}$ is the maximum junction temperature in [°C]

The expected ambient temperature is 40°C (that is temperature inside the transmitter enclosure).

Thermal resistance for a standard board (Θ_{JA}) is $62.5 \left[\frac{^{\circ}C}{W} \right]$ [6].

From the simulation the total power dissipation is 1 W.

From the recommended operating conditions the maximum junction temperature is 150°C [6].

Based on the data from the simulation and the datasheet the maximum ambient temperature can be determined

$$\begin{aligned} T_{A(MAX)} &= T_{J(MAX)} - R_{TH} * P_{TOT} \\ T_{A(MAX)} &= 150 - 62.5 * 1 = 87.5^{\circ}C \end{aligned}$$

The expected ambient temperature is lower than the maximum temperature calculated based on simulation data. Therefore, this part will operate within specified recommended conditions in the datasheet.

G. Charging Subsystem

The LTC4162-L is designed to manage a power path between an external input power source V_{in} , an output power V_{out} , and an installed battery pack. When external input power greater than the battery voltage is available at V_{in} , the LTC4162 will route V_{in} to V_{out} and charge the connected battery. If external power is interrupted or falls below V_{bat} , battery power will be automatically routed to V_{out} . As long as the battery has charge or a power source exists at V_{in} , V_{out} will be supplied with power, but the voltage will range from V_{bat} to V_{in} . In order to provide consistent voltage to the target device output power should be drawn directly from the battery. Leaving V_{out} unused allows the maximum power point tracking feature to operate with optimal efficiency.

The LTC4162 draws power directly from V_{out} and has its own internal LDO linear regulators. All other components of the wireless receiver PCB must be powered by an appropriate DC-DC stage at V_{out} that can convert any potential input voltage (i.e. 7.4-35 V) to the required operating voltages of 5 V and 3.3 V. In the event that the battery is severely depleted and cannot power the microprocessor and Bluetooth interface, it will be necessary for the transmitter to be capable of initiating charging independently.

Since the LTC4162 has only an internal buck voltage regulator, the wireless power receiver subsystem must provide power to V_{in} that is higher than the voltage of the battery but below the maximum input voltage of 35V.

The LTC4162 approaches 95% efficiency at recommended switching frequency when the input voltage is no more than approximately 5V above battery charging voltage, and surpasses 90% in less ideal configurations. Heat losses will be in the range of three watts or less. It has a Θ_{JC} of $3.4 \left[\frac{^{\circ}C}{W} \right]$ and will be soldered to a four-layer PCB. The team does not anticipate any thermal management issues with this circuit.

H. Battery Considerations

Li-Ion batteries offer superb performance and high energy density, but require special attention to safety. Under normal circumstances the LTC4162-L will monitor battery voltage and avoid overcharging. A NTC thermistor will allow the LTC4162 to monitor local charging temperatures and limit current in accordance with JEIDA recommendations.

For safety reasons, the team requires stricter battery specifications than originally planned. While our charger's thermistor can limit charging current in response to ambient temperature extremes, it cannot monitor individual cells—particularly if the battery pack is intended to be modular. While it can recognize and respond to abnormal battery voltages or short conditions, it cannot automatically determine maximum safe charging current. Any battery pack used must have a maximum charge current greater than the maximum current delivery of the charger. Battery packs must also meet UL1642 and IEC61960 standards and contain internal protection circuitry to limit charge and discharge currents and protect against thermal runaway.

The LTC4162 can deliver a maximum of 3.2 amps and has an efficiency of up to 95%. Assuming optimal efficiency and 26 W output from the wireless receiver, the charging voltage must be at least $\frac{25W}{3.2A} = 7.8$ V in order to fully utilize the available power. Since the voltage of a typical Li-Ion cell is 3.7 V and the charging voltage is 4.2 V, the target battery pack should consist of two or more cells in series. The LTC4162 supports 1 to 8 cell series arrangements provided the input voltage is adequate. Optimal arrangements would include a 7.4V pack rated for 3.2 A charging, a 11.1 V pack rated for 2.2 A charging, or a 14.8 V pack rated for 1.7 A charging. The number of cells is set by selection pins and may be configured by a DIP switch or jumpers. It is not necessary to specify a specific number of cells for suitable battery packs, provided that they meet UL1642 and IEC61960 standards. The optimal balance of safe charging rates and performance will likely be found with packs utilizing six to eight 18650 cells or the equivalent. The power delivery estimates above are optimistic and actual power delivery from the charger may not reach these levels. As prototyping progresses, it will be possible to refine battery recommendations and expected charging times.

Ideally, up to 25 W will be delivered to the battery pack, making the battery the largest potential source of heat in our system. Since the battery pack is intended to be a modular, removable component with flexible specifications, it will not necessary for it to be enclosed with the wireless receiver PCB and receiving coil. It will be connected by an appropriate low-loss cable and connector, and exact placement will be determined by the user application. For this reason, the team has specified that only battery packs with internal temperature monitoring and protection circuitry should be used with this charger.

Our original specifications suggested that the charging subsystem would be capable of detailed monitoring of battery health and charge state. The team has learned that this type of information must be obtained at the individual cell level by a specialized controller which is usually integrated into the battery pack itself. Our charge subsystem can only recognize an approaching low-battery condition by a drop in voltage, and cannot estimate battery capacity except by calculation using charging voltage, charge times and currents, and such data would be of limited use considering battery aging and user-replaceability. It will be possible to notify the user and target device of a drop in battery voltage, but more detailed fuel gauge and battery health information will require an SMBus enabled smart battery. An I²C line on the MSP430FR5994 will be reserved for

communication with an optional SMBus capable smart battery pack. If feasible, optional battery pack telemetry may be polled by firmware and reported to the user along with the data already available from the LTC4162.

All the parts and design resources needed to complete the charging and power subsystem are readily available. Constructing this subsystem within the projected time-frame is feasible.

Table 5: Final Design's Charging Subsystem Specifications

DC-DC stage from wireless receiver to V_{in}	May not be necessary, pending further determination of wireless receiver output voltage
DC-DC stage from V_{out}	5V at 100mA; 3.3V at 100 mA
Battery Requirements	UL1642 and IEC61960 compliant Li-Ion packs with 7.4-15 V_{DC} nominal output voltage
Maximum Charging Current	3.2A (7.4V); 2.2A (11.1V); 1.7A (14.8V)
Provision for optional smart battery health and fuel gauge monitoring	Reserved I ² C line from MSP430FR5994 with buffering

I. Microcontroller Considerations

The MSP430FR5994 has a body size that ranges from 6mm by 6mm to 12mm by 12mm depending on the package the group purchases, 8KB RAM, 68 GPIO pins, 4 I²C, 4 UART, up to four serial communication ports, and 20 ADC channels. The MSP430 series include limitations that range from safety to performance [3].

Relevant limitations to the project include:

1. ESD (Electrostatic discharge) ratings. For a human-body model, safe discharge ratings are around 500 V to 1000 V, while for a charged-device model, safe discharge ratings are around 250 V. These regulations are taken from JEDEC JS-001 and JESD22-C101 respectively [3].
2. Absolute maximum ratings: voltage applied to any pin must be within -0.3 V to 4.1 V, voltage difference between DVCC and AVCC pins must stay within -0.3 V to 0.3 V (if not, writing errors could occur to RAM and FRAM), and current at any device pin must have a maximum of -2 to 2 mA [3].
3. Supply voltage applied should be within 1.8 V to 3.6 V, maximum ACLK frequency should be 50 kHz, and maximum SMCLK frequency should be 16 MHz [3].

4. For the eUSCI I²C, eUSCI (enhanced universal serial communication interface) input clock frequency should not exceed 16 MHz, SCL clock frequency should not exceed 400 kHz [3].

J. Firmware Requirements: Transmitter

The Wireless Power Transmission Stage (Transmitter) will be controlled by an MSP430FR5994 running custom firmware. The firmware must meet the following requirements:

- 1.) Activate or deactivate wireless transmitter.
- 2.) Respond to commands received from a Bluetooth link with the Wireless Power Receiver Stage (Receiver), which may include requests for power delivery measurements or instructions to initiate or cease charging.
- 3.) Continuously monitor wireless power transmitter current and voltage and calculate delivered power.
- 4.) Automatically cease power transmission when the Receiver requests a shutdown or if severe interference is detected.
- 5.) Communicate operating status to the Receiver via Bluetooth, and directly to the user via fault LED's or an installed LCD.

K. Firmware Requirements: Receiver

The Wireless Power Receiver Stage (Receiver) will be controlled by an MSP430FR5994 running custom firmware. The firmware must meet the following requirements:

- 1.) Link to the Transmitter over Bluetooth.
- 2.) Link to user GUI device over Bluetooth.
- 3.) Link to an optional UART connection with the target device.
- 4.) Respond to queries or instructions from the Bluetooth connection to the user GUI or from the optional UART connection.
- 5.) Monitor charging state and battery status though I²C connection with LTC4162 and optional SMBus link with smart battery.
- 6.) Recognize low voltage state or optional low capacity battery warning and notify the user and target device.

- 7.) Signal the Transmitter via Bluetooth to initiate charging when instructed by the user or target device.
- 8.) Continuously monitor wireless power receiver current and voltage and calculate delivered power.
- 9.) Monitor reported power transmission from the Transmitter, compare it with received power, and recognize excessive power losses that could indicate unsafe interference conditions
- 10.) In the event of excessive transmission losses, instruct the Transmitter to cease power transmission. Notify the user and target device of the error condition.

The Transmitter and Receiver firmware will be developed with Texas Instruments Code Composer Studio. The team has suitable Launchpad development boards and access to all necessary documentation and libraries are available. The team is composed of multiple experienced programmers in our group. The firmware requirements are limited and well-defined and completing it within our scheduled time-frame is feasible.

L. Software Requirements: GUI

The GUI will be operated on multiple platforms and rely upon QT5 to operate. The software must fulfill the following requirements:

- 1.) Provide connection to transmitter and receiver for the product's user that grants sufficient control over the product's hardware
- 2.) Serve as a platform for custom messages to and from the user's device connected to the receiver.
- 3.) Provide alert system via push notifications and continuous monitoring of the transmitter and receiver.

M. Coil Considerations

Table 6: Final Design's Coil Tubing Specifications

Material	122 Copper
Tube Size	1/8 [in]
Outer Diameter (OD)	1/4 [in]
Wall Thickness	0.049 [in]
Inner Diameter (ID)	0.152 [in]
Fabrication	Seamless
Bending Method	By hand
Temper Rating	Soft
Compatible Tube Fittings	Compression, Solder Connect
Specifications met	ASTM B75 RoHS 3(2015/863/EU) Compliant
Resistivity	$1.68 \times 10^{-8} [\Omega/m]$
Conductivity	$5.96 \times 10^7 [S/m]$

This tubing has good corrosion resistance and excellent heat transfer qualities. All tubing meets international standards for copper tubing. Important to note: Tube size is an accepted industry designation, not an actual size [7].

Table 7: Final Design's Receiver Coil Specifications

Outside Diameter of Coils (Do)	90 mm
Number of Turns	4
Length	729.6 mm
Spacing	4.81 mm
Width of Tubing	3.175 mm
Inner Diameter (Di)	26.12 mm
Winding Radius	29.03 mm
Radial Depth	31.94 mm
Inductance	909.66 nH.
Capacitance	150.55 pF
Frequency	13.6 MHz
Resistance (Dc)	1.5462 mΩ
Total Resistance	69.46 mΩ
Quality Factor	1119.09

N. Specification Summary

Table 8: Final Design's Receiver Specifications

Charge time(4Ah Battery Pack)	5 Hours Max
Battery pack voltage	User Selectable: 7.4V-14.2 V
Coupling Efficiency Transmitter to Receiver	90%
AC-DC Conversion Efficiency	80%
Charging Controller DC-DC Converter	85%
Overall Receiver Conversion Efficiency	61.2%
Battery Requirements:	UL1642 and IEC61960 compliant Li-ion packs.
Maximum Battery Charging Current	3.2A (7.4V); 2.2A (11.1V); 1.7A (14.8V)
Charger Subsystem Charge Protocol	Constant Current Constant Voltage (Li-Ion Battery)
Battery Type	UL1642 and IEC61960 compliant Li-Ion packs; 7.4-15 VDC nominal output voltage.
Power Negotiation	Using Bluetooth 5 LE
Deliverables	Wireless resonant charger with approximately 30W power transmission capability. Stretch Goal: a mobile device to demonstrate autonomous charging.
Telemetry	Report State to GUI Device
LCD display	Diagnostic Data Character String Display

Table 9: Final Design's Transmitter Specifications

Operating Frequency	13.56 MHz
RF Power Output	30 W
Max. Charging Distance	30 cm
DC Power supply	48V 1.25A min.
Conversion Efficiency	80%
DC-AC	
Telemetry	Report State to Receiver

Table 10: Final Design's Communication Link Specifications

Communication Medium	Bluetooth 5 LE
Protocols	GUI: Host Controller Interface (HCI) Receiver-transmitter: Synchronous Connection-Oriented (SCO) link

Table 11: Final Design's GUI Specifications

OS	WinOS, IOS, Linux, & Android
License	LGPL 3.0
Software Architecture	Model-Controller-View (MCV) Architecture
Delivery Model	Open Source Free App Download

O. Ethical and Professional Considerations

1.) *Public Health* Life preserving medical equipment requires concern in the transmission of powerful RF charging signals that may interfere with the medical equipment. We will adhere to FCC standards for intentional radiators and ensure that the charger transmitter does not exceed FDA guidelines for RF emission. Our design will be informed by the guidelines of the National Council on Radiation Protection and Measurements (NCRP) and the Institute of Electrical and Electronics Engineers (IEEE).

2.) *Safety and Welfare* Our design may contribute to public safety and welfare by easing the development of robotic systems intended to handle hazardous materials, work in narrow spaces, high temperature environments, or in vacuum. We will follow industry best practices for safe charging, such as current limiting and temperature monitoring, to minimize the risk of battery failure.

3.) Global Factors The pressures of governing bodies are to be taken into consideration in any choice this project takes; however, we are primarily concerned with the US governing bodies and then the EU bodies in order to streamline our development process to hit the largest market base possible. Additionally, Canadian and Mexican regulations would be considered as immediate market options.

In an alternate vein, there are sourcing questions that must be investigated before production in order to conform with international laws and prevent being banned from specific global markets whether at home or abroad.

4.) Societal factors The source code will be educational as well as providing value to the device itself. The design's modular intention will permit versatile implementations at work or at home. The product should serve influenceable groups such as teenagers, helping them enter STEM related fields.

The product as a whole should be considered in a way that would encourage further education in the classroom in physics. Likewise, the production of the product should foster a community between the product's programmers and engineers.

5.) Environmental factors This concern requires continual attention for any anomalies concerning the battery cells. The device cannot account for all of these concerns, but should maintain labeling that makes the customer aware of such concerns that may be caused by their device. The project must provide a means of emergency shut off by some interrupt port that is always active. The operating robot, the user via a GUI, and the receiver itself must have this ability to turn off the charging feature of the receiver.

6.) Economic factors The device could fulfill legal requirements for a client, and, in that case, a custom suite would be developed in the software at a premium to satisfy a client's needs. Additionally, creating a lightweight, low-cost production process is critical in maximizing profits. The open-source market also provides extensive free advertising momentum when capitalized successfully. Additionally, the product would assist in producing other products, especially in research and development.

Table 12: Ethical and Professional Considerations

Public Health	<ul style="list-style-type: none"> · Medical Equipment RF Exposure · Electrical Shock · Chemical Exposure
Safety and Wellness	<ul style="list-style-type: none"> · RF Bandwidth Jamming · Electrical Shock · Chemical Exposure
Global Factors	<ul style="list-style-type: none"> · International Governing Bodies · Sourcing Restrictions · Inter-Market Penetrability
Societal Factors	<ul style="list-style-type: none"> · Open-Source Capitalization · STEM Educational Resources · Professional Organizations · Customer Privacy & Security
Environmental Factors	<ul style="list-style-type: none"> · Chemical Pollution · User Environmental Awareness · Emergency Shut Off Cases
Economic Factors	<ul style="list-style-type: none"> · Open-Source Capitalization · Specialty Clientele · Rapid Agile-Deployment · Light-Weight Production

III. DESIGN SOLUTION

A. Product Architecture

The wireless charger system consists of two main subsystems, the receiver and the transmitter. The transmitter is powered by an external AC/DC 48 V power supply. The transmitter subsystem converts DC power into RF power to drive the transmitter coil. The transmitter has a microcontroller that communicates with the receiver and controls its wireless power transfer. The receiver has a receiving coil and capacitor that completes a 13.56 MHz parallel LC resonant circuit. The magnetic field generated by the transmitter induces an electric current in the receiving coil. The received power is rectified and transferred to the battery charger circuit. Also, the receiver has a microcontroller that communicates with the transmitter and indirectly controls transmitter circuits such as the wireless power transfer circuit. The receiver also communicates with remote devices such as tablets, phones, or computers to provide telemetry data.

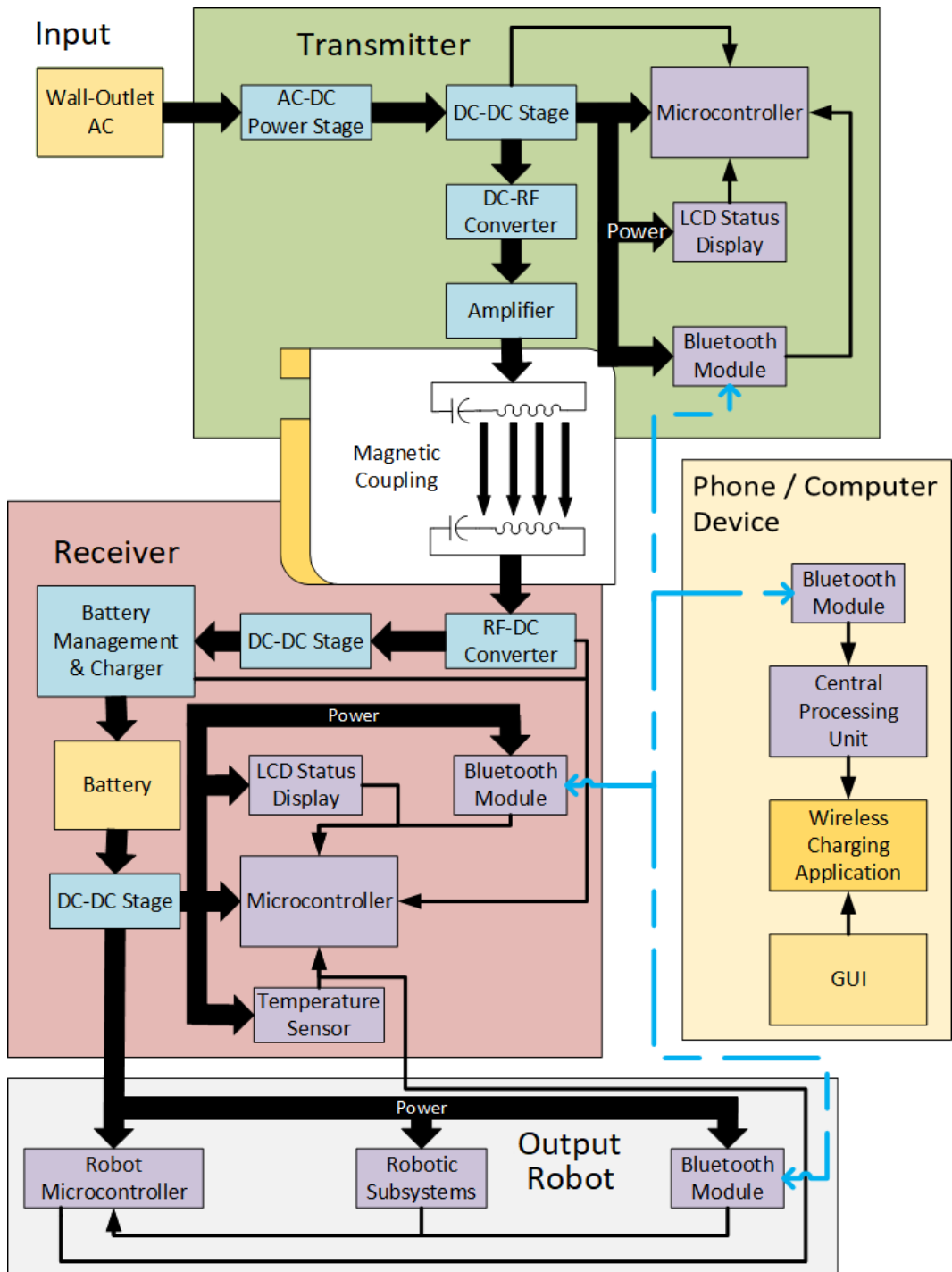


Figure 5: System Level Block Diagram

The graphical user interface (GUI) displays information with lists, data feeds, and visual aids that keep track of the battery's charge and any information passed along by the receiver to the user's remote device. The GUI's information on each device's connection and charging status allows real-time troubleshooting of each device.

The GUI Wireframe image below provides an example of how the GUI is structured. The selection widget shall be used to select between receiver devices to connect to. The top panel is reserved for battery monitoring. The Info panel utilizes wifi symbols to indicate connection status between devices while the lightning bolts reflect their on-going charging status. The bottom text panel is reserved for general warnings and information.

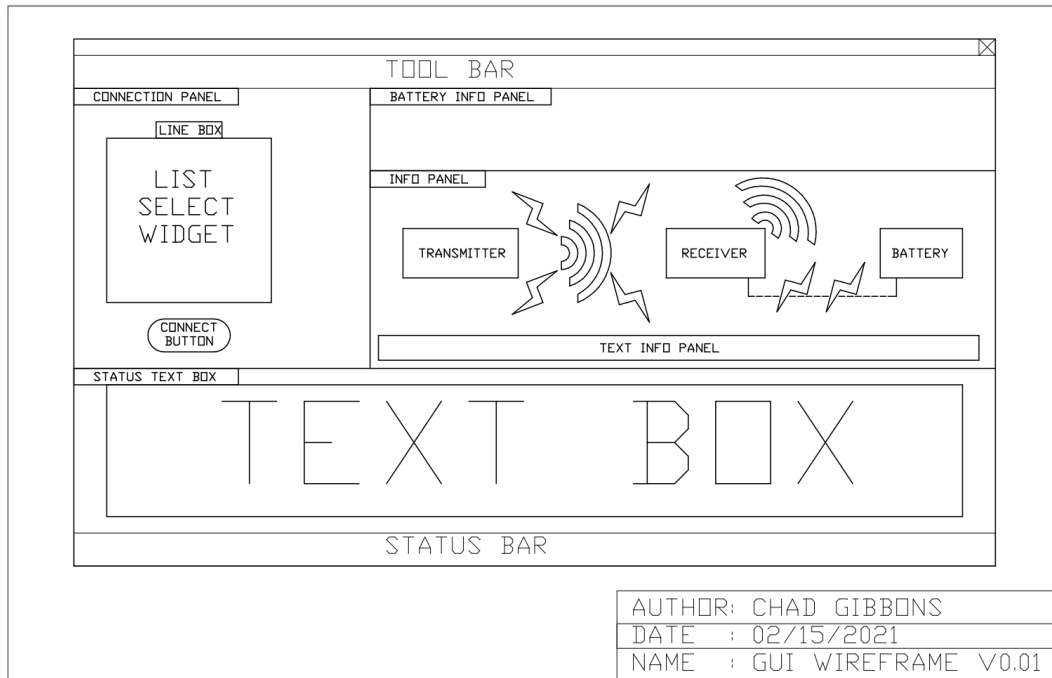


Figure 6: GUI Wireframe Diagram

B. Hardware Subsystems

1.) *Transmitter Subsystem* The transmitter circuit requires a 48 V power supply that will be down-regulated to 30V, 5V, and 3.3V. 30V is used by a coil driver (class E amplifier). 5 V supply will be used for the LCD and class E amplifier buffer. 3.3V is used by digital circuits such as microcontroller and Bluetooth.

The block diagram below shows internal voltage regulator connections.

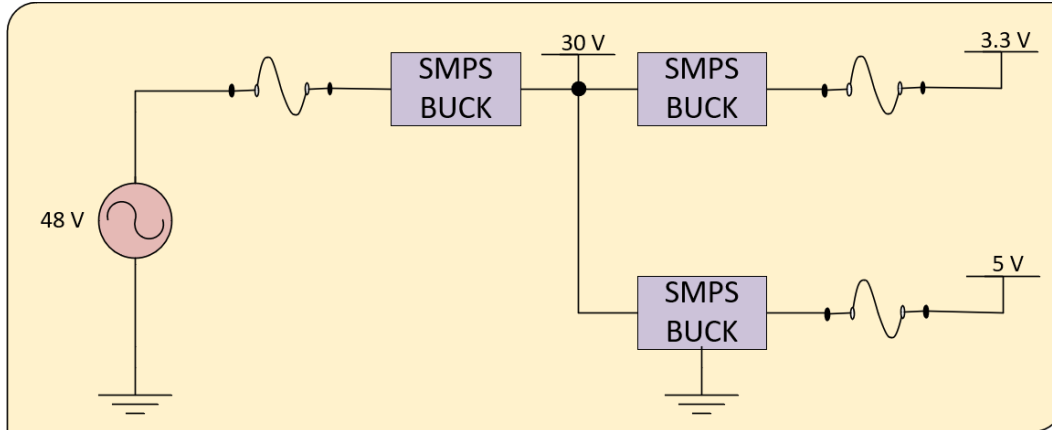


Figure 7: Transmitter Subsystem Voltage Regulator

The transmitter subsystem block diagram below illustrates how transmitter subcircuits interact with each other. The microcontroller is used to control most of the circuits in the transmitter subsystem. The Bluetooth module is connected to the microcontroller using the UART interface with flow control (RTS and CTS lines). The Bluetooth module is connected to the circuit that controls display contrast. The display parallel I/O interface is connected to the microcontroller through a level shifter. Also, the transmitter has four multipurpose user buttons that can be used to set the different modes of operations.

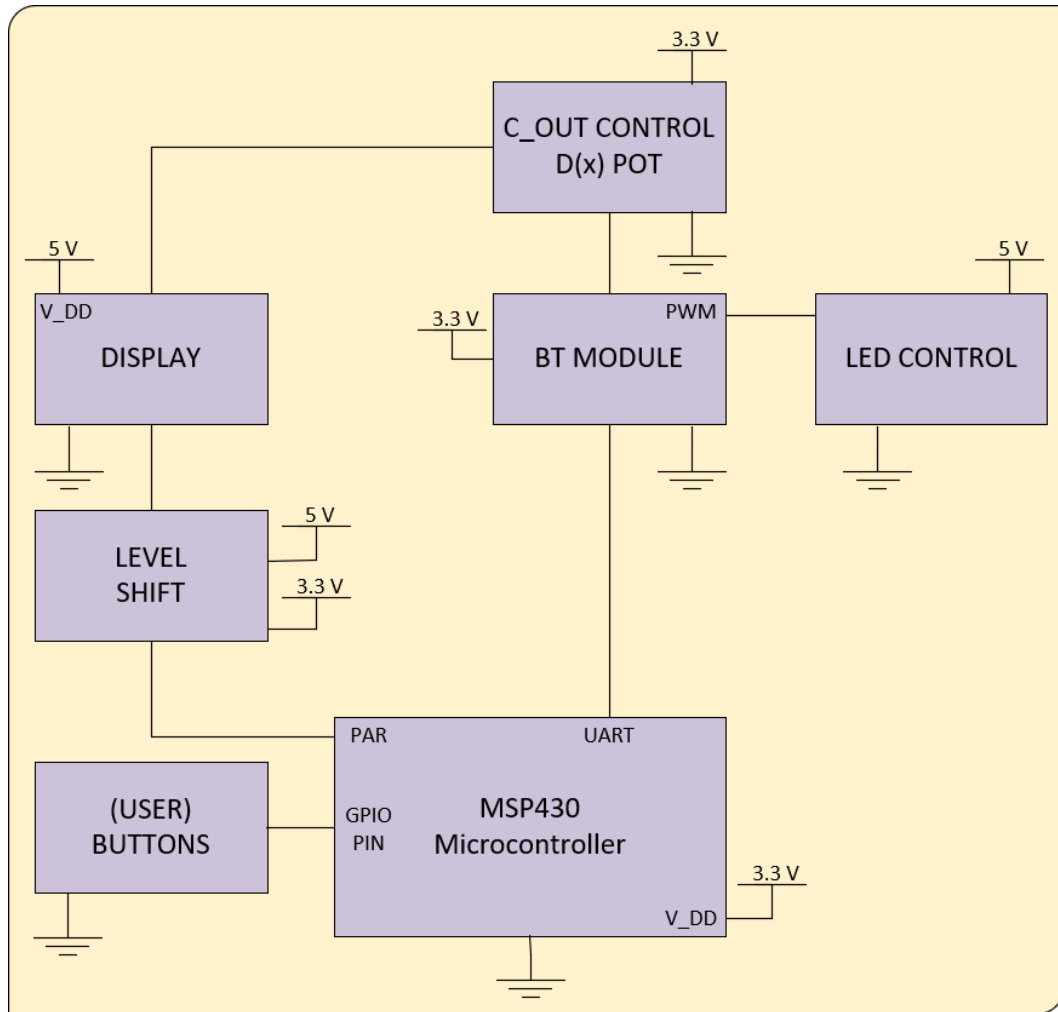


Figure 8: Transmitter Subsystem Block Diagram

The block diagram below illustrates the power transmission or DC to RF converter subcircuit. The subcircuit has an oscillator, buffer, and a coil driver. The 13.56 MHz signal is generated by a temperature-compensated crystal oscillator. The output of the oscillator is buffered using the GaN FET driver. A tuned switching power amplifier, also known as a Class E amplifier, is used to drive the transmitter coil where a GaN FET is used as a single-pole switching element. The transmitter coil and capacitors in series create the resonant LC circuit.

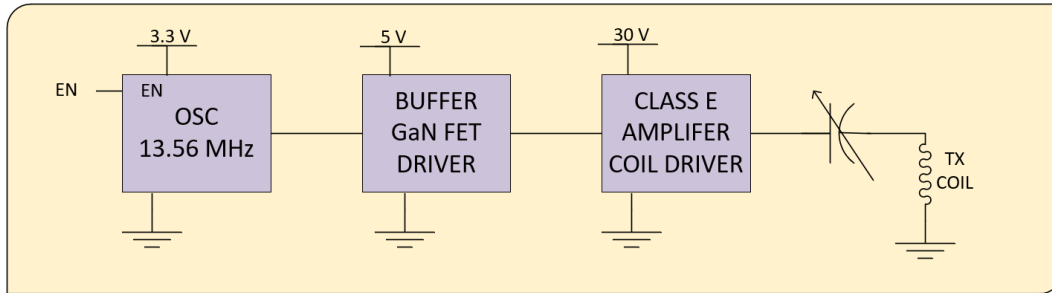


Figure 9: Coil Driver Subcircuit

The schematic diagram for the microcontroller (U2: MSP430FR5994), Bluetooth module (MD1 RN4870) display connector P3, the display illumination control (U5: MCP6001T-I/OT, U6: NUD3112LT1G), and LCD contrast control (U7: MCP4531-103E/MS) can be found in appendix NN.

The input power is supplied by an external AC/DC SMPS (Switched Mode Power Supply) converter. The power output of the buck SMPS is protected by a PPTC resettable fuse as short circuit protection. The fuse rating is 2.5A. A 48V power is converted to 30V which is used by the class E amplifier's 5V buck converter and 3.3V buck converter. Each SMPS module output has overcurrent protection using resettable PPTC fuses. Both fuses are 0.5A rated. Both low voltage regulators (5V and 3.3V) have additional filtering at their outputs using ferrite beads and 0.1 μ F capacitors.

Voltage regulators are shown below

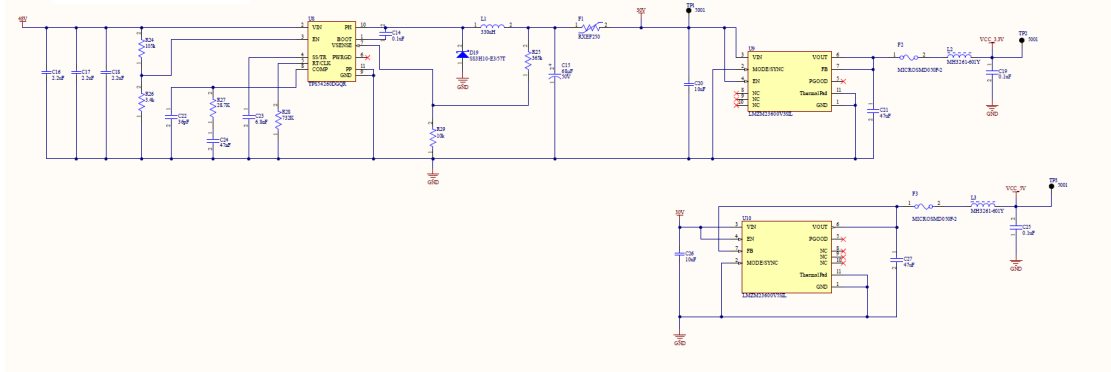


Figure 10: SMPS Subcircuit

The output of the temperature-compensated crystal oscillator (Y2) is connected to the GaN FET driver (U11: LM5112) which is connected to a GaN FET (Q1: EPC2019). the output of the class E amplifier is connected to the transmitter coil. The amplifier circuit has a peak detector (R30, R35, D20, C36 and R36) to detect the peak voltages of its output. The voltage on the peak detector will be sampled using the microcontroller's ADC in order to validate the receiver's presence via loading effects on the coil.

The coil driver circuit is shown below

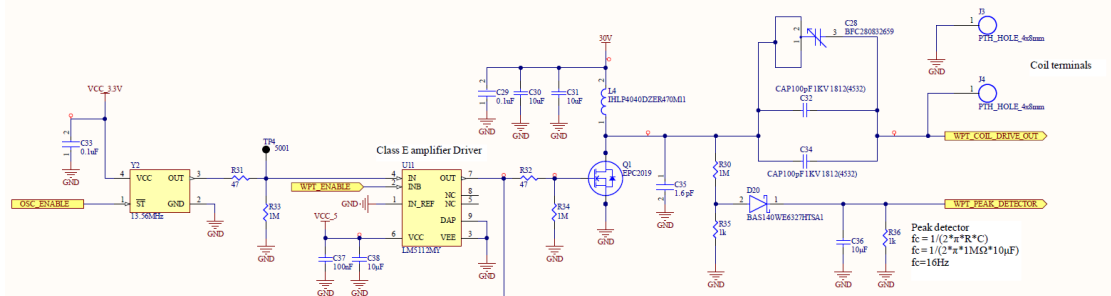


Figure 11: Transmitter Subcircuit

The transmitter subsystem function control and communication circuits schematic diagram shows the microcontroller (U2: MSP430FR5994), Bluetooth module (MD1 RN4870) display connector P5, the display illumination control (U5: MCP6001T-I/OT, U6: NUD3112LT1G), and LCD contrast control (U7: MCP4531-103E/MS). The schematic diagram can be found in appendix NN.

2.) *Receiver Subsystem* The main components in the receiver microcontroller subcircuit are identical to the transmitter microcontroller subcircuit.

The diagram below shows connections between receiver subcircuits.

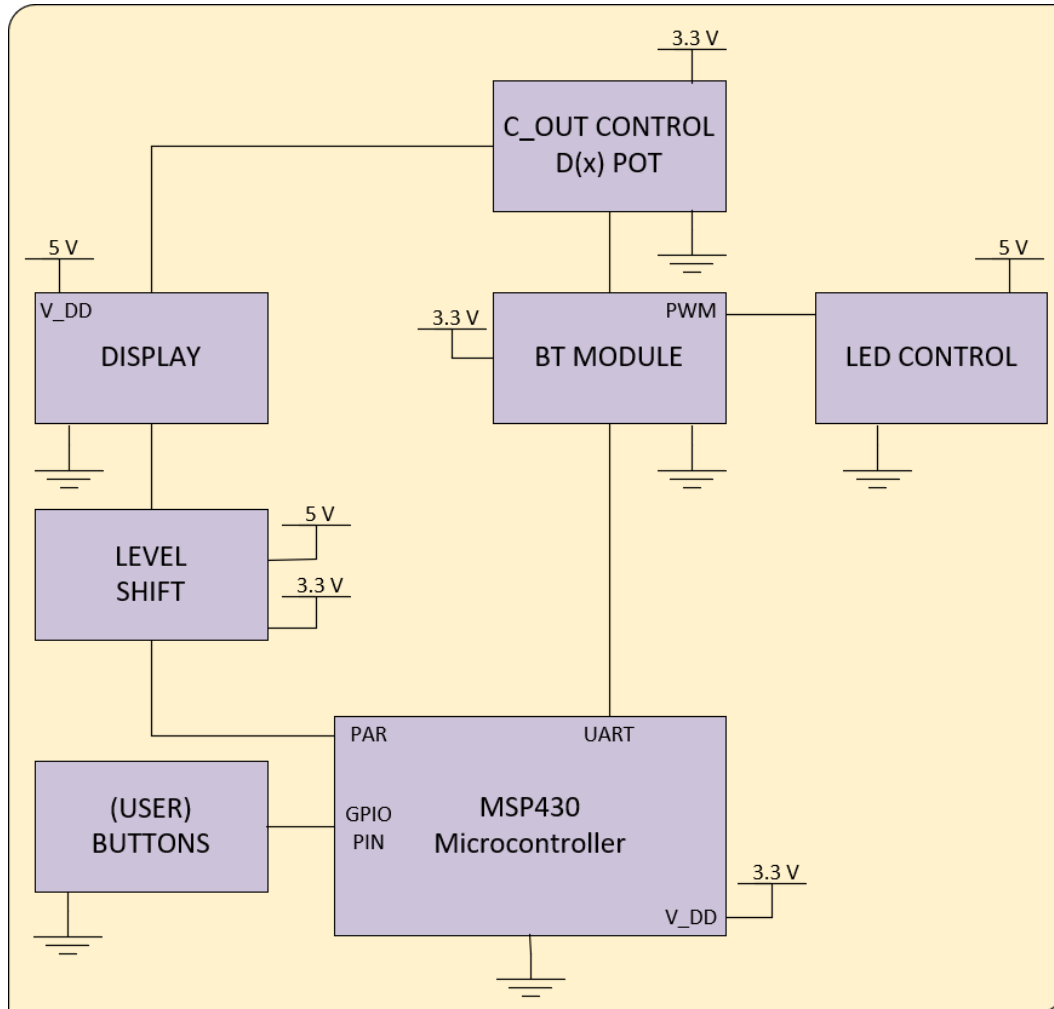


Figure 12: Receiver Subsystem Block Diagram

The receiver coil and parallel capacitor are acting as resonant tank circuit at a frequency of 13.56 MHz. The received power is rectified using a full wave rectifier bridge and then supplies to the battery charger circuit. The rectifier output voltage and current are constantly sampled by the microcontroller to determine instantaneous received power. The battery pack is connected to the charger for charging and the battery pack SMBus interface is connected to the microcontroller.

The diagram below shows the receiver's charging subcircuits.

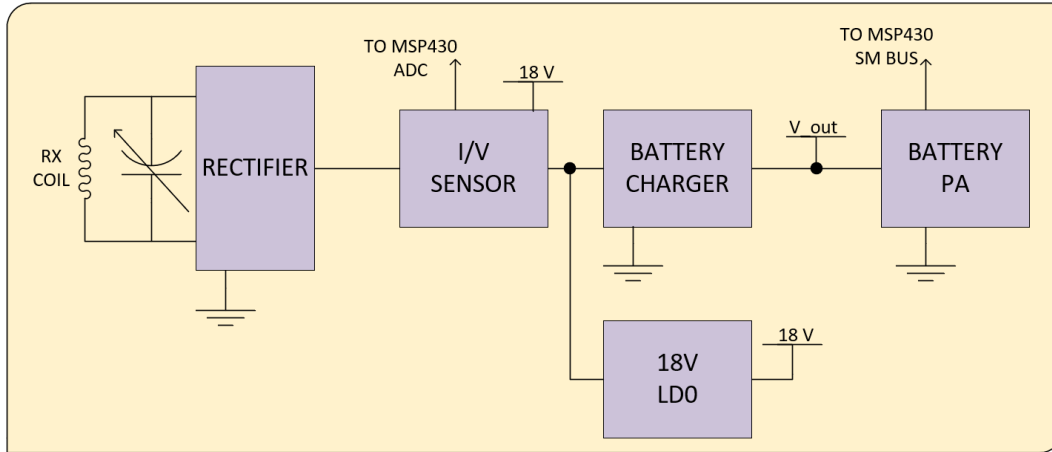


Figure 13: Receiver Coil Subsystem Block Diagram

The diagram below shows the voltage regulators utilized in powering the receiver's digital circuits and draws power from the battery pack directly.

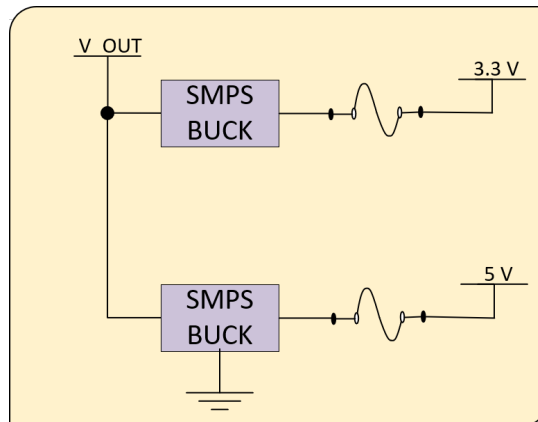


Figure 14: Receiver Voltage Regulator

On the receiver, battery management and power delivery functions are performed by the LTC4162-L monolithic charging controller. It handles many important battery testing and safety procedures automatically. Batteries are tested before charging, and should abnormal charging currents or voltages be detected the LTC4162-L will cease charging without firmware intervention. If conditions fall outside the preset limits a microcontroller interrupt may be triggered via the SMBALERT line for further error handling. The microcontroller firmware may read and change the LTC4162 status over an SMBus interface at any time.

A RRC smart battery will handle cell monitoring, balancing, and charging capacity measurement. It will automatically limit charge and discharge current to ensure safe functioning. Any one of a family of smart batteries may be connected to a keyed cable connector that ensures correct polarity and an SMBus connection. The SMBus interface will communicate with the microcontroller firmware to provide battery charge capacity and health information to the user.

Charger subcircuit is realized using LTC4162EUFD-SAD integrated circuit and may be found in Appendix A.2.

The power receiver subcircuit consists of the receiver coil, rectifier bridge, voltage sensor, and current sensor on the DC side of the circuit and feeds into the battery charging subcircuit. The rectifier bridge is designed using silicon carbide Schottky diodes.

DC Voltage detector and current sensor will be used to determine received power levels which can be used as an indication of transmitter-receiver inductive coupling. DC Voltage levels and current are sampled using the MSP430FR5994 AD converter.

The RF receiver rectifier and power sensor are shown below and can be found in larger print in Appendix A.3.

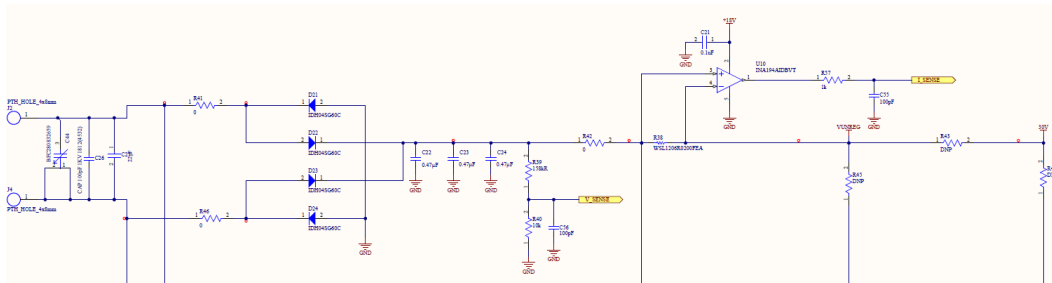


Figure 15: Rectifier and Power Sensor Subcircuit

3.) *Planar Coil Inductor* The transmitter and receiver utilize identical planar coils in the wireless power transfer process with an inductance of $0.909 \mu\text{H}$. The coils utilize copper tubing to reduce weight and costs.

The dimensions of the coil are shown below.

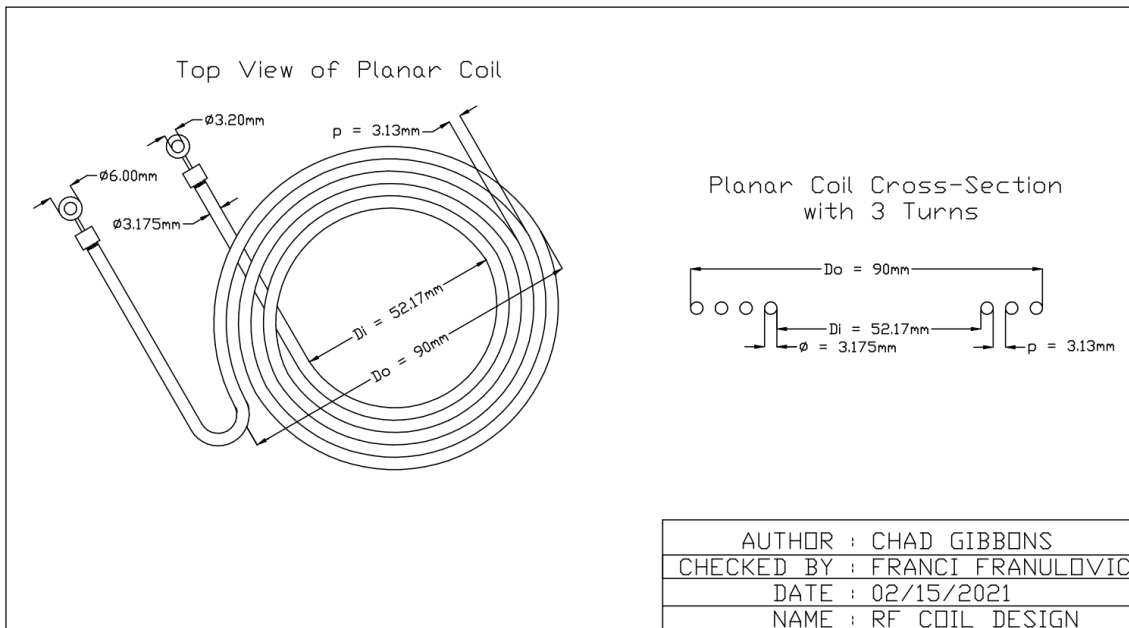


Figure 16: Planar Coil CAD Drawing

C. Software Architecture

1.) *Firmware Architecture* The microcontrollers' firmware architecture is split into two general categories: core functionality that is required for the microcontroller to operate and utilities that handle specific tasks that the microcontrollers need to complete. The core functions primarily stem from interrupt calls and setup sequences. The util functions will communicate through the bluetooth, display information, and handle or monitor power transmission.

Below is an example of the firmware architecture.

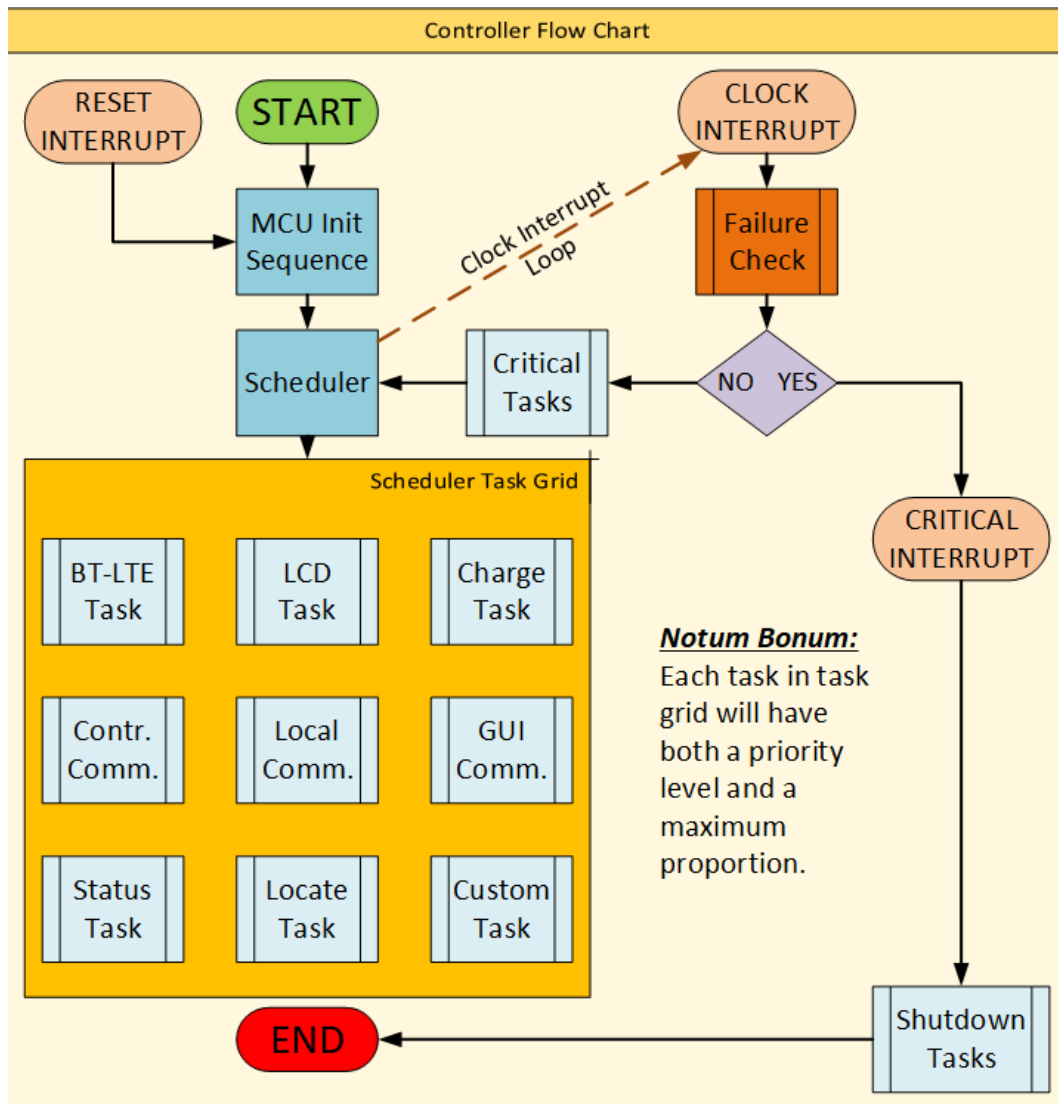


Figure 17: Controller Flow Chart

2.) *GUI Software Architecture* The GUI Software architecture is split into three general categories: Model, Controller, and View (MCV) components. Each general category is then subdivided into layers of functionality to maintain modularity. The Model is critical for handling data classes and storing data into files. The Controller is responsible for operating the visual components and model objects. The view category is utilized strictly for showing the graphical displays and are passive elements in the design's architecture.

The figure below shows the GUI 's Model-Controller-View (MCV) Architecture

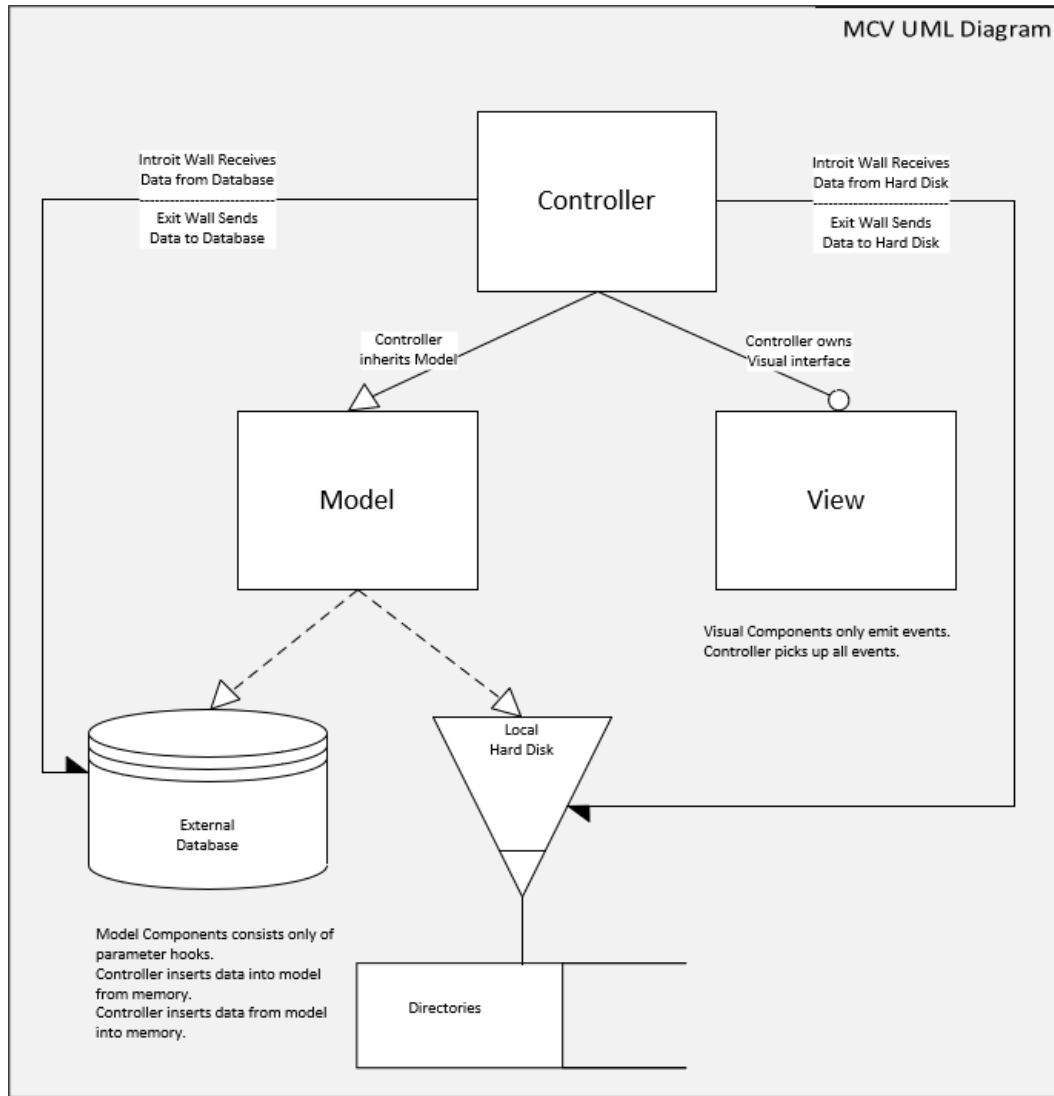


Figure 18: High Level GUI Software Architecture Example

D. Software Modules

1.) Firmware Modules Programmed on TI's Code Composer software and tested on TI's MSP430FR5994 Launchpad Kit

* = confer to both header and C files.

Microcontroller Setup

Location: Firmware\{MSP430FR5994_MCU\}\core\mcu_setup.*

Function: Activates port settings and instantiates utility functions that operate the program.

Microcontroller Reset

Location: Firmware\{MSP430FR5994_MCU\}\core\mcu_reset.*

Function: Resets microcontroller to initial setup configuration.

Task Queue Scheduler

Location: Firmware\{MSP430FR5994_MCU\}\util\Scheduler\scheduler.*

Function: Creates and operates the scheduler method class that selects the next task to be run in the main loop based on task priorities.

Clock Interrupt

Location: Firmware\{MSP430FR5994_MCU\}\core\Interrupts\clock_interrupt.*

Function: The code uses Timer A and SMCLK (1 MHz) to test clock interrupt. Once the program starts running, the timer counts up to 4 ticks to emit the clock interrupt signal every 250 ms period. Additionally, it instantiates utility functions considered critical to repeat frequently.

Button Interrupt

Location: Firmware\{MSP430FR5994_MCU\}\core\Interrupts\button_interrupt.*

Function: Four buttons are set up within a port. The code sets up an interrupt service routine to run when a button is pushed, so that their respective function is called.

Pin Input Voltage Reader

Location: Firmware\{MSP430FR5994_MCU\}\core\Interrupts\pins.*

Function: The function reads the analog 12 bit ADC input voltage at a port's pin.

Communication Transmission

Location: Firmware\{MSP430FR5994_MCU\}\util\Bluetooth\bluetooth_trans.*

Function: The code permits the transmitter to communicate directly with the receiver. Alternatively, it permits the receiver to communicate with both the transmitter and a mobile device.

Communication Received

Location: Firmware\ MSP430FR5994 MCU\ util\ Bluetooth\ bluetooth_recv.*

Function: The code facilitates the reception and reaction to bluetooth messages received.

2.) GUI Software Modules

+++ = architecture layer (Abstract - Base - Panel - Page - Window - App)

* = confer to both header and C++ files

Controllers

Location: Software\ controller\ +++_controller.*

Function: The doer or agent component of the program. Controllers allocate functions to particular events in the UI or manipulations to data models.

Widget Constructor

Location: Software\ controller\ widget.setter.*

Function: The factory class that is dedicated to building widgets in a panel with the proper hierarchy of inheritance in order to give the controller mediate control of all widgets.

Bluetooth Low Energy

Location: Software\ core\ Bluetooth\ Protocols\ bt_le.*

Function: The concrete method class handling Qt5 Bluetooth classes.

App Initialization

Location: Software\ core\ app.init.*

Function: Configure all initial settings and ensure that the program is properly installed.

Models

Location: Software\ model\ +++_model.*

Function: Data classes that can be pickled into compressed and encrypted binary data files. These models provide the stable memory of the application.

Canvas

Location: Software\ ui\ CanvasTools\ +++_canvas.*

Function: Concrete instances of Qt5's QCanvas class for graphical displays of information.

Canvas Shapes

Location: Software\ ui\ CanvasTools\ +++_canvas_shape.*

Function: Individual images used as graphical displays of information and placed on their respective canvases.

Panels

Location: Software\ui\Panels***_panel.*

Function: Concrete instances of movable panels used to hold widgets or canvases in GUI.

Toolbar Tools

Location: Software\ui\ToolbarTools\win_bar_tools.*

Function: Flushes out available toolbar icons and functions. Can also expand or limit drop down menu options at top of window.

Widgets

Location: Software\ui\Widgets

Function: Too many individual modules to account for in this document. See GitHub repository https://github.com/gibbs212521/HEC_2_senior_design for further detail. These modules are Abstract-Concrete constructor classes that build their respective widgets with additional custom methods or attributes.

Windows

Location: Software\ui\Windows***_window.*

Function: Abstract-Concrete constructor classes that permit the appearance of various types of windows in the application (restricted in tablet/cellphone device compilation).

Power Monitor

Location: Software\util\power_monitor.*

Function: Method class that ascertains whether the transmitter is sending power currently or not. Collects additional ancillary charging data.

Ticker Class

Location: Software\ui\Ticker***_ticker.*

Function: Collects or alters LCD ticker read out on the microcontroller.

App Configurations

Location: Software\config.h

Function: Global variable module. Ideally this file remains blank.

Application's Hidden Settings

Location: Software\.settings

Function: This file shall operate as a flat file to write or read current or most recent states in the application.

Main Program

Location: Software\app.cpp

Function: The proverbial main.cpp that handles all dependencies of the application's program.

E. Hardware Off The Shelf Items

The table below provides links and information on hardware incorporated in the post-production of the PCB. Further information can be found in the BOM Appendices in Appendix C, D, and E.

Table 13: Off The Shelf Items Utilized in Prototype

Description [Name]	Part Number	Link
Line Power Adapter: 65W 48V DC	DT62PW480D	https://product.tdk.com/en/search/power/switching-power/ac-dc-converter/info?part_no=DT62PW480D
74.52 Wh Li-Ion Battery	RRC RRC2040-2	https://www.rrc-ps.com/en/battery-packs/standard-battery-packs/products/rrc2040-2/
LCD Display	NHD-0420DZ-FSW-FBW	https://www.newhavendisplay.com/specs/NHD-0420DZ-FSW-FBW.pdf

F. Software Off The Shelf Items

The table below includes all software used to develop hardware and the software for the wireless charger project.

Table 14: Off The Shelf Software Items

Name and Version	License Type	Restrictions	Link
National Instruments Multisim 14.1	Commercial	None	https://www.ni.com/en-us/shop/software/products/multisim.html
Altium 21.0.9	Commercial	None	https://www.altium.com/
Altium 365	Commercial	None	https://www.altium.com/altium-365
Gerbv 2.6A	GPL 2.0	None	http://gerbv.geda-project.org/
Saturn PCB Design Inc. – PCB Toolkit ver.7.13	Commercial Freeware	None	https://saturnpcb.com/pcb_toolkit/
TI Code Composer	Commercial Freeware	None	https://www.ti.com/tool/CCSTUDIO
Qt5	LGPL 3	Code must be Open Source and Free to Download	https://doc.qt.io/qt-5/licensing.html
MS Visio	Personal License	No Corporate Use	https://www.microsoft.com/en-us/microsoft-365/visio-flowchart-software
NanoCAD	Personal License	No Corporate Use	https://nanocad.com/products/nanoCAD/
GCC	GPL 2.0	None	https://nanocad.com/products/nanoCAD/

G. Schematics / Wiring Diagrams / Technical Drawings

The schematics utilized can be found in appendices A and B with respect to the receiver, transmitter, and battery charger.

The coil design and GUI wireframe can be found in appendices I and J.

H. Custom Software

All code is written modularly, to inspect functions or objects individually see repository of https://github.com/gibbs212521/HEC_2_senior_design.

1.) Firmware Main Program msp430_proj.c

```
#ifndef __MC_MSP430_H
#define __MC_MSP430_H
#include <msp430fr5994.h>
#endif
#include "util/Scheduler/scheduler.h"
#include "core/mcu_setup.h"
short main(){
    mc_setup(); // Setup Interrupts and Core Functions
    struct MCScheduler mc_scheduler; // Instantiate Scheduler Class Object
    buildScheduler(&mc_scheduler); // Build Out Scheduler
    mc_scheduler.run(&mc_scheduler); // Begin Utility Function Loop
    return 1; // Returns 1 since this point should never be reached
}
```

2.) GUI Software Main Program app.cpp

```
#include "Core\app_init.h"

int main(){
    AppController MotherController;
    MainWindow MainWin;
    AppModel PrimaryModel;
    MainWin.owner = &MotherController; // use only for signaling
    PrimaryModel.owner = &MotherController; // use only for signaling

    AppController.getSettings(); // collect stable memory in .settings file
    AppController.setModel(&PrimaryModel); // giving control over model
    AppController.setUI(&MainWin); // giving control over window ui
    // AppController.setChildrenControllers() // Currently only one page
    AppController runApp();
    return 0; // emits 0 on successful closure of application
}
```

IV. PROTOTYPE DESIGN AND FABRICATION

A. Transmitter Subsystem Prototype Production

1.) *PCB Manufacturing* The transmitter boards are manufactured at JLC PCB factory in China. The PCB specification shown below makes this board producible by many manufacturers because it does not require special manufacturing processes.

For the fabrication process, Altium PCB CAD software is used to generate board manufacturing files (Gerber X2).

Gerber files include the following files:

Transmitter_RevA_Copper_Signal_Top.gbr	TOP SIGNAL
Transmitter_RevA_Copper_Plane_1.gbr	GROUND PLANE
Transmitter_RevA_Copper_Signal_1.gbr	MID1 SIGNAL
Transmitter_RevA_Copper_Signal_Bot.gbr	BOTTOM SIGNAL
Transmitter_RevA_Soldermask_Top.gbr	TOP MASK
Transmitter_RevA_Soldermask_Bot.gbr	BOTTOM MASK
Transmitter_RevA_Legend_Top.gbr	TOP SILK
Transmitter_RevA_Legend_Bot.gbr	BOTTOM SILK
Transmitter_RevA_Paste_Top.gbr	TOP PASTE
Transmitter_RevA_Paste_Bot.gbr	BOTTOM PASTE

Reference Drill files

Transmitter_RevA_PTH_Drill.gbr	Plated through holes
Transmitter_RevA_NPTH_Drill.gbr	Non-plated through holes

NC DRILL

Transmitter_RevA-RoundHoles.TXT	N/C DRILL ROUND HOLES
Transmitter_RevA-SlotHoles.TXT	N/C DRILL SLOT HOLES

The transmitter boards are manufactured using the following specification:

Material: FR4 (135degC Tg) RoHS COMPLIANT

Board Thickness: 0.063"

Surface finish: Immersion Gold (Electroless Nickel Gold - ENIG)

Solder Mask Color: Green

Silkscreen Color: White

Min. Drill: 8 mils

Min. Line Width: 8 mils

Min. Spacing: 4 mils

The layers are stacked up as follows:

1. TOP SIGNAL
2. GROUND PLANE
3. MID1 SIGNAL
4. BOTTOM SIGNAL

The transmitter board size is 5.702 inches (144.821 mm) X 4.203 inches (106.76 mm).

2.) Transmitter Prototype Board Assembly The group plans to assemble two transmitter boards. Parts for two boards are ordered using part numbers and quantities specified in the bill of materials. Quantities for small parts such as resistors, capacitors, some diodes, and some transistors are rounded to the nearest hundred because of the price break.

The assembly is performed manually using solder paste stencil and manual surface mount component placement. The solder paste stencil is custom made and is manufactured in the same facility as the PCB. Soldering is performed using a reflow oven. Through-hole parts are added after reflow oven soldering and soldered using standard solder pencil. All materials used in the assembly process are RoHS compliant.

For manual PCB assembly the group must provide detailed drawings of the PCB with visible reference designators, the bill of materials (BOM) that includes components reference designators, component description, and part numbers.

Required assembly documentation for the transmitter subsystem includes the following documents:

1. PCB Top silk layer and top copper layer drawings (c.f. Appendix B)
2. Bill of materials (c.f. Appendix D)

The figure below shows the PCB Top silk layer.

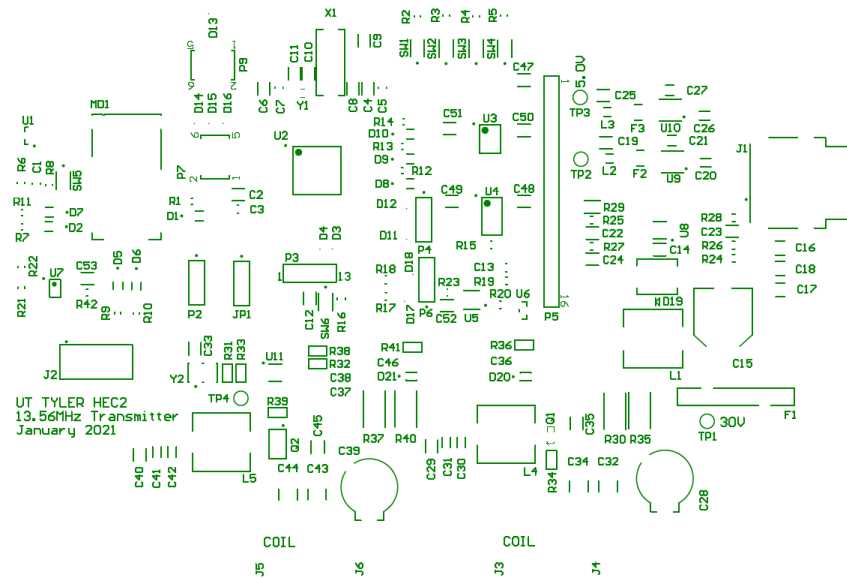


Figure 19: Transmitter Top Silk Layer

The figure below shows the PCB Top copper layer.

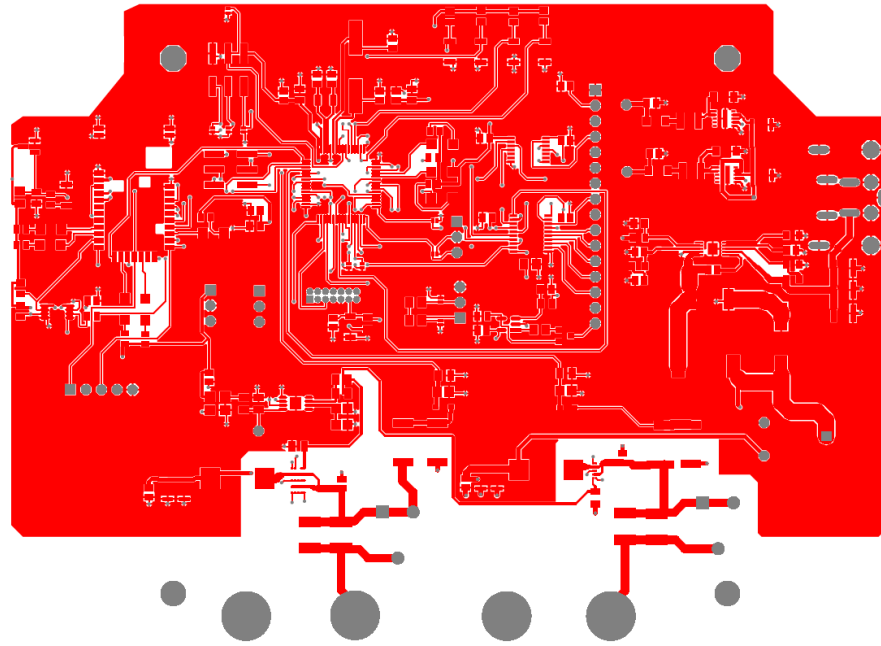


Figure 20: Transmitter Top Copper Layer

The assembly is performed by a professional worker. The assembly process consists of the following steps:

1. Solder paste printing on the PCB
2. Manual placement of surface mount components
3. Soldering using a reflow oven.
4. Through-hole soldering by hand using a solder iron pencil

All materials used in the assembly process are RoHS compliant. Also, all tools used in this process are standard tools used for the PCB assembly process.

3.) Post Assembly Inspection After the boards are assembled, they must be inspected for solder quality and possible assembly errors. Components values such as resistance, capacitance, and part numbers must be compared against the BOM and the board drawing. Also, the inspection step includes component polarity and solder quality inspection. After this step, the transmitter boards are ready for electrical verification and tests.

The transmitter prototype design is intended to match the final hardware design. The enclosure selection may change depending on the thermal behavior of the transmitter subsystem. Also, the differences that may exist between the transmitter prototype and the final design solution are not known at this stage because the transmitter electronics performance and efficiency need to be validated. Depending on the test results the group may apply changes in the transmitter circuits.

B. Receiver Subsystem Prototype Production

1.) PCB Manufacturing The receiver boards are manufactured at JLC PCB factory in China. The PCB specification shown below makes this board producible by many manufacturers because it does not require special manufacturing processes.

For the fabrication process, Altium PCB CAD software is used to generate board manufacturing files (Gerber X2).

Gerber files include the following files:

HEC2_Receiver_RevA_Copper_Signal_Top.gbr	TOP SIGNAL
HEC2_Receiver_RevA_Copper_Plane_1.gbr	GROUND PLANE
HEC2_Receiver_RevA_Copper_Signal_1.gbr	MID1 SIGNAL
HEC2_Receiver_RevA_Copper_Signal_Bot.gbr	BOTTOM SIGNAL
HEC2_Receiver_RevA_Soldermask_Top.gbr	TOP MASK
HEC2_Receiver_RevA_Soldermask_Bot.gbr	BOTTOM MASK
HEC2_Receiver_RevA_Legend_Top.gbr	TOP SILK
HEC2_Receiver_RevA_Legend_Bot.gbr	BOTTOM SILK
HEC2_Receiver_RevA_Paste_Top.gbr	TOP PASTE
HEC2_Receiver_RevA_Paste_Bot.gbr	BOTTOM PASTE

Reference Drill files	
HEC2_Receiver_RevA_PTH_Drill.gbr	Plated through holes
HEC2_Receiver_RevA_NPTH_Drill.gbr	Non-plated through holes

NC DRILL
HEC2_Receiver.TXT N/C DRILL ROUND HOLES

The receiver board is manufactured using the following specification:

Material: FR4 (135degC Tg) RoHS COMPLIANT
 Board Thickness: 0.063"
 Surface finish: Immersion Gold (Electroless Nickel Gold - ENIG)
 Solder Mask Color: Green
 Silkscreen Color: White
 Min. Drill: 8 mils
 Min. Line Width: 8 mils
 Min. Spacing: 4 mils

The layers are stacked up as follows:

1. TOP SIGNAL
2. GROUND PLANE
3. MID1 SIGNAL
4. BOTTOM SIGNAL

The receiver board size is matching the enclosure recommended board dimensions.

The receiver prototype design is intended to match the final hardware design. The enclosure selection may change depending on the thermal behavior of the receiver subsystem. Also, the differences that may exist between the transmitter prototype and the final design solution are not known at this stage because the transmitter electronics performance and efficiency need to be validated and compared to the product specification. Depending on the test results the group may apply changes in the receiver circuits. The receiver board size is 5.702 inches (144.821 mm) X 4.203 inches (106.76 mm).

2.) Receiver Prototype Board Assembly The group plans to assemble two receiver boards. Parts for two boards are ordered using part numbers and quantities specified in the bill of materials. Quantities for small parts such as resistors, capacitors, some diodes, and some transistors are rounded to the nearest hundred because of the price break. The assembly is performed manually using solder paste stencil and manual surface mount component placement. The solder paste stencil is custom made and is manufactured in the same facility as the PCB. Soldering is performed using a reflow oven. Through-hole parts are added and soldered after reflow oven soldering using standard solder pencil. All components and materials used in the assembly process are RoHS compliant.

For manual PCB assembly the group must provide detailed drawings of the PCB with visible reference designators, the bill of materials (BOM) that includes components reference designators, component description, and part numbers.

Required assembly documentation for the transmitter subsystem includes the following documents:

1. PCB Top silk layer and top copper layer drawings (ic.f. Appendix A)
2. Bill of materials (c.f. Appendix C)

The figure below shows the PCB Top silk layer.

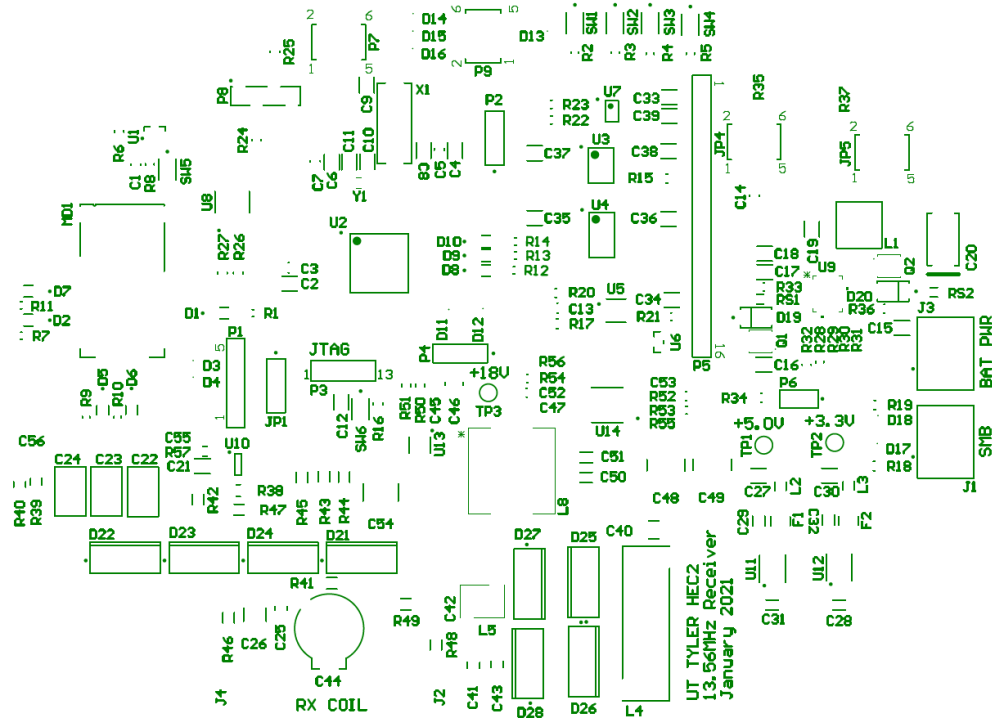


Figure 21: Receiver Top Silk Layer

The figure below shows the PCB Top copper layer.

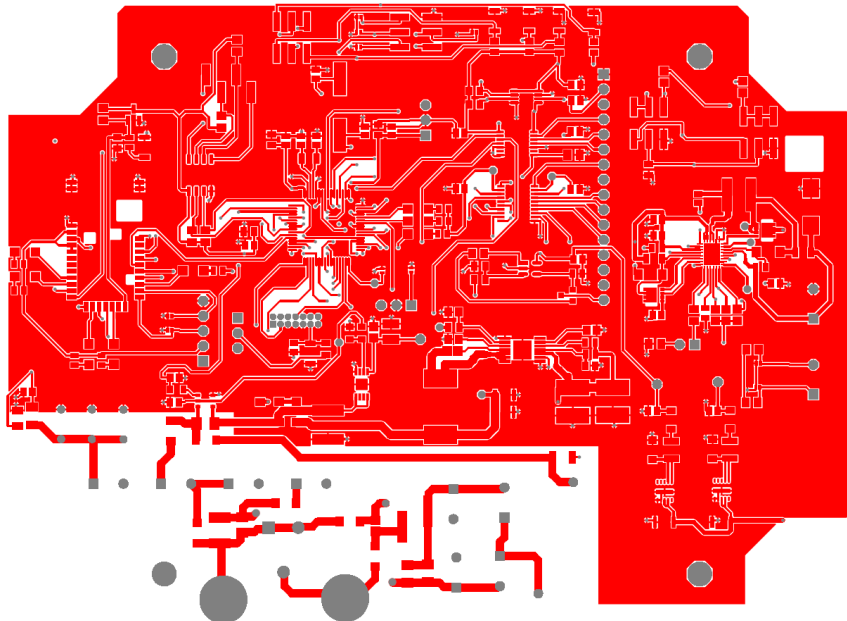


Figure 22: Receiver Top Copper Layer

The assembly will be performed by a professional worker. The assembly process consists of the following steps:

1. Solder paste printing on the PCB
2. Manual placement of surface mount components
3. Soldering using a reflow oven.
4. Through-hole soldering by hand using a solder iron pencil

All materials used in the assembly process are RoHS compliant. Also, all tools used in this process are standard tools used for the PCB assembly process.

3.) Post Assembly Inspection After the boards are assembled, they must be inspected for solder quality and possible assembly errors. Components values such as resistance, capacitance, and part numbers must be compared against the BOM and the board drawing. Also, the inspection step includes component polarity and solder quality inspection. After this step, the receiver boards are ready for electrical verification and tests.

The receiver prototype design is intended to match the final hardware design. The enclosure selection may change depending on thermal behavior of the receiver subsystem. Also, the differences that may exist between the receiver prototype and the final design solution are not known at this stage because the receiver electronics performance and efficiency need to be validated. Depending on the test results the group may apply changes in the receiver circuits.

C. Coil Production

The coil development process involves printing a 3-dimensional hollow plastic fixture. The interior of the fixture contains a spiral bas-relief that shall fix the coil in the specified spiral form. The coil shall be connected to the PCB board using stranded copper wire. For ideal performance conditions, the coil must withstand 600V rms as well as possess a resistance of 69.906 mΩ. The coil is encased in a plastic enclosure to prevent electric shock. The plastic enclosure specification will have a size of 130mm x 110mm x 20mm. MFG alpha rated wire will be soldered to the coil and the other end of wire will be terminated with the ring terminal.

D. Expenditure Report

The list below shows development tools and assembly tools cost that are used as an aid to design and produce the wireless charger system. This list does not include the cost of components that are part of the system.

Evaluation Kits for Firmware

Bluetooth Development Tools (802.15.1) RN4870 Sensor Board

Manufacturer part number: RN-4870-SNSR

Mouser part number: 579-RN-4870-SNSR

Cost: \$91.80

Ordered: 1 unit

Total cost: \$91.80

Bluetooth Development Tools (802.15.1) RN4870 click

Manufacturer part number: MIKROE-2543

Mouser part number: 932-MIKROE-2543

Cost: \$33.00

Ordered: 3 units

Total cost \$99.00

Development Boards & Kits - MSP430 MSP430FR5994 LaunchPad Dev Kit

Manufacturer part number: MSP-EXP430FR5994

Mouser part number: 595-MSP-EXP430FR5994

Cost: \$20.39

Ordered: 5 units

Total cost \$101.95

Hardware Evaluation Kits

Power Management IC Development Tools LTC4162 DC2038= Li-ion,adjustable, MPP
Manufacturer part number: DC2038A-J

Mouser part number: 584-DC2038A-J

Cost: \$150.00

Ordered: 1 unit

Battery packs for charger controller testing

Battery Packs 11.1V, 6.4Ah, 72Wh battery (3s2p)

Manufacturer part number: RRC2040-2

Mouser part number: 328-RRC20402

Ordered: 1 unit

Cost: \$105.00

Solder Stencil Production

Solder paste stencils are ordered for each subsystem.

Manufacturer: JLC PCB

Manufacturer part number: Custom order

Solder paste stencil \$7.05

Total cost \$14.10

Table 15: Summary of Expenditures

	Expenditure Description	Subsystem	Cost
1	Hardware development kits	Receiver	\$255.00
2	Firmware evaluation kits	Transmitter/ Receiver	\$226.75
3	Solder paste stencils (board assembly)	Transmitter/Receiver	\$14.10
	TOTAL COST		\$495.85

The tables below account for man-hours expended in development and prototyping.

Table 16: Man-Hours Expenditure Report in Development and Prototyping

Task Description	Man-Hours
Coil Production	
Francisco Sosa worked on coil	8
Franci Franulovic worked on coil	8
Subtotal	16 hours
Schematic design and capture	
David Flory	90
Franci Franulovic	12
Subtotal	102 hours
PCB Layout Design	
Franci Franulovic	10
David Flory	9
Subtotal	19 hours
PCB Assembly	
Estimated time required to assemble four prototypes	16
Subtotal	16 hours
Post Assembly Inspection	
Assembly verification	1
Solder quality inspection	1
Subtotal	2 hours
GUI Software Development	
Chad Gibbons on GUI Software Architecture	5
Chad Gibbons	2
Subtotal	7 hours
Firmware development	
Natasha Franca	25
Francisco Sosa	8
Chad Gibbons	32
Chad Gibbons worked on test suite	10
Subtotal	75 hours

Man-Hours Report Continued

Task Description	Man-Hours
Learning Curves and Used Skilled Resources	
David Flory on Altium	7
Firmware Team studied C/C++	15
Franci Franulovic developed PCB Schematic Drawing	11
Natasha Franca learned Object Oriented Programming in C	2
Subtotal	35 hours
Subsystem Prototyping	
Receiver PCB assembly	8
Parts procurement	2
Coil assembly	8
Coil Test	5
Hardware test	17
Firmware test	6
Quality control inspection	8
Subtotal	54 hours

Table 17: Development and Prototyping Summary of Man-Hours

Task Description	Man-Hours
Time Learning	35
Software Development	82
Hardware Development	137
Assembly	36
Quality Assurance	36
Total	326 hours

E. Budget

This budget lists the expenses for development hardware, prototyping materials, and skilled labor necessary to realize and test the prototype.

Table 18: Development and Prototyping Budget

Item Description	Price	Qty.	Totals
Microchip Bluetooth RN4870 Sensor Board	\$91.80	1	\$91.80
Mikroe Bluetooth RN4870 click	\$33.00	3	\$99.00
TI MSP430FR5994 LaunchPad Dev Kit	\$20.39	5	\$101.95
Analog Devices LTC4162-L Evaluation Board	\$150.00	1	\$150.00
RRC Battery Packs 11.1V, 6.4Ah, 72Wh battery (3s2p)	\$105.00	1	\$105.00
16x2 Parallel LCD Display (for evaluation)	\$20.63	3	\$61.89
Receiver BOM	\$77.30	2	\$154.59
Transmitter BOM	\$128.78	2	\$257.55
System BOM	\$136.92	1	\$136.92
Total Hardware			\$1,158.70

F. Current Manufacturing Abilities

The process starts with the purchase of the necessary components. Having the PCBs' Altium CAD Software drawings, the transmitter and receiver board files are sent for manufacturing at JLC PCB factory in China. Shipping time for the boards are around seven days. Small parts for the boards are also generated in the Altium software as a bill of materials, and those include but are not limited to resistors, capacitors, transistors, and diodes. Those can be ordered anywhere online and take up to seven days for delivery. Small parts can be purchased at local electronics stores. Hardware off-the-shelf items include power adapter, Li-Ion battery, and LCD display, and those can also be readily purchased at any local electronics store. Assembling is done by soldering the components according to the board layout, and each board takes approximately four to five hours to assemble by hand. The last setup step is to load the firmware onto the boards which requires less than one hour. In that same hour, testing the prototype can be completed if there are no issues hindering the charging process. The board would need to be troubleshooted for firmware, software, or hardware issues; the troubleshooting can take minutes or hours to fix.

Table 19: Prototype Production Timetable

Description	Time Required
Shipping Time for PCBs and other components	7 days
Manual receiver PCB assembly	5 hours
Manual transmitter PCB assembly	5 hours
Parts procurement process for each subsystem	2 hours
Coil assembly for each subsystem	1 hour
Coil Test	1 hour
Hardware test	1 hour
Firmware load and test	1 hour
Quality control inspection	8 hours
Total	8 days

V. TESTING AND VALIDATION

Validation of a product prototype is an important step to determine the performance, reliability, and durability of the designed product. Without proper testing, the product life cycle can be severely limited due to component failure or subcircuit malfunction. All basic functionality for each subsystem is verified by following standard test practices. The transmitter and receiver subsystems were subjected to validation tests described below to observe their actual performance.

TRANSMITTER TESTS

A. *Transmitter Power Supply Tests*

The transmitter prototype board testing starts by applying DC voltage on pins 3, and 4 positive terminals and pins 1-7 negative terminals. DC voltage is supplied using a bench power supply with the current limit set to 0.3A. The power supply voltage is gradually increased from 0V to the nominal voltage of 48V while the bench power supply current was constantly monitored. The 30V regulator will start regulating if the input voltage is higher than 38.3V. The expected output voltage on TP 1 is 30V +/-2% due to reference voltage tolerance and resistors used for setting the output voltage.

After the 30V regulator test, the voltage output is verified the following low voltage regulators are verified:

- 3.3V regulator (U11) test point TP2 nominal voltage 3.3V tolerance +/- 1.5%
- 5V regulator (U11) test point TP3 nominal voltage 5V tolerance +/- 1.5%

Below is the part of the schematic diagram showing test points TP1, TP2, and TP3.

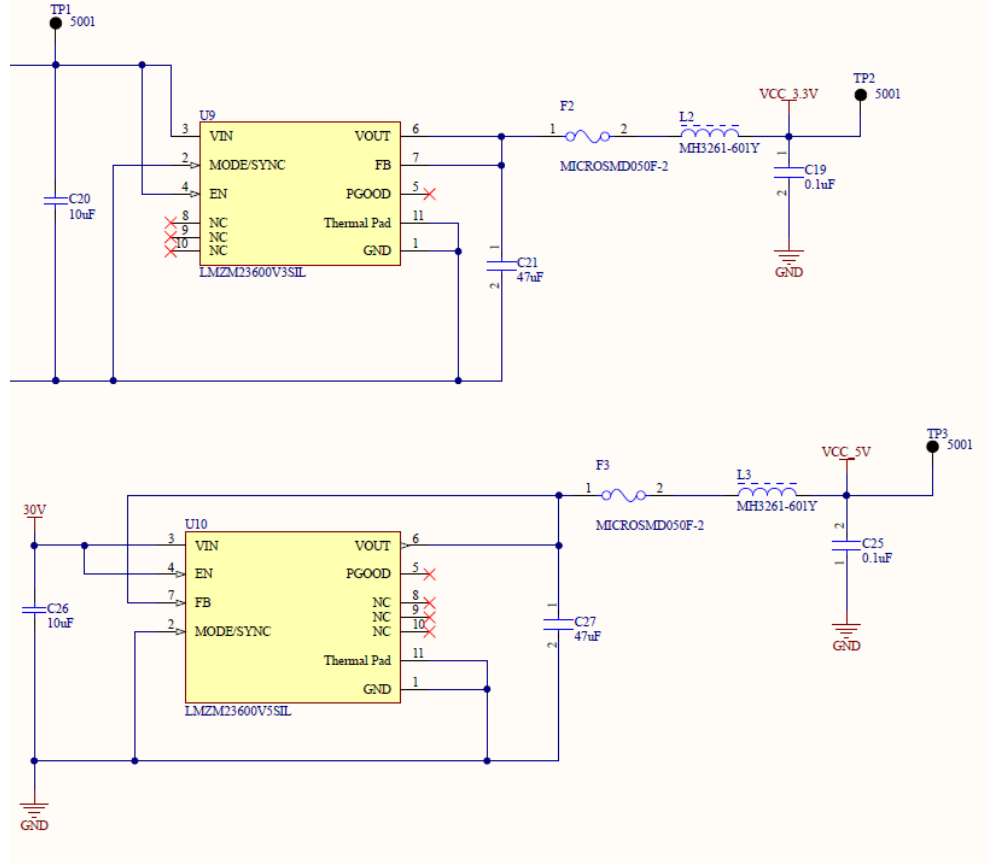


Figure 23: Transmitter Voltage Regulator Circuits

After power modules are verified the test firmware can be loaded using a JTAG connection on the board. The firmware sets all parameters in the default state for testing. The coil driver is disabled and all peripherals are turned off.

B. Transmitter Coil Driver Tests

After the firmware is loaded the board is turned off and the transmitter coil is connected to the terminals J3 and J4. The coil driver circuit is tested using a variable voltage supply. To perform this test PPTC fuse, F1 is removed and the bench power supply is connected to the TP1 (positive terminal) and the negative terminal is connected to the ground. The oscilloscope probe is attached to the drain of Q1 (GaN FET transistor). The second probe is connected to the output of the 13.56MHz temperature compensated oscillator (TP4).

After the test equipment is attached the power supply is turned on and the output voltage is gradually increased. When the power supply is higher than 5V voltage regulators (3.3V and 5V) are enabled and they provide power to the transmitter subcircuits. The temperature compensated oscillator (TXCO) enable line is controlled by push buttons. When the oscillator enable line is set to a high level a 13.56MHz signal is enabled and 13.56MHz is fed into the Class E amplifier driver (U11). The expected voltage from the TXCO on TP4 is $3.3V_{pp}$. After the oscillator subcircuit is verified the oscilloscope probe is placed on one of the terminals of jumper R32 to verify the functionality of U11. The expected amplitude on the output of the Class E amplifier driver is $5V_{pp}$.

The figure below presents the subcircuit wherein the transmission signal is generated and tested.

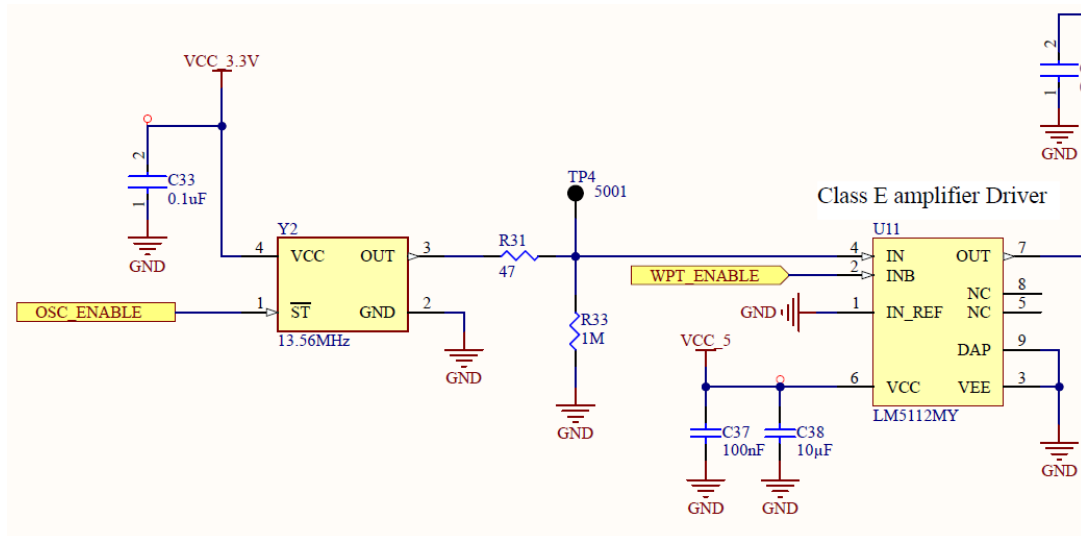


Figure 24: Oscillator and Buffer Subcircuit

The GaN FET switching is verified by observing the GaN FET drain voltage waveform that will have a voltage swing from 0V to 117V if the power supply voltage is set to 30 V. For lower supply voltages the swing will be lower but it always should swing from 0V to some positive voltage. After the GaN FET switching is verified the transmitter coil resonance will be adjusted.

To set transmitter coil resonance a variable capacitor (C28) must be adjusted while the voltage across the coil is monitored using a 100X oscilloscope probe attached to J4 (transmitter board coil terminal). The trimmer capacitor must be adjusted until the voltage across the transmitter coil reaches the maximum value. After the resonance is achieved the power supply voltage is gradually increased to 30V while the supply current is constantly monitored. The expected voltage on the drain of the GaN FET is $117V_{pp}$. The measured voltage is recorded. The 30V power supply current should be 120mA if there is no load present (no receiver coil in the front of the transmitter coil).

The figure below presents the subcircuit wherein the transmission signal is amplified and observed by a Class E amplifier.

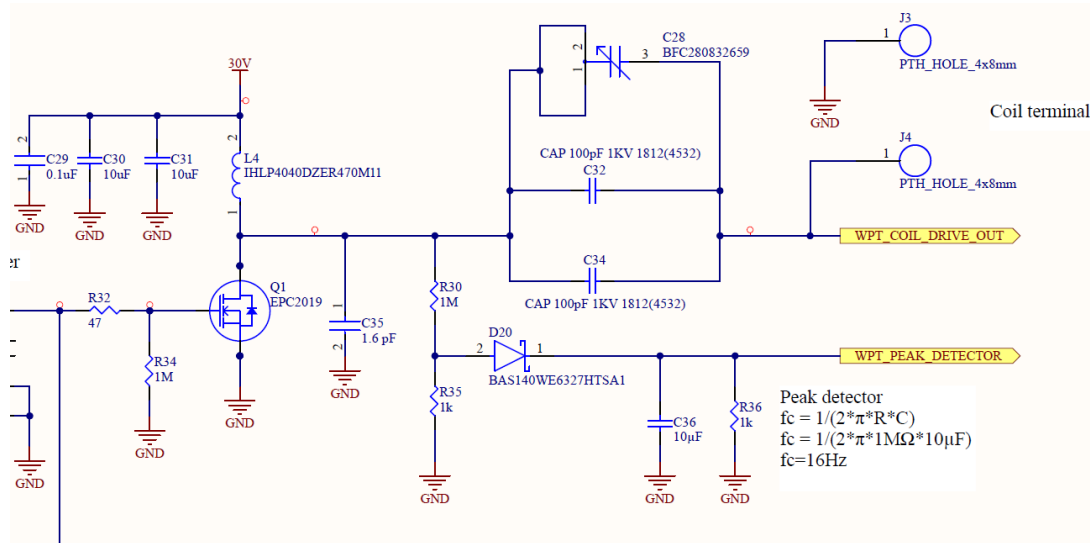


Figure 25: Transmission Signal Class E Amplifier Subcircuit

Transmitter power output is measured when the class E amplifier is verified and the amplifier power supply voltage is 30V. The specified transmitter power output is 30W. The power output is measured by placing receiving LC circuit loaded with a 50Ω high power resistor in the front of the transmitter coil at a distance of 5 cm. The peak to peak voltage across the load is measured using the oscilloscope and recorded in the table. This process is repeated for distances of 4 cm, 3 cm, 2 cm, and 1 cm.

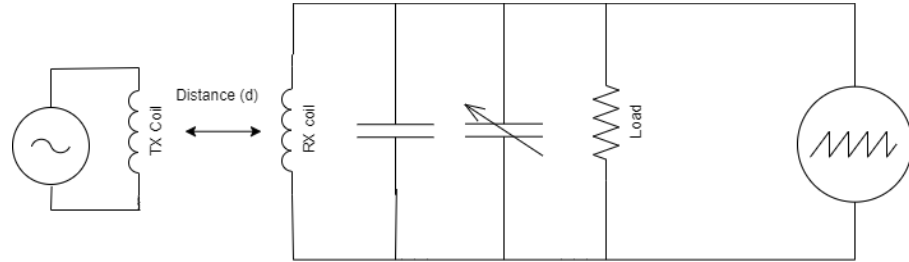


Figure 26: Received Power vs. Distance Test Setup

C. Transmitter Firmware Tests

The figure below is a reference for the transmitter part numbers and pin numbers. The part numbers can be found adjacent to the part outline with a prefix of P, J, U, Q, F, D, R, C, or L. Pin numbers are found without a prefix adjacent to the first and last pin with their respective number in any part denoted by the prefix P where space provides.

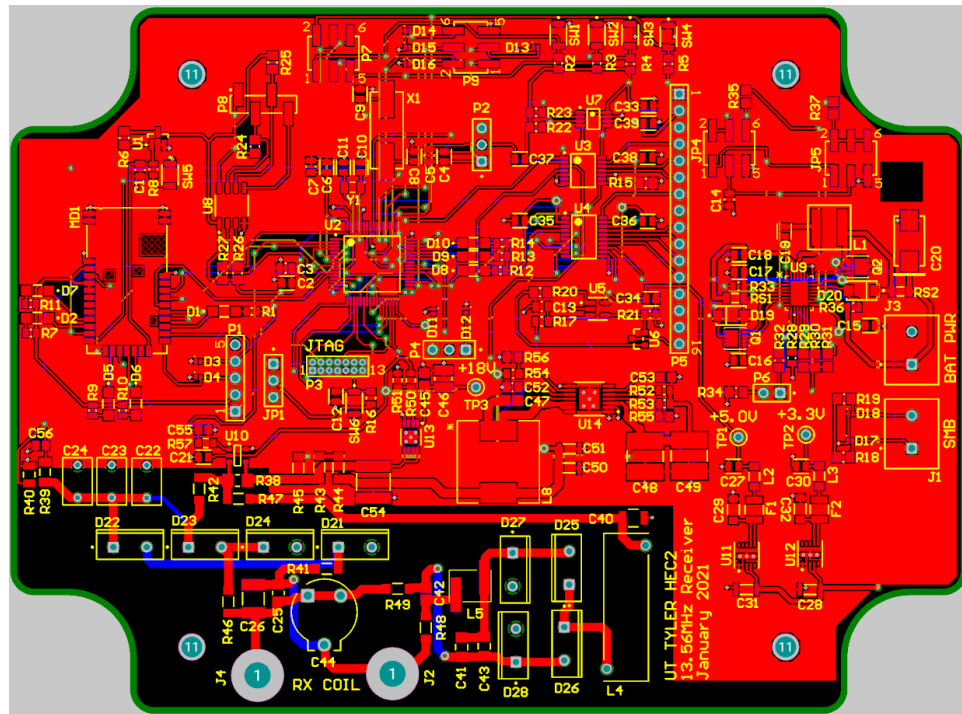


Figure 27: Reference Layout for Part and Pin Numbers

D. Transmitter Firmware Tests

The first recommendation in any trouble rise of troubleshooting of quality assurance is to check the mcu_setup.c and mcu_setup.h files. Additionally, it is good to note that a unit test is a type of software test that only requires building a small portion of the codebase in order to test a set of specific modules. Unit testing reduces the total amount of time dedicated into the development of any software.

The MCU Clock On LED (MCU_Clock_on or D8 by the microcontroller) should be blinking at a rate of approximately twice every second. If this is not occurring, the clock interrupt routine is not operating properly. Investigate for over-polling at the UART RX Pins (P2.0 and P2.5) is occurring. Alternatively, the TX Pins could be written out of turn (P2.1 and P2.6) which would thus initiate the UART Interrupts EUSCI_A0_VECTOR (located at P2.0 and P2.1) or EUSCI_A1_VECTOR (located at P2.5 and P2.6). If this is not the case, the next step would be to troubleshoot the ADC (Analog to Digital Converter) Pins (P3.0, P3.1, P3.2, and P3.3). If this issue where the ADC12_B_VECTOR interrupt contravenes the clock interrupt is detected, the error is likely caused by a breakdown in the hierarchy of interrupts. In such a case, the code must be provided additional logic on how to handle specific interrupts in the scheduler's run method.

The LCD Ticker Panel should display some coherent statement or acronym. If it does not, running of a “Hello World” unit test to the LCD is required for appropriate troubleshooting. The unit test should utilize the identical function used in the production code. If the unit test passes without errors, the error would reside in the accumulation of text that is meant to be passed into the LCD Ticker Panel.

The UART (RX/TX) CON tests require unit tests. There are four unit tests to be done to test the non-Bluetooth UART ports (P2.5 and P2.6). The first involves transmitting a ‘A’ character to the same PCB’s RX_CON Pin (P2.5). The next unit test would involve transmitting a string and acknowledgment TCP handshake. These same unit tests are repeated with a secondary PCB.

The Bluetooth validation tests will involve a unit test from the personal computer that connects to the receiver and sweeps through a set of pre-programmed unit tests that provide specific responses and sample data points.

The Wireless Power Transmission (WPT) Signal Generation test should be conducted prior to connecting the transmitter’s WPT coil. Press Button 0 at SW1 to turn on the signal generator and measure the voltage at the transmitter WPT Coil Junction points (J3 with J4 as well as J5 with J6). Once the voltage is observed, press Button 1 at SW2 to turn off the signal generator, and a drop off of voltage should be observed. (NOTE: The button closest to the microcontroller is Button 0 while the button furthest from the microcontroller and closest to the pins of Part P5 is Button 4. The buttons are arranged in sequential order.)

RECEIVER TESTS

E. Receiver Power Supply Tests

The receiver prototype board testing starts by applying DC voltage across coil terminals for power supply verification at the Receiver Coil Junction Points (J2 and J4). The Coil terminal subcircuit is shown in the figure below.

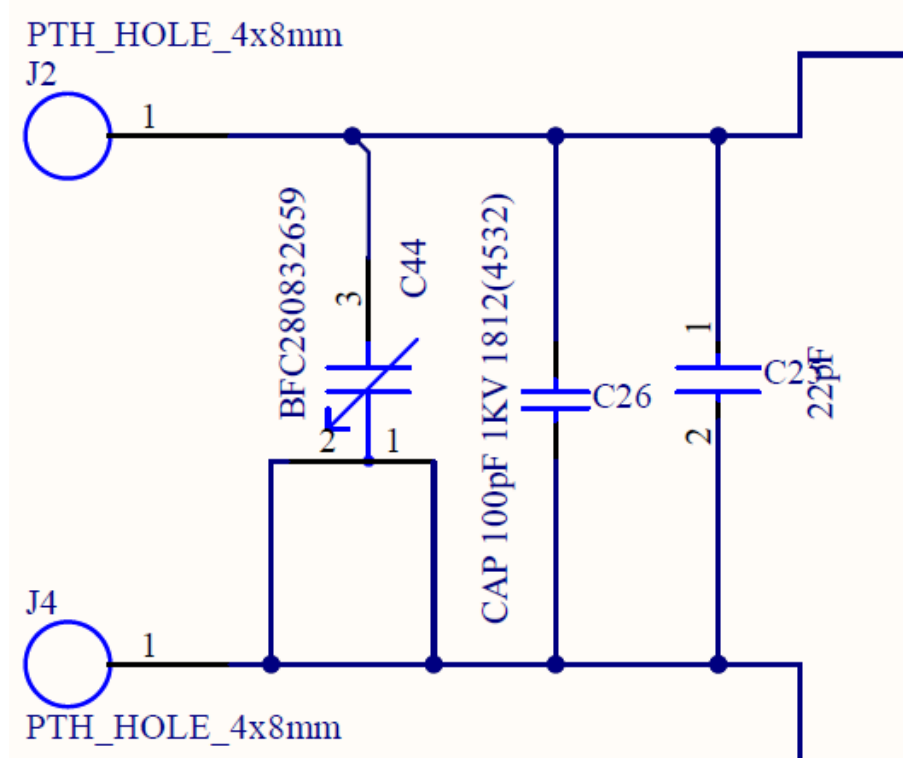


Figure 28: Receiver Coil Terminal Subcircuit

This test is necessary for determining whether the voltage regulators output voltages are matching the design specification.

The following voltage regulators are verified in this test:

- .3.3V regulator (U12) test point TP2 nominal voltage 3.3V tolerance +/- 1.5%
- .5V regulator (U11) test point TP1 nominal voltage 5V tolerance +/- 1.5%
- .18V regulator (U13A) test point TP3 nominal voltage 18V tolerance +/- 2%

After power module verification the test firmware can be loaded using a JTAG connection on the board. The firmware sets all parameters in the default state for testing.

F. Receiver Wireless Power Rectifier Tests

Specification for AC-DC (RF-DC) conversion efficiency is 80%

Conversion efficiency is tested using resistive load and without any other circuit attached to the DC side of the converter (R43 is removed). The load voltage and current are continuously measured. The specified receiver coil distance from the charger coil is 5 cm max.

Efficiency Test Protocol

This test determines the efficiency of the power transfer at various distances:

- The transmitter RF output is set to output 30W.
- The receiver coil is placed at a 5 cm distance from the transmitter
- Current and load voltage are recorded

Previous steps are performed for distances 4 cm, 3 cm 2 cm, and 1 cm. Using collected information load power is calculated. Efficiency is calculated using the following equation:

$$\eta = \frac{P_{receiver}}{P_{transmitter}} \cdot 100\% \quad (3)$$

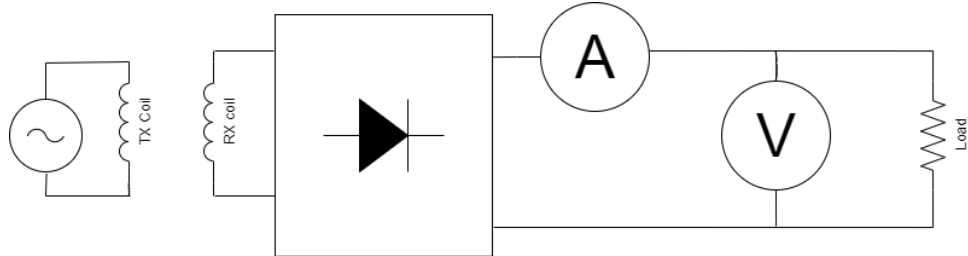


Figure 29: Receiver RF-DC Converter Efficiency Test Setup

G. Receiver Battery Charger Tests

The bench power supply current should initially be limited to 1A and the initial voltage should be set to 20V. There are two diode voltage drops (1.4V) in the full wave rectifier bridge circuit. 18.6V on charger input is high enough for the proper operating voltage for the LTC4162-L battery charger. The charger is functional without the battery pack and according to the datasheet, the voltage on the charger output will rise to the programmed constant-voltage value. By measuring this voltage it is possible to determine whether the charger regulates the proper voltage for a given programmed value.

A 18650 battery with two cells in series discharged to 3.2-3.8V per cell may be used for constant current and constant voltage charge testing. The bench power supply should be connected followed by the battery and no change in MCU behavior should be noted. Constant current charging should begin. The current limit of the bench power supply may be increased and the charging current should increase up to a maximum of 3.2A. The maximum charging current, charging voltage, cell count, and power supply current and voltage should be recorded and efficiency calculated.

Then the power supply should be disconnected and reconnected and there should be no effect on the MCU power state. Charging should automatically resume when the power supply is reconnected. The battery should be allowed to charge until it enters constant voltage mode, which may be recognized by a slowly decreasing charge current that is much lower than the maximum current observed during constant current charging. A 2 ohm load should be connected to the battery under charge for at least 30 seconds and removed without any effect on MCU operation.

H. Receiver Firmware Tests

The first recommendation in any trouble rise of troubleshooting of quality assurance is to check the mcu_setup.c and mcu_setup.h files. Additionally, it is good to note that a unit test is a type of software test that only requires building a small portion of the codebase in order to test a set of specific modules. Unit testing reduces the total amount of time dedicated into the development of any software.

The MCU Clock On LED (MCU_Clock_on or D8 by the microcontroller) should be blinking at a rate of approximately twice every second. If this is not occurring, the clock interrupt routine is not operating properly. Investigate for over-polling at the UART RX Pins (P2.0 and P2.5) is occurring. Alternatively, the TX Pins could be written out of turn (P2.1 and P2.6) which would thus initiate the UART Interrupts EUSCI_A0_VECTOR (located at P2.0 and P2.1) or EUSCI_A1_VECTOR (located at P2.5 and P2.6). If this is not the case, the next step would be to troubleshoot the ADC (Analog to Digital Converter) Pins (P3.0, P3.1, P3.2, and P3.3). If this issue where the ADC12_B_VECTOR interrupt contravenes the clock interrupt is detected, the error is likely caused by a breakdown in the hierarchy of interrupts. In such a case, the code must be provided additional logic on how to handle specific interrupts in the scheduler's run method.

The LCD Ticker Panel should display some coherent statement or acronym. If it does not, running a “Hello World” unit test to the LCD is required for appropriate troubleshooting. The unit test should utilize the identical function used in the production code. If the unit test passes without errors, the error would reside in the accumulation of text that is meant to be passed into the LCD Ticker Panel.

The UART (RX/TX) CON tests require unit tests. There are four unit tests to be done to test the non-Bluetooth UART ports (P2.5 and P2.6). The first involves transmitting a ‘A’ character to the same PCB’s RX_CON Pin (P2.5). The next unit test would involve transmitting a string and acknowledgment TCP handshake. These same unit tests are repeated with a secondary PCB.

The Bluetooth validation tests will involve a unit test from the personal computer that connects to the receiver and sweeps through a set of pre-programmed unit tests that provide specific responses and sample data points. The Bluetooth tests for the receiver should also include data requests pertaining to the voltage from the battery, the battery’s current charge, and any data utilized in the battery charger.

I. GUI Software Tests

The GUI's UI Evaluation validation test attempts to execute the GUI program and expose its components. The GUI should represent the GUI wireframes to be considered successful. The image below shows the furthest extent of the GUI's visual components available after one hour's work.

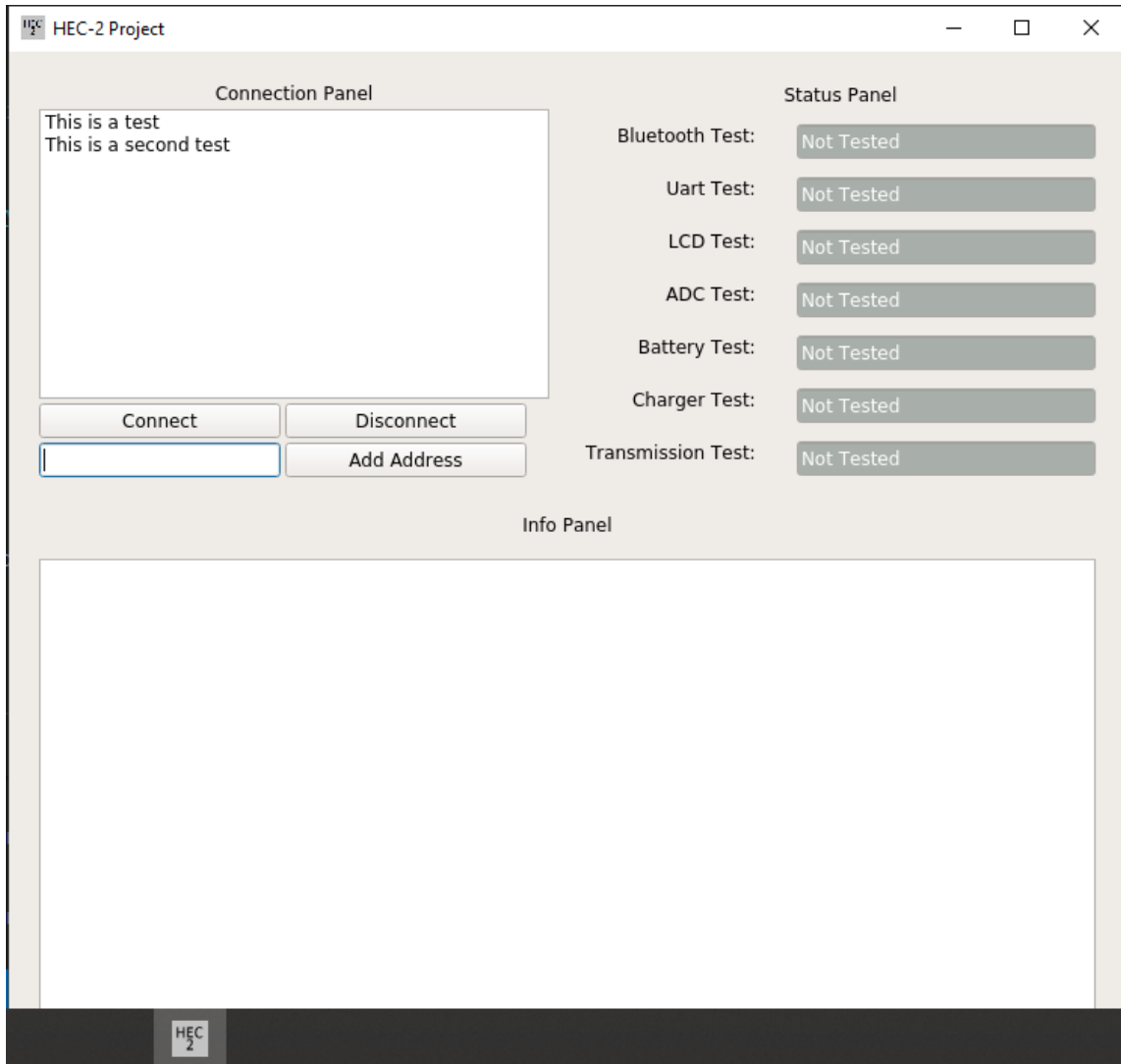


Figure 30: Current GUI Visual Components Exposed

The GUI's Functionality Evaluation validation test would run through the series of modules that fulfill the bluetooth tests on the Transmitter and Receiver. The GUI's UI would reflect the pass or fail state of each test as they are run.

SYSTEM TESTS

J. Coil Test

Coil impedance is measured using a Vector Network Analyzer (VNA). The impedance measurement is obtained by setting the instrument to measure S-parameters (S_{11}) at 13.56 MHz. Before measurements, the instrument must be calibrated using calibration standards (short circuit, open circuit, and 50ω load). The measured impedance is in complex form $R+jX$ form.

Specified inductance: 909.66 nH

The coil's inductance is determined using the formula below:

$$L = \frac{X_L}{\omega} \quad (4)$$

Where $\omega = 2 \pi f$

The figure below shows the equivalent circuit of how the transmitter / receiver coils were evaluated using a Vector Network Analyzer.

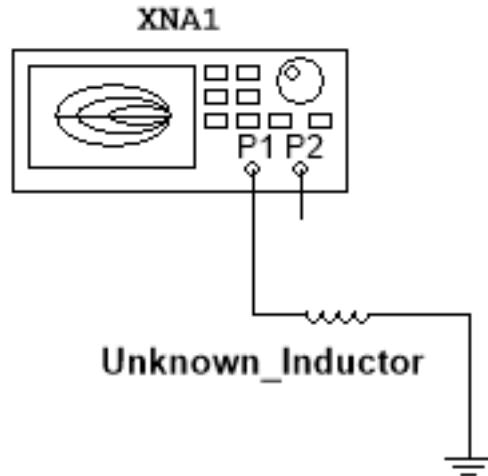


Figure 31: VNA Test Setup

Although VNA is not very precise for quality factor measurements it still can be used for estimation. The quality factor is determined by obtaining S₂₁ parameter (forward voltage gain).

Specified Q factor: 1119

The quality factor also can be determined by dividing reactance by the resistance the formula is shown below:

$$Q = \frac{X_L}{R} \quad (5)$$

K. System Level Firmware Tests

The Bluetooth Localization Test utilizes the “M” command on the RN4870 BLE chip with 3 prior locations to triangulate which direction is moving towards the transmitter. This test begins with a computer provided unit test that accepts four distances, the first three that are used to triangulate the receiver in reference to the transmitter and a fourth that must be closer than all three triangulating distances to be considered passing.

L. Test Results Summary

1.) Transmitter Evaluations

DC Power Test

30 V regulator no-load condition measured output voltage 30.04 V

5 V regulator measured output voltage TP3 5.03 V

3.3 V regulator measured output voltage TP2 3.33 V

Coil Driver Test

Oscillator output voltage TP4 3.69 V_{pp}

Oscillator output Frequency (13.56 MHz) measured: 13.56 MHz

Class E amplifier driver voltage jumper R32 (nominal 5 V_{pp}) measured 5.80 V_{pp}

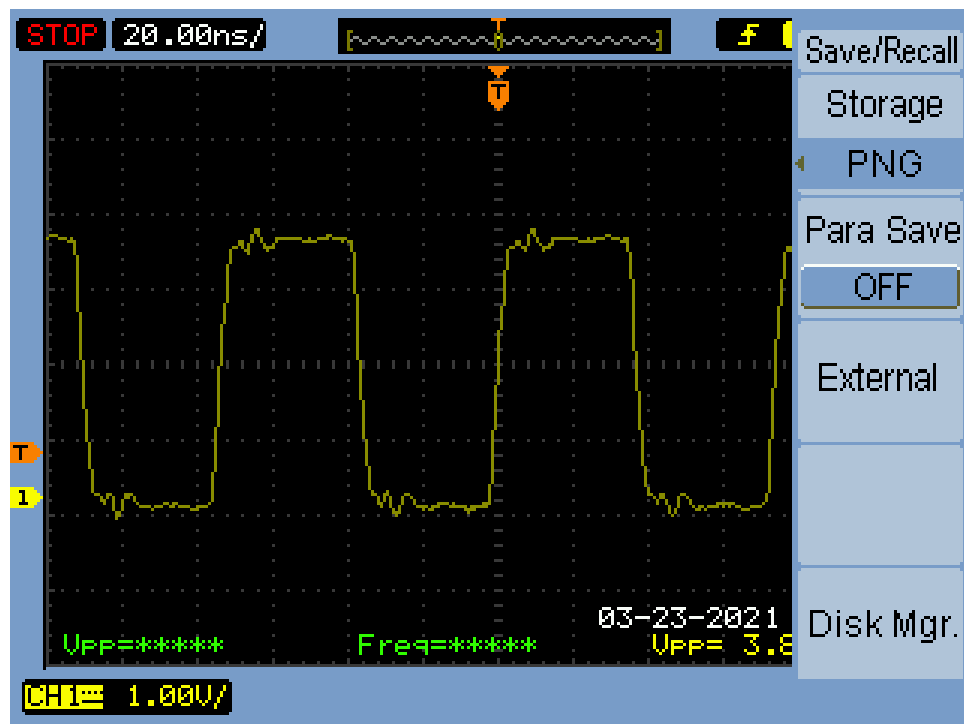


Figure 32: Class E Amplifier Driver Output

Q1 Dran nom. 117 V_{pp} (30 V supply) Measured 102 V_{pp}

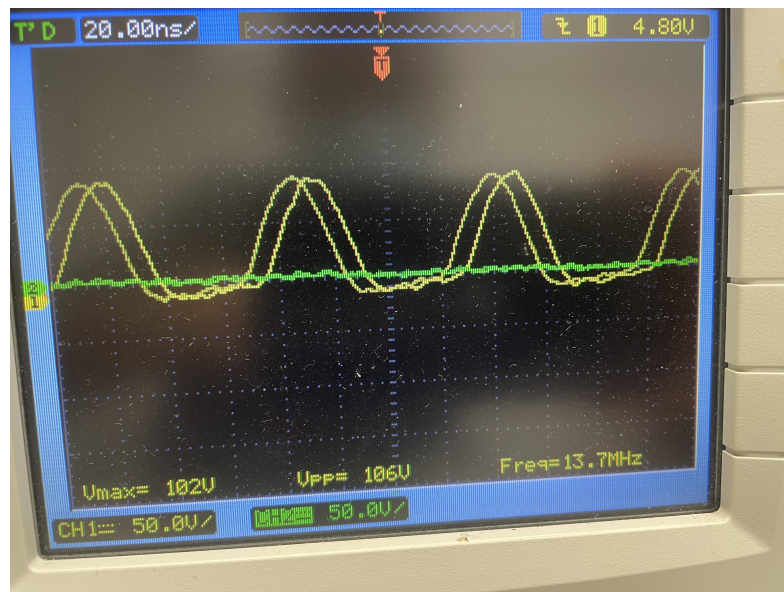


Figure 33: Q1 Drain Voltage Waveform

Transmitter coil voltage 117 V_{pp} (30 V supply) Measured 204V_{pp}

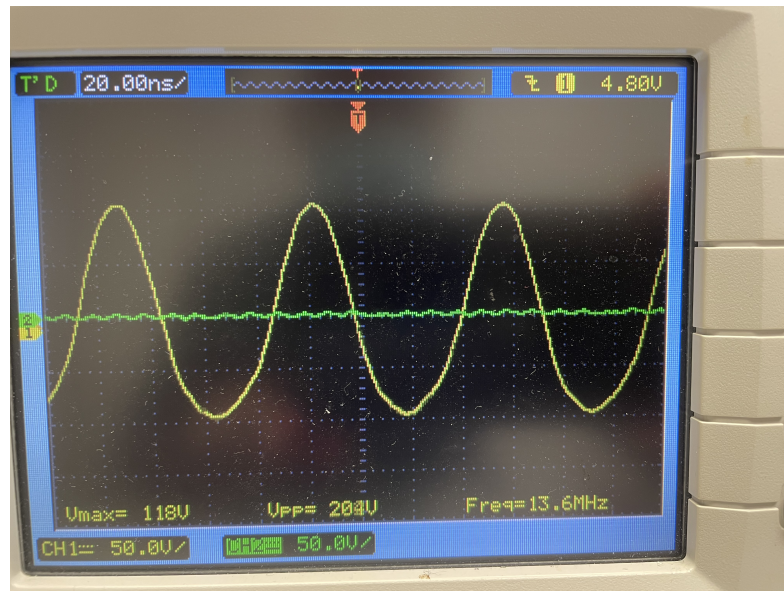


Figure 34: Q1 Drain Voltage Waveform

Transmitter subsystem input current at 30 V supply (120 mA nom. no load) Measured 140 mA

Table 20: Transmitted Power vs. Distance Test

Distance [cm]	V_{Load} [V _{pp}]	P_{Load} [W]	$V_{Transmission}$ [V _{pp}]	I_{DC} [A]	$P_{Transmission}$ [W]	Efficiency [%]
0	61.6	9.486	13.8	0.73	10.074	94.2
1	30.4	2.310	13.8	0.18	2.484	93.0
2	20.0	1.000	13.8	0.15	2.070	48.3
3	11.6	0.336	13.8	0.10	1.380	24.4
4	8.8	0.194	13.8	0.09	1.242	15.6
5	6.2	0.096	13.8	0.09	1.242	7.7

Where the load resistance is 50 Ω.

2.) Receiver Evaluations

DC Power Test

5 V regulator measured output voltage TP1 5.07 V

3.3 V regulator measured output voltage TP2 3.33 V

18 V regulator measured output voltage TP3 18.26 V

After several experiments with various diodes and rectifier circuit topology, the best performance was achieved using a full-wave bridge with small Schottky diodes. RF power is converted into DC power by rectification using a full-wave rectifier. Full-wave rectifier Schottky diodes part number is RB168MM100TFTR . Received power (DC) vs. distance test is performed with 50 Ω load on DC output of the receiver subsystem. At a 0 cm distance, the energy transfer efficiency for the entire system is close to the specified efficiency.

Table 21: Received Power (DC) vs Distance Test

Distance [cm]	V_{Load} [V _{DC}]	P_{Load} [W]	$V_{Transmission}$ [V]	I_{DC} [A]	$P_{Transmission}$ [W]	Efficiency [%]
0	18.0	6.480	13.8	0.709	9.7842	66.23
1	5.12	0.524	13.8	0.137	1.8906	27.73
2	3.16	0.200	13.8	0.095	1.3110	15.23
3	2.27	0.103	13.8	0.104	1.4352	7.18
4	1.45	0.042	13.8	0.099	1.3662	3.08
5	0.9	0.016	13.8	0.95	13.11	0.12

Where the load resistance is 50 Ω.

The efficiency test was repeated at 0 cm distance with different loads to determine the effect of load impedance on the power transfer efficiency.

Table 22: Power Transfer vs Load Test

V_{Load} [V _{DC}]	R_{Load} [Ω]	P_{Load} [W]	Coil V_{tx} [V _{pp}]	Amplifier V_{ds} [V _{pp}]	V_{Supply} [V]	I_{Supply} [A]	$P_{Received}$ [W]	Eff. [%]
18.00	50	6.48	192	73	13.8	0.714	9.8532	65.77
4.09	8	2.09	264	84	13.8	0.717	9.8946	21.13

This test is performed with a limited power output of the transmitter at 10 W. The battery charging current is set to 0.32 A by replacing the current sense resistor from 10 mΩ to 0.1 Ω. The transmitter is powered using a 12 V power supply and the distance between the receiver and transmitter coils is 0 cm. The transmitter DC power supply voltage and current are measured. The receiver DC output voltage, battery current, and battery voltage are measured.

$$P_{TX} = V_{DC} \cdot I_{DC} \quad (6)$$

The received power is determined by adding power dissipated in the load and power absorbed by the battery.

$$P_{RX} = P_{LOAD} + P_{BATT} \quad (7)$$

Table 23: Overall Efficiency Test

V_{Trans} [V]	I_{Trans} [A]	P_{Trans} [W]	V_{Recv} [W]	R_{Load} [Ω]	$I_{Battery}$ [A]	$V_{Battery}$ [V]	$P_{Battery}$ [W]	Eff. [%]
12.4	0.84	10.42	8	50	0.2	7.74	2.83	27.2

Coil Design Validation

Specified inductance: 909.66 nH

Measured impedance at 13.56 MHz: $0.43 + j78.28 \Omega$

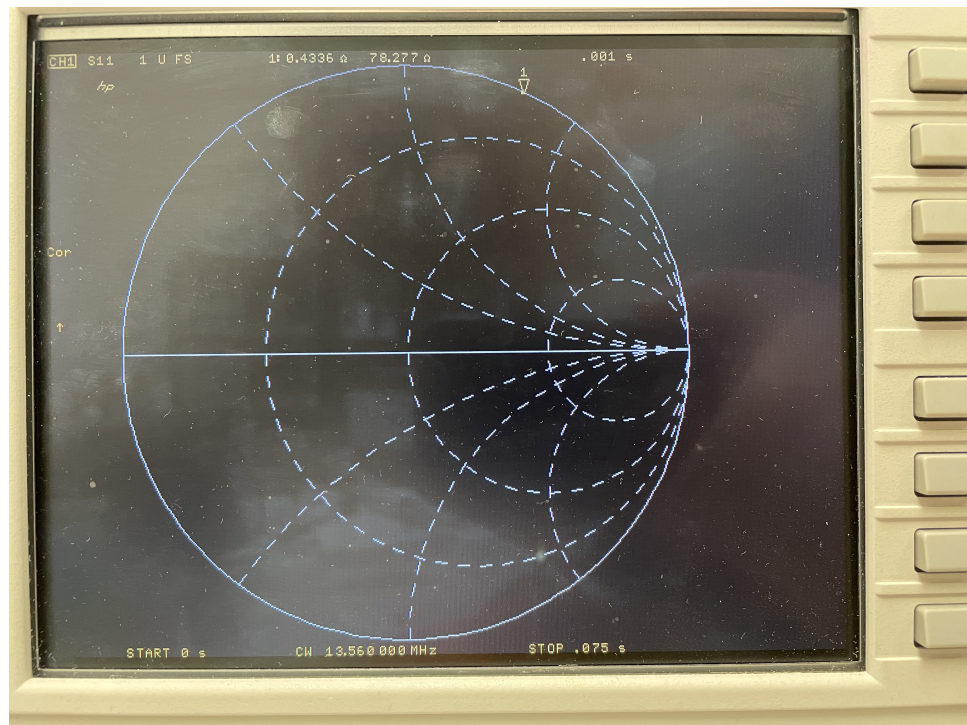


Figure 35: VNA TX/RX Coil Impedance Measurement

Measured inductance using VNA (HP8753E) $0.917 \mu\text{H}$

Measured inductance using LCR meter (HP4262A) $0.97 \mu\text{H}$

Q factor from VNA impedance measurement: 182

M. Experimental Data Collection Sheets with Results

Below are the data collect sheets intended for testing and validation that are filled out in the test sheets below. If a result is not filled it, it is either on account of not being able to conduct the test as planned.

1.) Transmitter Subsystem Data

Transmitter Subsystem Data

Test Description	Test Results
30V power supply voltage nominal 30V +/-2% Measured (TP1)	____ V Pass / Fail
3.3V regulator (U11) test point TP2 nominal voltage 3.3V tolerance +/- 1.5%	3.33 V Pass / Fail
5V regulator (U11) test point TP3 nominal voltage 5V tolerance +/- 1.5%	5.03 V Pass / Fail
TXCO Voltage and Frequency Test	<u>3.69</u> V _{pp} & <u>13.56</u> MHz Pass / Fail
Coil Driver (U11) Output Test	5.80 V _{pp} Pass / Fail
Voltage V _{DS} Test of Class E Amplifier GaN FET	____ V Pass / Fail
Peak to Peak Voltage Load Test	61.60 V Pass / Fail
Transmitter Power Output Test	10 W Pass / Fail
Firmware Upload JTAG Test	Pass / Fail

2.) Receiver Regulators Subsystem Data

Receiver Regulators Subsystem Data

Test Description	Test Results
DC voltage across coil terminals (J2 & J4)	<u>20</u> V Pass / Fail
5V regulator (U11) test point TP3 nominal voltage 5V tolerance +/- 1.5%	<u>5.07</u> V Pass / Fail
3.3V regulator (U11) test point TP2 nominal voltage 3.3V tolerance +/- 1.5%	<u>3.33</u> V Pass / Fail
Firmware Upload JTAG Test	Pass / Fail

3.) Receiver Rectifier Subsystem Data

Receiver Rectifier Subsystem Data

Test Description	Test Results
Transmitter RF Output Test	<u>10</u> W
Coil Placement Distance	<u>0</u> cm
Load Voltage (Test Load: <u>50</u> Ω)	<u>18</u> V Pass / Fail
Load Power	<u>6.46</u> W Pass / Fail
Efficiency	<u>66.23</u> % Pass / Fail

4.) *Charger Subsystem Data*

Charger Subsystem Data

Test Description	Test Results
Set Bench Power Supply Current Limit: 1 A Voltage Limit: 20V	<u>18.6</u> V Supplied
Number of Cells Attached	<u>2</u> Cells
Verify Charge Current Target Current : 3.2 A	<u>3.2</u> A
Peak Charge Current	<u>200</u> mA Pass / Fail
Query Battery Cell of SMBus	Response : <u>20E2</u> Pass / Fail

5.) *SMBus Subsystem Test Data*

SMBus Subsystem Test Data

Test Description	Test Results
Verify Interface Functionality SMBus Read/Write	Pass / Fail
Verify Interface Functionality SMBus Read/Write with MSP430	Pass / Fail
Verify Interface Functionality SMBus LTC4162	Pass / Fail
Target Charge Current SMBus RRC Smart Battery	Pass / Fail
Input Current Limit Target SMBus Read	Pass / Fail

6.) Coil Subsystem Test Data

Coil Subsystem Test Data

Test Description	Test Results
Complex Impedance @ 13.56 MHz	<u>0.43</u> + j <u>78.28</u> Ω
Inductance	<u>0.917</u> μH Pass / Fail
Quality Factor Estimation	<u>182</u> Pass / Fail

VI. BROADER IMPACTS OF THE PROJECT

This product follows FDA, IEE, and government safety regulations. A few ethical issues faced by our design include high voltages across the coil, excessive heat generation within the receiver, and electromagnetic field interference. During simulation stages, high voltages were observed across the coil which increases the risk of electric shock hazard. In order to lower this risk, the coil insulation will adhere to a wider voltage range. Within the receiver, excessive heat generation along high current levels can cause damage to batteries. Therefore, lower charging currents will be used in order to prevent damage. Excessive heat also increases the cost of the project as fans would need to be added. Electromagnetic field interference caused by the transmitter coil can disrupt the charging circuit and cause battery failure. To prevent this issue, additional shielding will be implemented.

During testing stages, minor ethical issues were faced by the design. Within the receiver board, there was an inductor that was not suited for a frequency of 13.56 MHz causing failure, and our rectifier circuits caused more loading than expected when tested with a signal generator. Also, the 48 V to 30 V buck stage microcontroller failed during testing for reasons that are yet to be further investigated by the team. When components get too hot, there's not only a risk of it failing, but also of leaking its chemicals which can be dangerous to human skin and eyes. Therefore, the group will adhere to safety procedures such as wearing personal protective equipment (PPE). Another risk observed here is electrical shock hazard due to the overloading in the circuit. To prevent this, the group will continuously measure the circuit for abnormal values while testing.

Our project's goal is to provide users a low-cost medium-power wireless charger. There are no products like this one in the market for a few reasons: chargers do not supply more than 5W via inductive charging, an existing industrial unit with same purposes as our product is priced at about \$2000 USD, and available wireless chargers are limited for charging a single type of device only. With our product, users will be able to charge a standard battery type and integrate it in their own design or use it for stand-alone operations. Our product communicates electronic circuits, electromagnetic fields, digital

systems, and microprocessors concepts to the audience. This product will not only be a low-cost wireless charger option, it will also provide customers with a charger for mobile devices of all shapes and sizes, no wiring exposure, apply greater range of tolerance for misalignment when charging, and provide a compact charging area.

Our product will be useful to robotics hobbyists and inventors who are developing new products that require wireless charging, serve to influence kids and teenagers interested in STEM, can be used for research and development, and capitalized in OEM market.

Ethical and Professional Considerations

Public Health	<ul style="list-style-type: none"> · Medical Equipment RF Exposure · Electrical Shock · Chemical Exposure
Safety and Wellness	<ul style="list-style-type: none"> · RF Bandwidth Jamming · Electrical Shock · Chemical Exposure
Global Factors	<ul style="list-style-type: none"> · International Governing Bodies · Sourcing Restrictions · Inter-Market Penetrability
Societal Factors	<ul style="list-style-type: none"> · Open-Source Capitalization · STEM Educational Resources · Professional Organizations · Customer Privacy & Security
Environmental Factors	<ul style="list-style-type: none"> · Chemical Pollution · User Environmental Awareness · Emergency Shut Off Cases
Economic Factors	<ul style="list-style-type: none"> · Open-Source Capitalization · Specialty Clientele · Rapid Agile-Deployment · Light-Weight Production

VII. CONCLUSION

Our current prototype successfully demonstrates that our wireless resonant power transfer system is capable of approaching our specified levels of efficiency, although not at our originally specified power. Experimental data gathered from testing was used to make multiple design improvements that are reflected in our final test results. A full design revision with the benefit of this experience in wireless power transfer might be expected to yield even greater efficiency and power transfer capability.

Our project goals did not merely specify a wireless power transfer system, but a fully developed product suitable for consumer or OEM use. Many of these specifications have not been met. Most show enough progress that the failings can be traced to correctable design errors, unexpected hardware failures, or errors in resource allocation.

The 48 V to 30 V buck stage control integrated circuit on the transmitter board self-destructed for as-yet unknown reasons. No obvious design errors were found. We performed no further diagnosis and completed our tests with a bench power supply.

Initial tests of the battery charging circuit were successful. A test battery of two fully charged 18650 cells was correctly detected and not charged further. After partial discharge the charger entered a constant-voltage charging mode and charged the battery at a slowly decreasing current of approximately 1 A. The receiver board continued to operate on battery power when simulated wireless power was removed. Further tests revealed that the charge controller was incorrect for Li-Ion chemistry. The controller was replaced but failed to detect connected batteries. We determined that the cause was inadequate grounding and excessive trace length to the output capacitor. Hand reworking succeeded in making the charger operational at less than full power. A full solution will require a PCB redesign.

An unexpected problem we encountered with the charging circuit was a failure to initiate charging when powered by the resonant link. The cause was determined to be inadequate regulation of the rectifier output voltage. The inrush current at the start of constant current charging causes a voltage drop that can trigger the LTC4162 to shut down. This issue is resolved in the prototype with the addition of a large (3.3 mF) capacitor to the rectifier bridge output.

The output of the bridge rectifier can reach unacceptably high voltages during no-load conditions before charging begins. A provisional solution is to maintain a $50\ \Omega$ resistive load on the output at all times. While this solution reduces efficiency, it permits testing of the charger pending the design of a suitable power regulation circuit.

Initial testing of the wireless power transfer resulted in a period of successful inductive power transfer and a brief success in achieving a resonant link. A failure on the transmitter board was traced to an inductor that was not suitable for operation at 13.56 Mhz. The inductor and damaged components were replaced and testing continued. A resonant link was achieved between the transmitter and receiver, but an unexpected transient destroyed the transmitter's amplifier transistor. Two other transistors were damaged by transients that we identified as high drain-source peak voltages that occurred when the transmitter coil was powered without any load on the receiver subsystem. We replaced the transistor successfully with more robust model (PN: TP65H480G4JSG-TR) with a higher drain-source breakdown voltage than the original transistor (PN: EPC2019). Unfortunately the greater capacity came at the cost of a relatively high drain-source on-resistance ($0.5\ \Omega$) compared to the drain-source on-resistance of the EPC2019 ($50\ m\Omega$).

The transmitter subsystem efficiency is approximately 93% and surpasses our original specifications. We are unable to meet our specified transmitting power due to our design's inability to tolerate the very high voltages that occur at resonant, no-load conditions. In order to proceed with our tests it is necessary to reduce the input voltage to 13.8 V for a maximum 10 W power transmission.

A future design capable of meeting our original specifications must tolerate high voltage peaks safely. The ideal Class E amplifier transistor will have a very small on-resistance and a drain-source breakdown voltage of 650 V or more. Since a short circuit in the receiver subsystem can cause high drain-source voltage and high current in the class E amplifier, the power supply must be capable of limiting current as needed to protect the transistor and other components. A revised design must provide for safe functioning and failure states while operating at the high voltages generated by 30 W resonant power transfer.

During the tests, the team observed that a strong magnetic field generated by the transmitter coil creates a disturbance in some parts of the transmitter and receiver circuit. Analog to digital conversion results are very noisy when the transmitter is on. The problem is partly resolved by performing moving average filtering on all measurements sampled by the ADC on both transmitter and receiver subsystems. EMI shielding should be considered in future revisions to lower the effects of the strong magnetic field on both internal circuitry and other nearby electronics.

Most of our wireless power losses were caused by poor receiver efficiency. The power transfer is performed at a high frequency (13.56 MHz). At high-frequency performance of the large power diodes becomes compromised due to junction capacitance. Large power diodes have a large junction area which results in larger junction capacitance than the junction capacitance in small diodes. Replacing these diodes with low power Schottky diodes (PN: RB168MM100TFTR) produced a dramatic improvement in efficiency at the cost of a maximum peak reverse voltage of 100 V and 1 A forward current.

For future rectifier designs, a synchronous rectifier may be a better solution than the diode rectifier bridge. Diode capacitance and forward voltage drop impose heavy costs in efficiency, and these phenomena are unavoidable in our present design. A synchronous rectifier circuit requires MOSFET gate drivers and is more complex, but it offers the possibility of achieving efficiencies at moderate to high power that would be impossible with diode rectifiers.

Our firmware was not completed in time and only minimal functions are available for testing. The firmware successfully reads power transmission data from the ADC inputs and reports it via the LCD. The transmitter firmware can determine if there is a resonant link with the receiver coil and automatically pause transmission if the link is lost. The bluetooth modules function correctly but remain unused in the current firmware version. All hardware issues were overcome that would prevent the firmware from being completed to our original specifications.

The firmware development was not given sufficient attention to meet all specifications with our programmers' primary efforts split between documentation and the hardware. The firmware ran into unexpected problems in the transition between the test board and the PCB prototype with respect to changes in ports and pin numbers as well as ADC functionality. We accept the recommendation that earlier testing with less mature prototypes would have helped the team overcome such issues earlier on. The operation of I²C and UART peripherals likewise could have been begun earlier with either further allocation of time to firmware or early prototyping.

If provided the opportunity, we would make our next prototype with a few minor and one major change in our hardware design process. The wireless power transfer circuit, being mostly a custom design, ideally would have been prototyped and tested much earlier in the design process. Our initial tests quickly brought to light certain design issues that would be fixed in its successive prototype. Designing the wireless power system on separate PCB's would have made it possible to perform multiple test and redesign iterations separately from the support circuitry.

More minor changes would include accepting the more limited selection of 3.3 V LCD's and deleting the 5 V rail and support circuitry. The 48V transmitter power supply and buck stage was chosen to minimize current and provide headroom for adjustments to the wireless transmitter voltage, but it now appears that a 30V supply with no further conversion would be sufficient.

If another team were to take up this project, we would recommend attention be given to the Hardware as mentioned above. However, certain questions pertaining to the firmware have been raised after implementing firmware onto the experimental hardware. We are uncertain as to the benefit vs complexity estimation of a minimal realtime operating system (RTOS) such as our scheduler as opposed to the actual risks that the product possesses if compiled in a basic loop that utilizes interrupts to handle extraordinary or dangerous events. The firmware still requires attention to the SMBus as well as the Bluetooth TX/RX UART communications in order to fulfill this product's specifications, especially those permitting additional safety features. The recommendation for providing directions to a user device, such as a robot, would be to do so over the auxiliary TX/RX UART Ports. All code is open-source and available on the team's GitHub repository, https://github.com/gibbs212521/HEC_2_senior_design. Lastly, the creation of a User's Guide would be the final task remaining in the project to bring it to completion.

VIII. REFERENCES

SOFTWARE REFERENCES

Block diagrams were rendered in Windows Visio Standard 2019.

Multisim circuits simulated in NI Multisim V.14.2 2019.

PCB Schematics rendered in Altium-365.

CAD Drawings rendered in NanoCAD.

DESIGN REFERENCES

- [1] “Standard High Power System”. In: *WIBOTIC Products* (2021). URL: <https://www.wibotic.com/products/high-power-dev-kit/>.
- [2] “Anatomy of a Create 2”. In: *iRobot Education: Create 2: Create | Advanced* (2021).
- [3] “MSP430FR599x, MSP430FR596x Mixed-Signal Microcontrollers”. In: *Texas Instruments Inc. SLASE54C - MARCH 2016 - REVISED AUGUST 2018* (2018), pp. 1–172. URL: https://www.ti.com/lit/ds/symlink/msp430fr5994.pdf?ts=1604041478538&ref_url=https%25A%252F%252Fwww.ti.com%252Fproduct%252FMSP430FR5994.
- [4] *Texas Instruments MSP430FR5994 Tool Description*. URL: <https://www.ti.com/tool/MSP-EXP430FR5994>.
- [5] “TPSM265R1 65-V Input, 100-mA Power Module with Ultra-Low IQ”. In: *Texas Instruments Inc. SNVSBF6A - OCTOBER 2019 - REVISED DECEMBER 2019* (2019), pp. 1–32. URL: https://www.ti.com/lit/ds/symlink/tpsm265r1.pdf?ts=1606735419804&ref_url=https%25A%252F%252Fduckduckgo.com%252F.
- [6] “TPS54160 1.5-A, 60-V, Step-Down DC/DC Converter with Eco-mode”. In: *Texas Instruments Inc. SLVSB56C - MAY 2012 - REVISED FEBRUARY 2014* (2014), pp. 1–58. URL: <https://www.ti.com/lit/ds/symlink/tps54160.pdf>.
- [7] *Conductor Bulk Resistivity & Skin Depths*. RF Cafe. URL: <https://www.rfcafe.com/references/electrical/cond-high-freq.htm>.

APPENDIX A: CODES, STANDARDS, AND CONSTRAINTS

Table 24: Relevant Codes and Standards

Organization	Engineering Standards
IEEE	<p>IEEE C95.1-2005 This standard defines exposure limits to the electromagnetic field This standard is adopted in many safety standards.</p> <p>IEEE 1625-2008 Standard for rechargeable batteries for multicell mobile computing devices.</p> <p>IEEE 802.15.1 Bluetooth standard</p>
Government	<p>FCC Part 15, FCC part 18 RF Power levels and communication links are defined by FCC Part 15 and Part 18. The RF transmitter power level limits in the US are much higher than in some other countries.</p> <p>FDA: 21 CFR 1000.15 FCC: KDB 680106 D01 Both standards define exposure limits to electromagnetic fields. The limits will be satisfied if the transmitter power is limited to 5W. Higher power levels are allowed if proper safety measures are implemented.</p>
International	<p>EN 55011:2016 This standard defines limits for unwanted emissions in the RF spectrum above 30MHz. The proposed WPT charger system must follow limitations for unwanted emissions.</p>

APPENDIX B: USER'S MANUAL AND INSTRUCTIONS

<User's Manual Not Written>

APPENDIX C: COURSEWORK RELATED KNOWLEDGE AND SKILLS

Table 25: Coursework Related Knowledge and Skills Table

Courses	Knowledge / Skills
EENG 3106 - Circuit Analysis I Lab	Laboratory Technique
EENG 3305 - Linear Circuits Analysis II	Circuit Analysis (RLC Circuits)
EENG 4109 - Electronic Circuit Analysis II Lab	Laboratory Technique
EENG 4309 - Electronic Circuit Analysis II	Amplifier Design Electronic circuit-analysis (amplifiers and rectifier circuits)
EENG 3303 - Electromagnetic Fields	Electromagnetic Theory Inductor parameters (inductance and resistance calculations based on shape and wire cross-section area and length.)
EENG 3302 - Digital Systems	Digital Troubleshooting
EENG 3307 - Microprocessors	Microcontroller Programming
EENG 4350 - Advanced Microprocessors	Microcontroller Programming

APPENDIX D: RECEIVER PCB SCHEMATICS

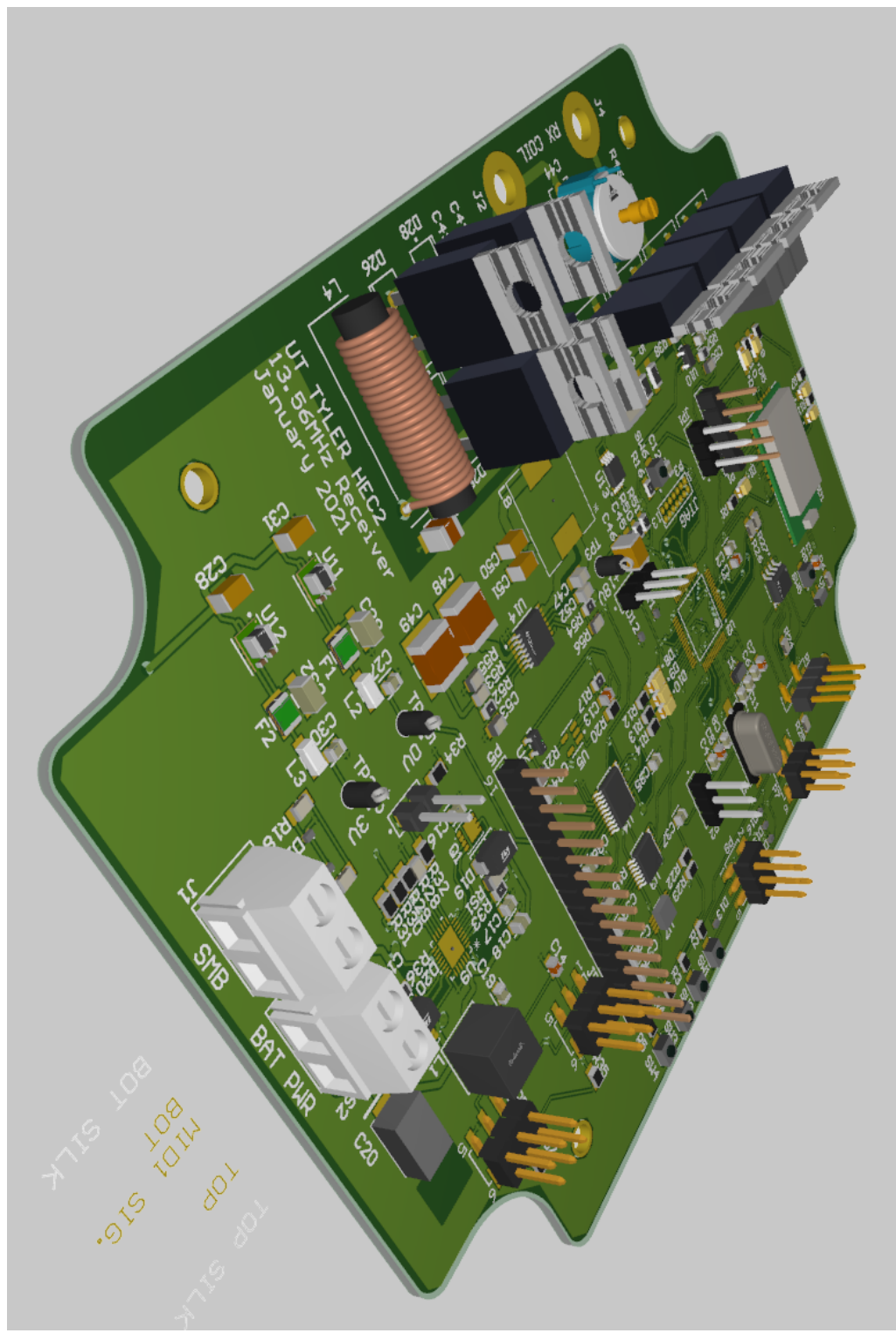
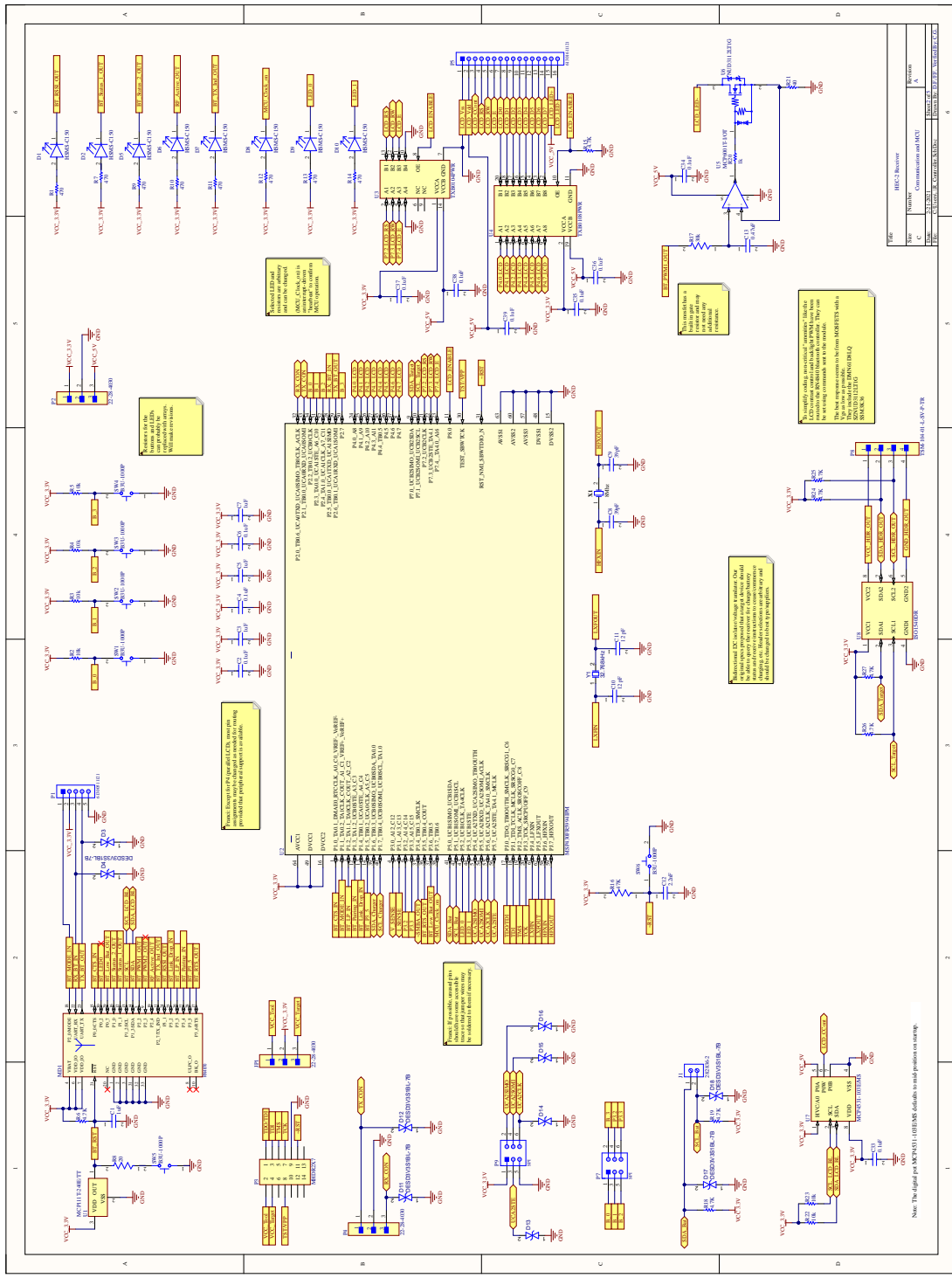
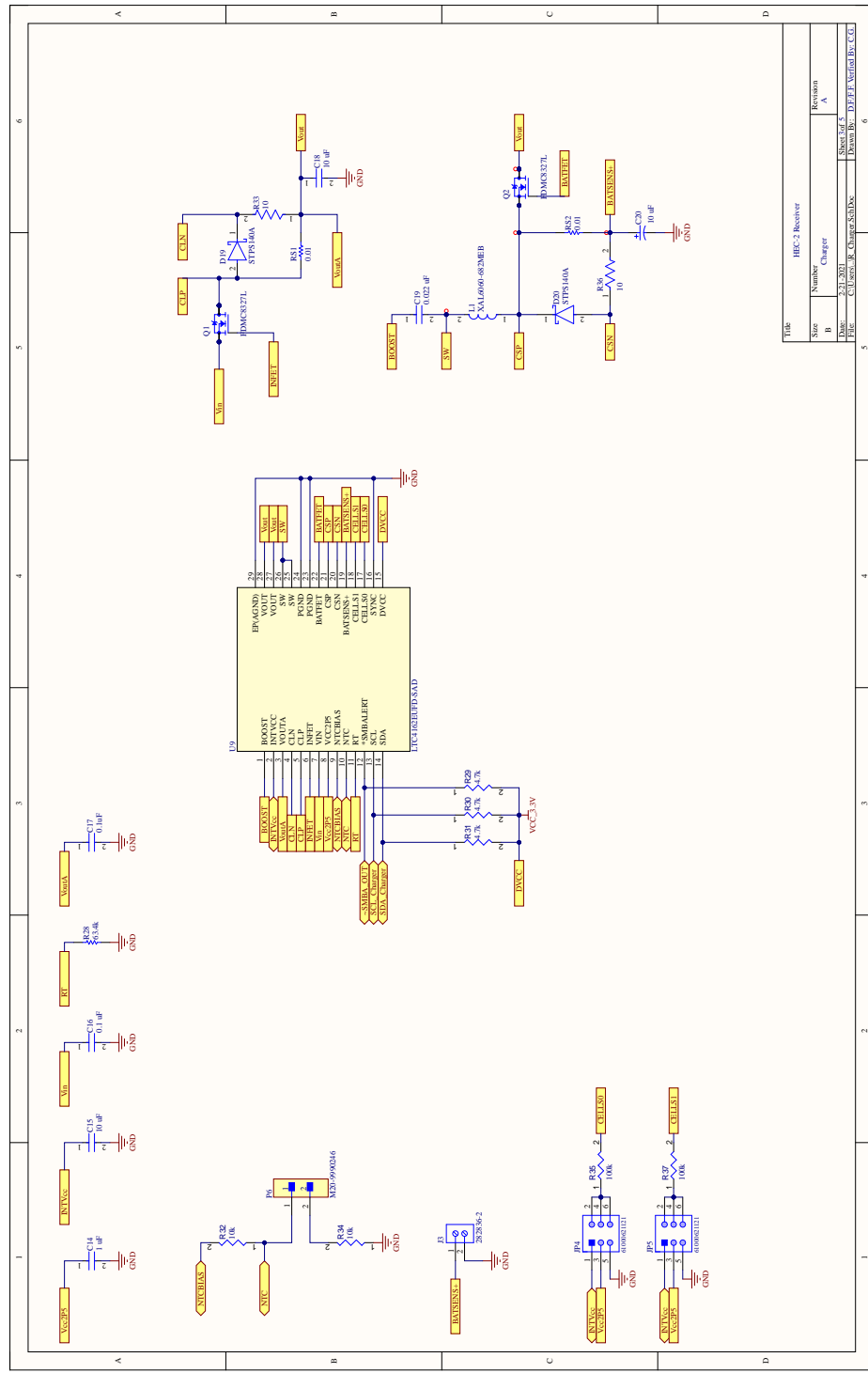


Figure 36: Isometric Image of Receiver PCB

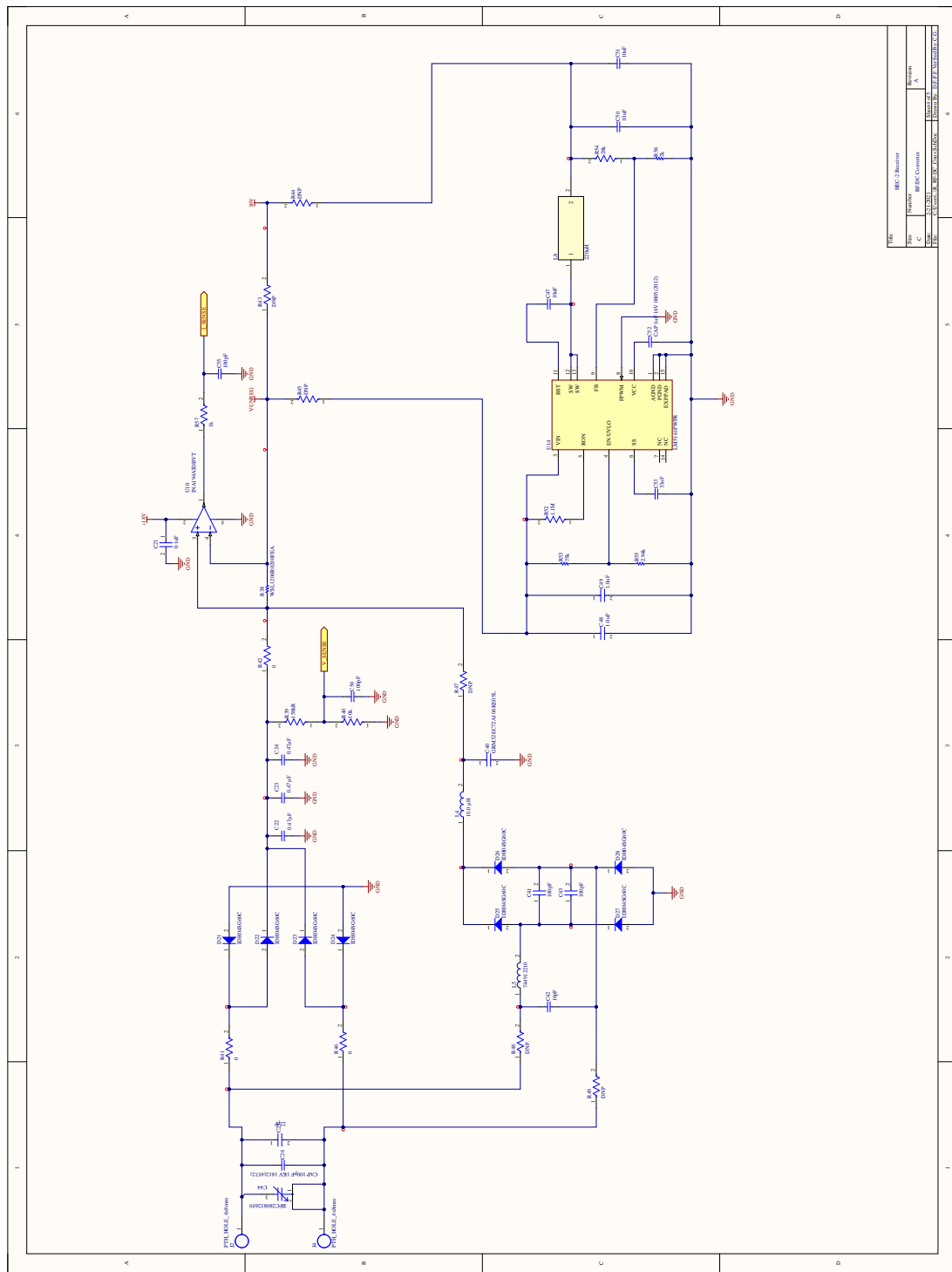
1. Receiver Controller



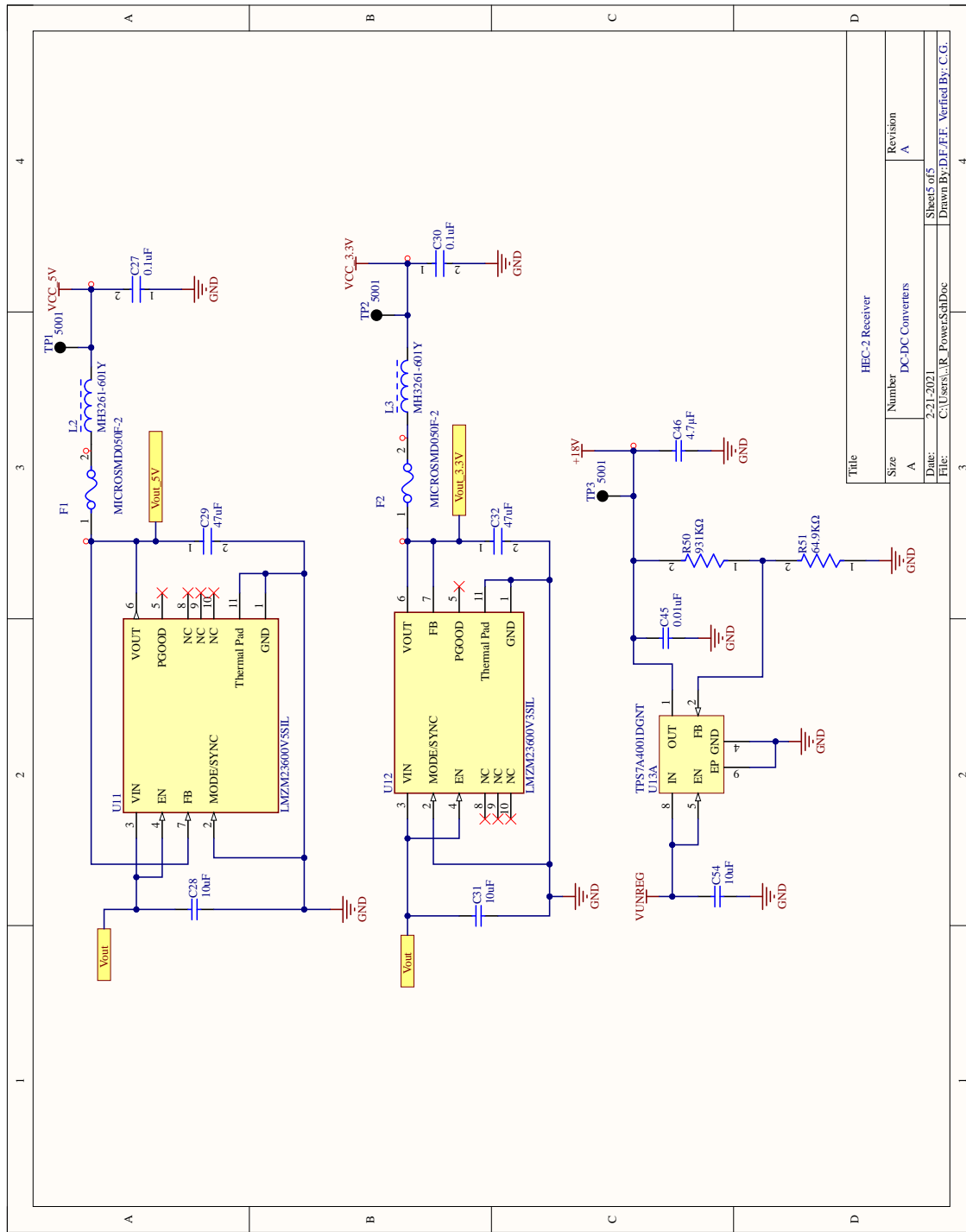
2. Receiver Battery Charger



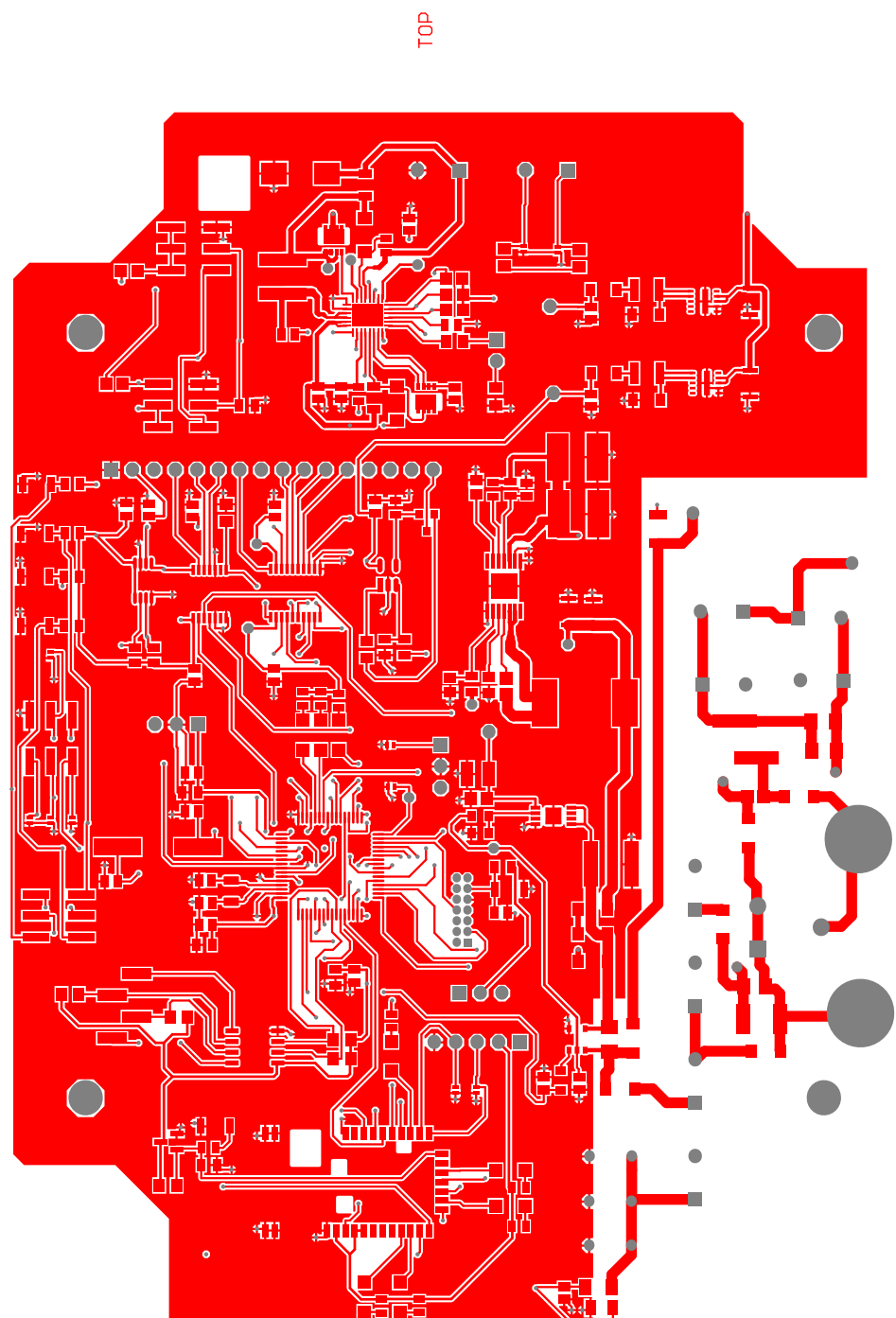
3. RF/DC Converter



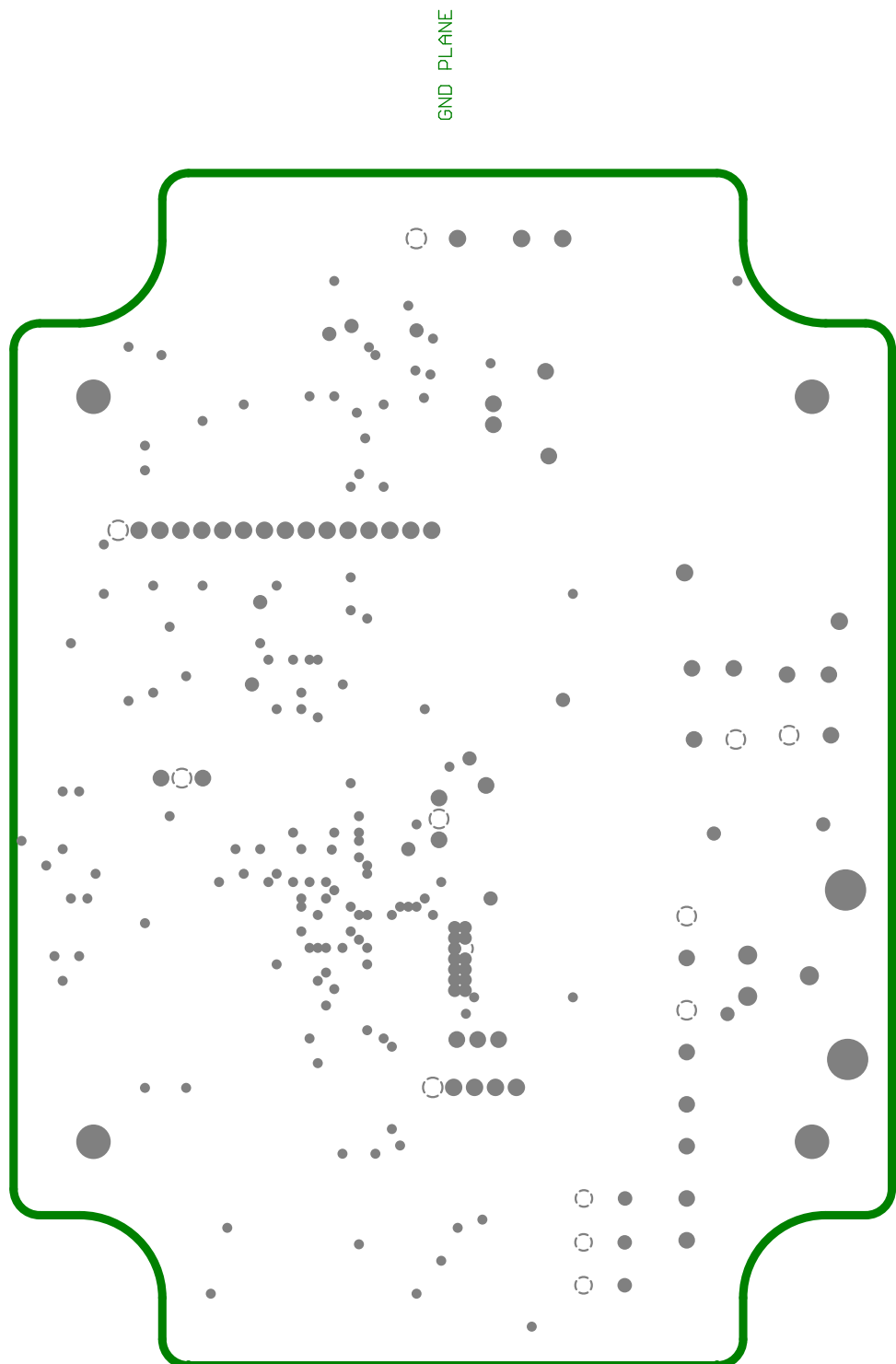
4. DC/DC Converter



5. Top Copper Layer



6. Top Silk Layer



APPENDIX E: TRANSMITTER PCB SCHEMATICS

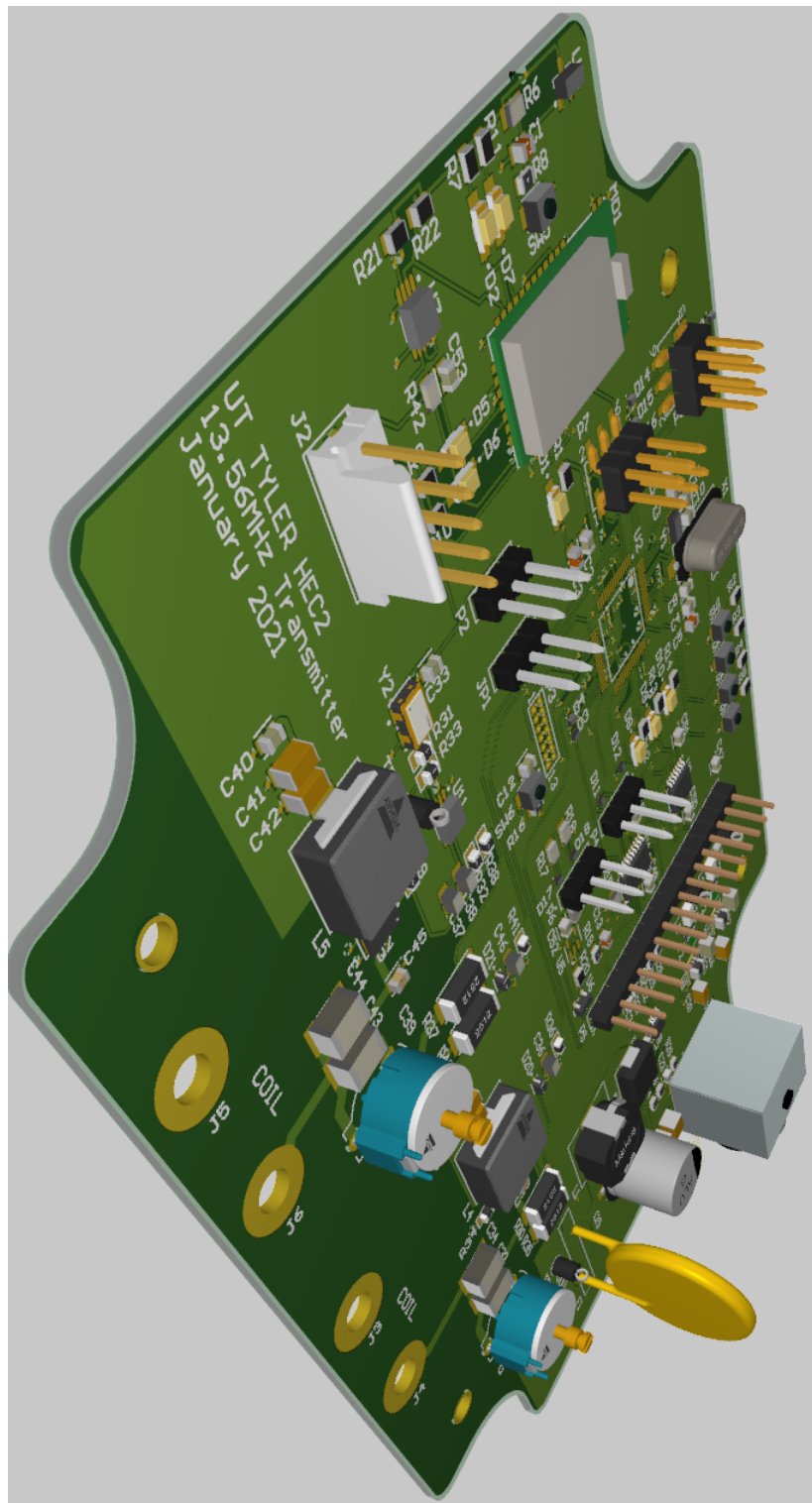
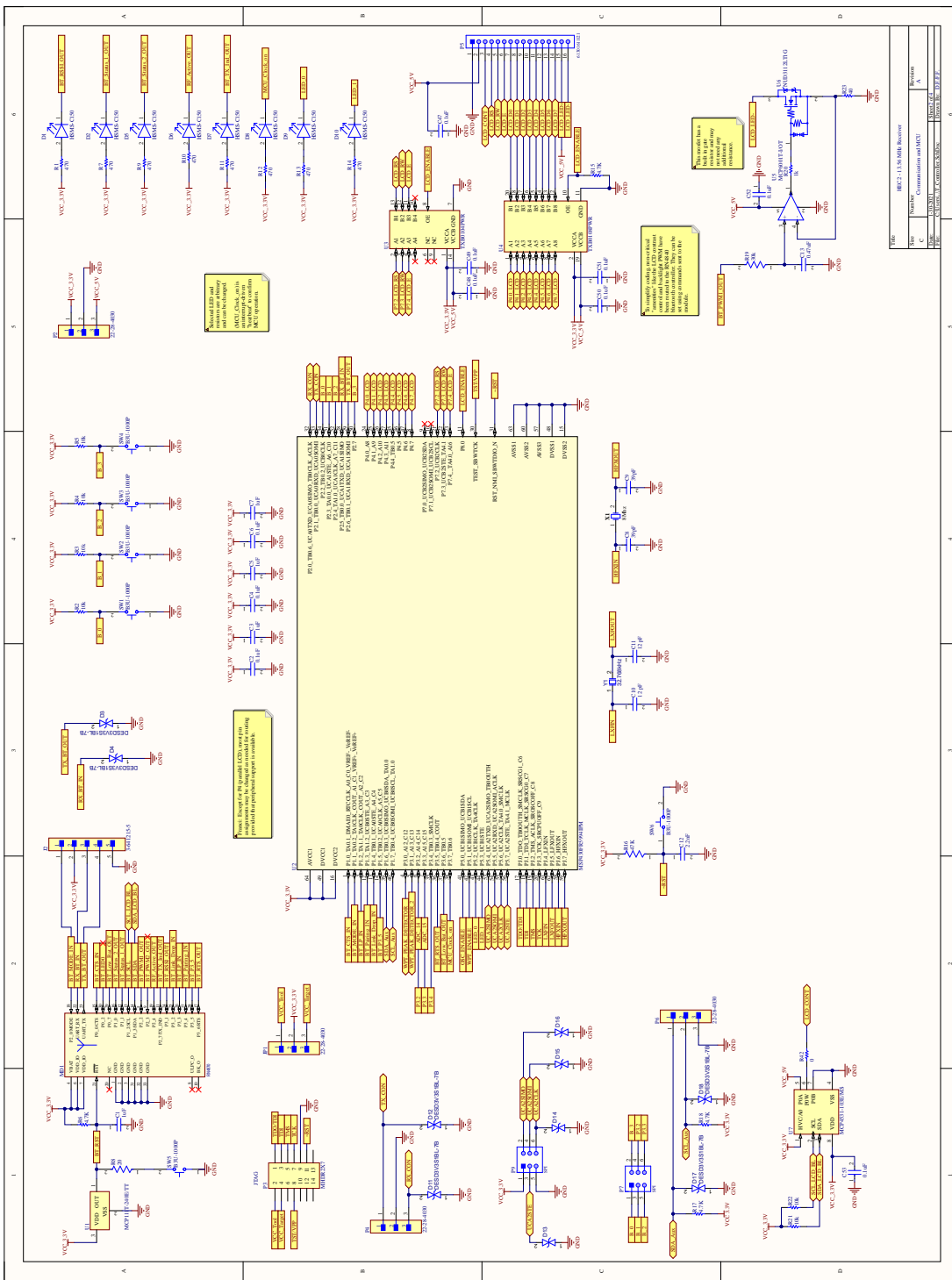
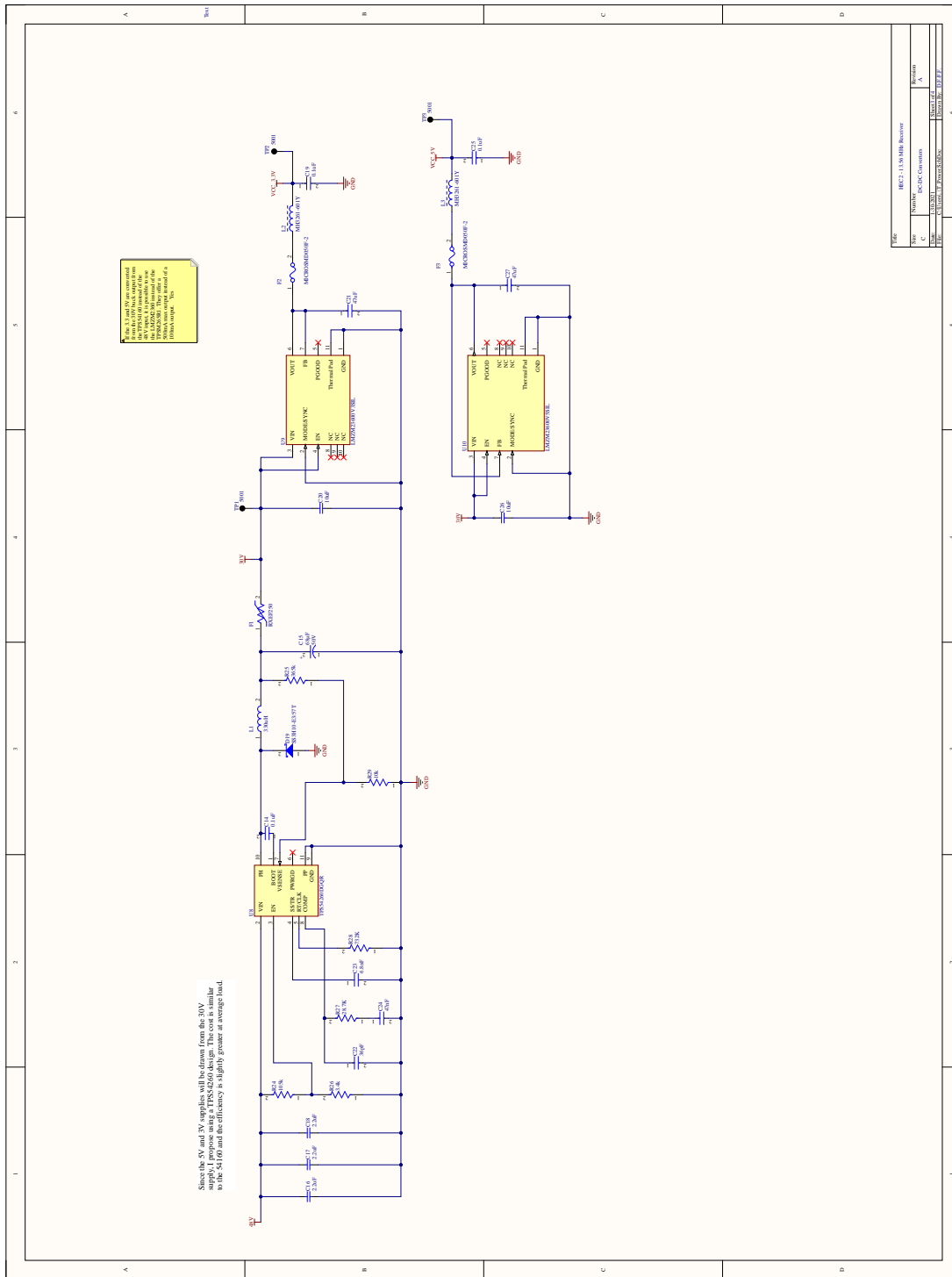


Figure 37: Isometric Image of Transmitter PCB

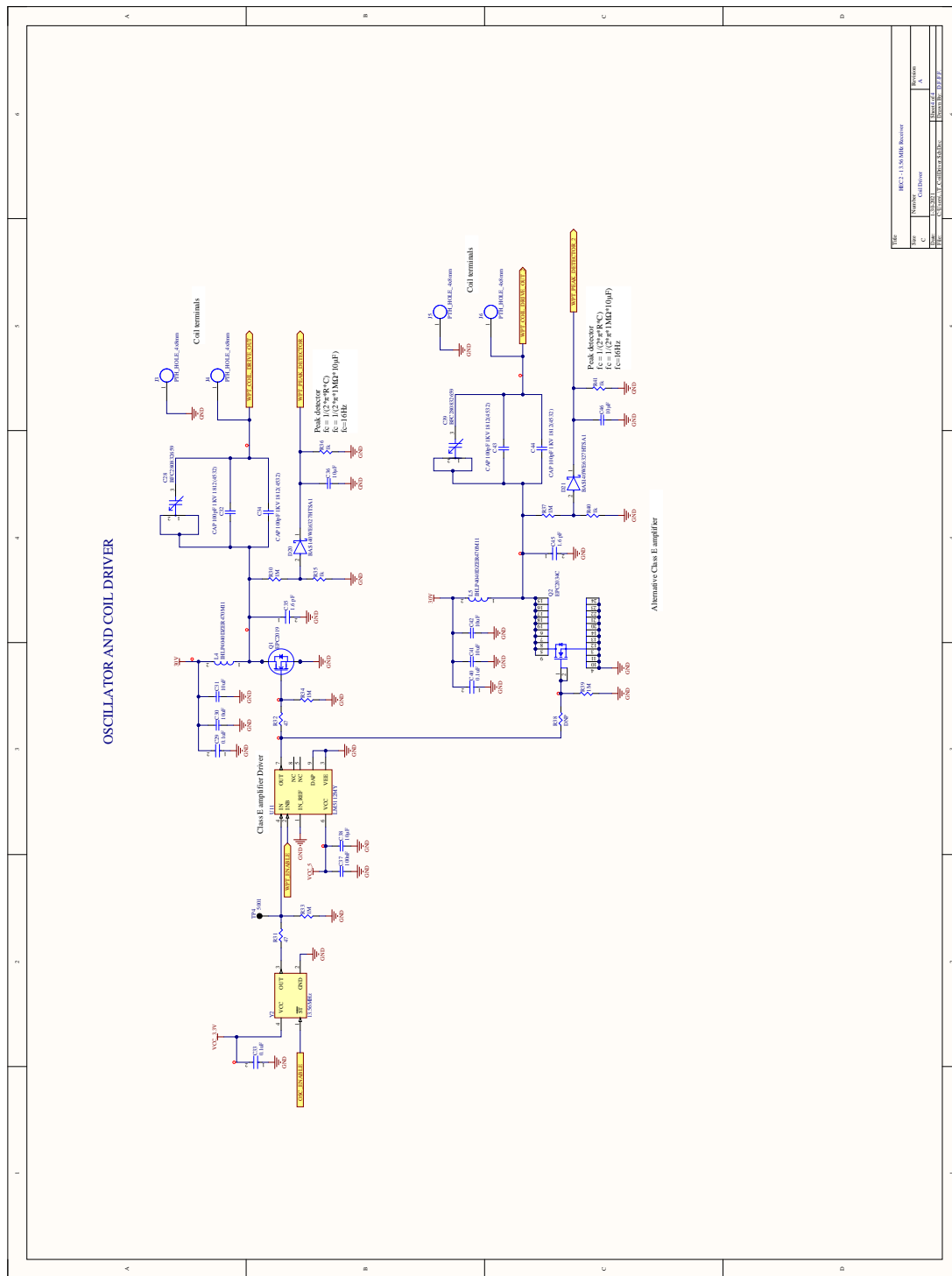
1. Transmitter Controller



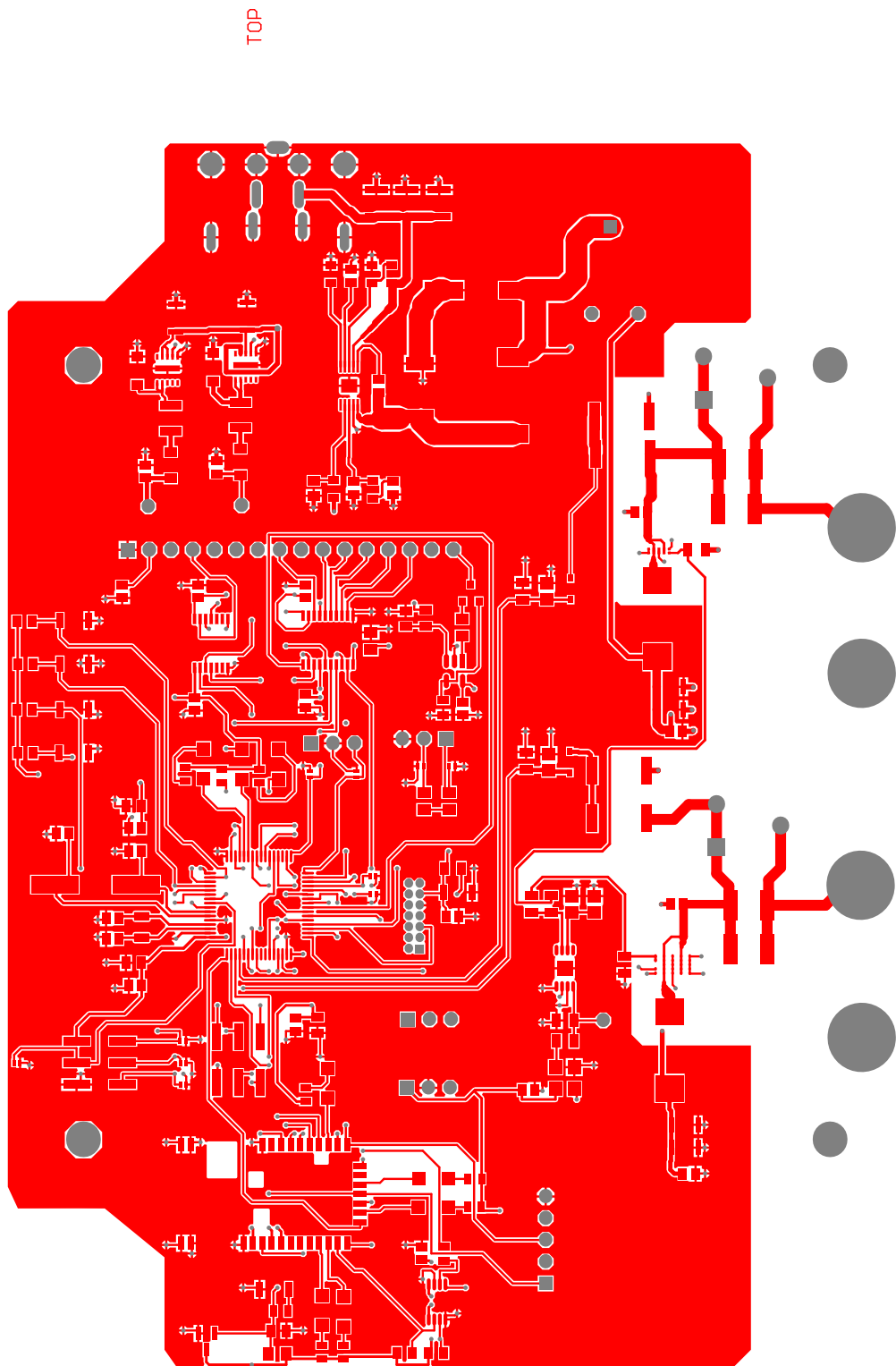
2. DC/DC Converter



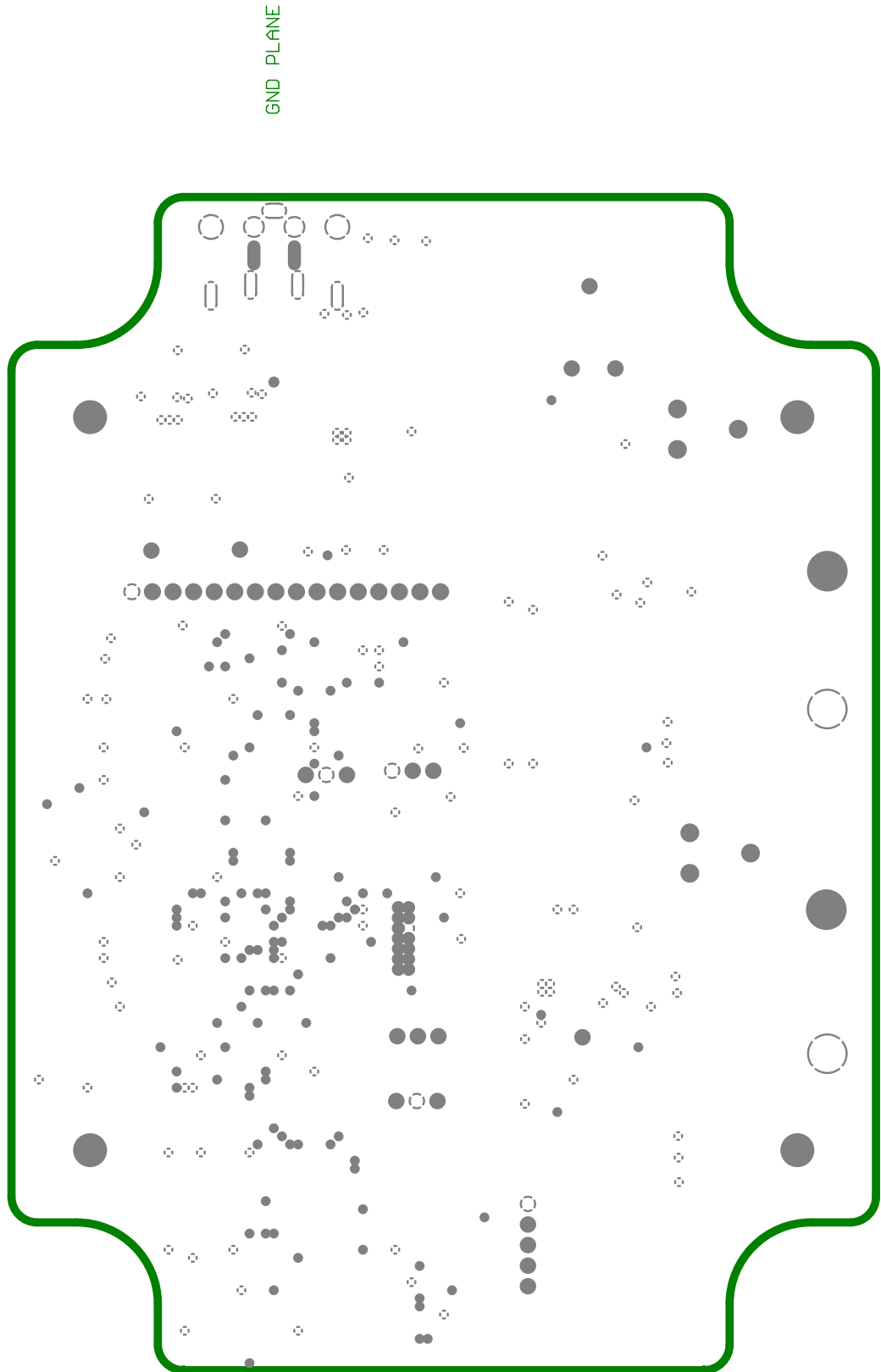
3. Coil Driver



4. Top Copper Layer



5. Top Silk Layer



APPENDIX F: RECEIVER BOM

ITEM	QTY	REFERENCE	DESCRIPTION	WFG	INFO/PIN	VENDOR	NOTE#	Notes/URL
		HEC Receiver						
		A						
		Lead-Free						
1	4	C1, C3, C5, C7	Multilayer Ceramic Capacitors MuCC - SMD/SMT	Yageo	CC0805KX7R6SB105	Mouse	663	https://www.mouser.com/datasheet/247/1/GMIC_X7R_6_3Vto3V_1s_15402.pdf
2	14	C2, C4, C5, C7, C11, C12, C13, C15, C17, C19, C21, C23, C24, C25, C26, C27, C29, C35, C39	Multilayer Ceramic Capacitors MuCC - SMD/SMT	KEMET	CB0805C10AKACTU	Mouse	80-C0805C1045R	https://www.mouser.com/datasheet/212/KEM_C1002_X7R_SMB_1102033.pdf
3	2	C8, C9	Multilayer Ceramic Capacitors MuCC - SMD/SMT	KEMET	CB0805C305GACTU	Mouse	80-C0805C3005G	https://www.mouser.com/datasheet/212/KEM_C1003_COG_S_MSD_101588.pdf
4	2	C10, C11	Multilayer Ceramic Capacitors MuCC - SMD/SMT	KEMET	CB0805C105GACTU	Mouse	80-C0805C12095G	https://www.mouser.com/datasheet/212/KEM_C1003_COG_S_MSD_101588.pdf
5	1	C12	Multilayer Ceramic Capacitors MuCC - SMD/SMT	KEMET	CB0805C227HAC1TU	Mouse	80-C0805C2229H	https://www.mouser.com/datasheet/212/KEM_C1007_X8R_UTRA_B5C_SMD102702.pdf
6	1	C13	Multilayer Ceramic Capacitors MuCC - SMD/SMT	KEMET	CB0805C305KX7R7B07A	Mouse	80-C0805C305KX7R7B07A	https://www.mouser.com/datasheet/212/KEM_C1003_X7R_S_MSD_101582.pdf
7	1	C14	Multilayer Ceramic Capacitors MuCC - SMD/SMT	Yageo	CC0805KX7R6SB105	Mouse	663-C0805KX7R6SB105	https://www.mouser.com/datasheet/247/1/GMIC_X7R_6_3Vto3V_1s_15402.pdf
8	2	C15, C18	Multilayer Ceramic Capacitors MuCC - SMD/SMT	KEMET	CB0805C305KX7R7B07A	Mouse	80-C0805C108K8P	https://www.mouser.com/datasheet/212/KEM_C1006_X8R_MSD_101349.pdf
9	1	C16	Multilayer Ceramic Capacitors MuCC - SMD/SMT	KEMET	CB0805C1045RACTU	Mouse	80-C0805C1045R	https://www.mouser.com/datasheet/212/KEM_C1002_X7R_S_MSD_1012033.pdf
10	1	C19	Multilayer Ceramic Capacitors MuCC - SMD/SMT	KEMET	CB0805C227HAC1TU	Mouse	80-C0805C2229H	https://www.mouser.com/datasheet/212/KEM_C1003_COG_S_MSD_101588.pdf
11	1	C20	Multilayer Ceramic Capacitors MuCC - SMD/SMT	KEMET	TAB106K050AT	Mouse	80-TAB106K050AT	https://www.mouser.com/datasheet/212/KEM_C1005_X7R_S_MSD_101556.pdf
12	1	C25	Multilayer Ceramic Capacitors MuCC - SMD/SMT	Murata	GRM12A17BA220W103D	Mouse	81-CER12A17BA220W103D	https://www.mouser.com/datasheet/212/KEM_C1003_X7R_S_MSD_101582.pdf
13	1	C26	Multilayer Ceramic Capacitors MuCC - SMD/SMT	Vishay	V1812A010KGAT	Mouse	77-V1812A010KGAT	https://www.mouser.com/datasheet/247/1/178415.pdf
14	4	C8, C11, C30, C51	Multilayer Ceramic Capacitors MuCC - SMD/SMT	TDK	CB126511H06K100A8	Mouse	80-C126511H06K100A8	https://www.mouser.com/datasheet/212/KEM_C1003_X7R_S_MSD_101582.pdf
15	2	C29, C32	Multilayer Ceramic Capacitors MuCC - SMD/SMT	TDK	C2165R1676M160AC	Mouse	81-C2165R1676M	https://www.mouser.com/datasheet/212/KEM_C1003_X7R_S_MSD_101582.pdf
16	1	C40	Multilayer Ceramic Capacitors MuCC - SMD/SMT	Murata	GRM12E72A105K055	Mouse	81-CRM12E72A105K055	https://www.mouser.com/datasheet/212/KEM_C1003_X7R_S_MSD_101582.pdf
17	1	C42	Multilayer Ceramic Capacitors MuCC - SMD/SMT	Vishay	V1812A010KGAT5Z	Mouse	77-V1812A010KGAT5Z	https://www.mouser.com/datasheet/247/1/178317.pdf
18	1	C44	Multilayer Ceramic Capacitors MuCC - SMD/SMT	Vishay	BCR08126569	Mouse	594-221208-2659	https://www.vishay.com/doc/28538
19	1	C46	Multilayer Ceramic Capacitors MuCC - SMD/SMT	KEMET	C1210475K5RAC1TU	Mouse	80-C1210475K5RAC1TU	https://www.mouser.com/datasheet/212/KEM_C1013_X7R_FT_Cap_SMD_103280.pdf
20	1	C47	Multilayer Ceramic Capacitors MuCC - SMD/SMT	AuV	00510A031A7A	Mouse	801-C0510A031A7A	https://www.mouser.com/datasheet/247/1/551274.pdf

21	2 C48, C49	Multilayer Ceramic Capacitors MLCC - SMD/SMT Multilayer Ceramic Capacitors MLCC - SMD/SMT 220uF 50Vt X7R 10%	GRM555DR72E105KWN01L Murata	GRM555DR72E105KWN01L Mouse	81-GRM555DR72E105K 5MW01_01-398382.pdf	https://www.mouser.com/datasheet/2/281/j/GRM55DR72E105KWN01L_01-398382.pdf	\$1.48
22	1 C52	Multilayer Ceramic Capacitors MLCC - SMD/SMT Multilayer Ceramic Capacitors MLCC - SMD/SMT 16V 1uF X7R 0805 10%	KEMET	C0805C105K4RACTU	89-C0805C105K4R	https://www.mouser.com/datasheet/2/212/kem-c1002_x7r_s_md1102033.pdf	\$0.13
23	1 C54	Multilayer Ceramic Capacitors MLCC - SMD/SMT Multilayer Ceramic Capacitors MLCC - SMD/SMT 100V 10uF X7R 220uF Tol High CV	AVX	22201C106MAT2A	581-22201C106MAT2A	https://www.mouser.com/datasheet/2/40/YTRD/electric-hem-cx-c55mfr2021-1827675.pdf	\$1.83
24	8 D1, D2, D5, D6, D7, D8, D9, D10	Standard ESD - SMD Standard Ld53 - SMD Red Diffused 656nm 10mcd	Broadcom Limited	H5K5-C150	630-15M5-C150	https://www.mouser.com/datasheet/2/1678/av02-0551-en-as-hsm-cx-c55mfr2021-1827675.pdf	\$0.41
25	5 D3, D11, D12, D17, D18	ESD Suppressors / TVS Diodes ESD Suppressors / TVS Diode Low Cap BiTVS 10pF 3.3V 8.8Vb 25kV ESD Suppressors / TVS Diodes ESD Suppressors / TVS Diode Low Cap BiTVS 10pF 3.3V 8.8Vb 25kV Diodes Incorporated	Diodes Incorporated	DES3VS1BL7B	621-DESDVS1BL7B	https://www.mouser.com/datasheet/2/115/DES3VS1BL7B_321080.pdf	\$0.29
26	5 D4, D3, D14, D15, D16	ESD Suppressors / TVS Diodes ESD Suppressors / TVS Diode Low Cap BiTVS 10pF 3.3V 8.8Vb 25kV Schottky Diodes & Rectifiers Schottky Diodes & Rectifiers 2.0Amp 40Volt	STMicroelectronics	STPS140A	531-STPS140A	https://www.mouser.com/datasheet/2/389/rtp140-1851573.pdf	\$0.44
27	2 D19, D20	D21, D22, D23, D24, D25, D26, D27, Rectifiers SiC D1D25 Resettable Fuses - PPTC Resettable Fuses - PPTC 5A 13.2V 40A iMax	Infineon	IDH045G60CKXS2	621-DESDVS1BL7B	https://www.mouser.com/datasheet/2/115/DES3VS1BL7B_321080.pdf	\$0.29
28	8 D28	D21, D22, D23, D24, D25, D26, D27, Schottky Diodes & Rectifiers Schottky Diodes & Rectifiers SiC D1D25 Resettable Fuses - PPTC Resettable Fuses - PPTC 5A 13.2V 40A iMax	Littelfuse	MICROSM050F-2	650-MICROSM050F-2	https://www.mouser.com/datasheet/2/40/littelfuse_ptc_mic_007960loc19e-specification-on-standard-or-control-partctx282385-2.pdf	\$0.47
29	2 F1, F2	Fired Terminal Blocks Fired Terminal Blocks 5.0MM PCB MOUNT 2P	TE Connectivity	282836-2	571-22-28-04030	https://www.mouser.com/datasheet/2/276/0022284030_pcb_headers-228162.pdf	\$0.80
30	2 J1, J3	Headers & Wire Housing Headers & Wire Housings 3P VERT HEADER Sn	Molex	22-28-4030	538-22-28-04030	https://www.mouser.com/datasheet/2/445/61/000621121-1717892.pdf	\$0.16
31	2 J2, J4	Headers & Wire Housing Headers & Wire Housings 3P VERT HEADER Sn	Molex	6100621121	710-61/000621121	https://www.mouser.com/datasheet/2/597/yal660x-70658.pdf	\$0.93
32	3 IP1, P2, P4	Headers & Wire Housing Headers & Wire Housings 3P VERT HEADER Sn	Molex	XA16060-682/MEB	994-XA16060-682/MEB	https://www.mouser.com/datasheet/2/54/m-777565.pdf	\$2.58
33	2 IP4, IP5	Housings WRPID 2.54mm SMT Gp Hrd Dual Srt Five Inductors Fixed Inductors 6.8uH Shld 0%	Collart	MH3261-601Y	652-MH3261-601Y	https://www.mouser.com/datasheet/2/445/744711005-1722097.pdf	\$0.10
34	1 L1	9a. 20.8mDoms AECQ2 Ferrite Beads Ferrite Beads 600 ohms 25% HIGH CURRENT	Bourns	744912105	710-744912105	https://www.mouser.com/datasheet/2/445/744912210-172335.pdf	\$1.83
35	2 L2, L3	Five Inductors Fixed Inductors WE5D Rad Core Five Inductors Fixed Inductors WECAIR Air Coil Five Inductors Fixed Inductors 200uH Shld 1%	Wurth Elektronik	744912210	710-744912210	https://www.mouser.com/datasheet/2/557/msi110-270677.pdf	\$1.16
36	1 L4	2.1A 245mOhms AECQ2 Bluetooth Modules (802.15.1) Bluetooth Modules Shielded, Antenna, ASCII Interface, 12x22mm	Microchip	RN4870-JRM140	994-M55120-224KEB	https://www.mouser.com/datasheet/2/445/RN4870-JRM140-Bluetooth-Low-Energy-Module-Data-Sheet-D-1658364.pdf	\$2.26
37	1 L5	Headers & Wire Housing Headers & Wire Housings WRPID 2.54mm Hot SP Single Str Gold	Wurth Elektronik	61300511121	70-61/000511121	https://www.mouser.com/datasheet/2/445/62/01421121-1717891.pdf	\$0.25
38	1 L8	Headers & Wire Housing Headers & Wire Housings WRPID 2.77mm Hot 14p Dual Str Gold Ferrite & Wire Housing Headers & Wire Housings WRPID 2.54mm Hot SP Single Str Gold	Wurth Elektronik	62201421121	710-62/01421121	https://www.mouser.com/datasheet/2/445/62/01421121-1717892.pdf	\$1.48
39	1 M01	Headers & Wire Housing Headers & Wire Housings WRPID 2.54mm Hot SP Single Str Gold Ferrite Beads Ferrite Beads 600 ohms 25% HIGH CURRENT	Wurth Elektronik	61302611121	710-61/000511121	https://www.mouser.com/datasheet/2/445/63/01611121-1717958.pdf	\$0.90
40	1 P1	Headers & Wire Housing Headers & Wire Housings WRPID 2.54mm Hot SP Single Str Gold	Harwin	M70-3990246	855-M70-3990246	https://www.mouser.com/datasheet/2/445/63/0090246-1218971.pdf	\$0.11
41	1 P3	Headers & Wire Housing Headers & Wire Housings WRPID 2.54mm Hot SP Single Str Gold Ferrite Beads Ferrite Beads 600 ohms 25% HIGH CURRENT	Wurth Elektronik	6100621121	710-61/000621121	https://www.mouser.com/datasheet/2/445/63/0090246-1218971.pdf	\$0.93
42	1 P5	Headers & Wire Housing Headers & Wire Housings 100° Surface Mount Terminal Strip Gold	Sumtec	TSM-104-01-L-SV-P-TTR	200-TSM1041LSVTPTR	https://www.mouser.com/datasheet/2/308/1807402.pdf	\$1.27
43	1 P6	Headers & Wire Housing Headers & Wire Housings 02 SIL VERTICAL PIN HEADER TIN	ON Semiconductor	FDMC8327L	512-FDMC8327L	https://www.mouser.com/datasheet/2/447/Pn0_RC_Group_51_R05_L_10-1564068.pdf	\$0.86
44	2 P7, P9	Headers & Wire Housing Headers & Wire Housings WRPID 2.54mm Hot SP Single Str Gold	Wurth Elektronik	6100621121	710-61/000621121	https://www.mouser.com/datasheet/2/445/63/0090246-1218971.pdf	\$0.93
45	1 P8	Headers & Wire Housing Headers & Wire Housings 100° Surface Mount Terminal Strip Gold	Sumtec				
46	2 Q1, Q2	PowerTrench MOSFET Thick Film Resistors - SMD Thick Film Resistors - SMD 470 OHM 1%	Yageo	RC0805FR-07470RL	603-RC0805FR-07470RL	https://www.mouser.com/datasheet/2/447/Pn0_RC_Group_51_R05_L_10-1564068.pdf	\$0.13
47	8 R1, R7, R9, R10, R11, R12, R13, R14						

48	6 R2, R3, R4, R5, R22, R23	Thick Film Resistors - SMD Thick Film Resistors - SMD 10K Ohm 1% Yageo	RC0805FR-0710KL	Mouse	603-RC0805FR-0710KL	https://www.mouser.com/datasheet/2/447/PLU_RC_Group_51_Rohs_L_10-166068.pdf	\$0.13	
49	8 R27	Thick Film Resistors - SMD Thick Film Resistors - SMD 1 Watt, 4.7Kohms 5% 100ppm	CRCW08054K0UNTA	Mouse	71-CRCW08054-4.7K	https://www.mouser.com/datasheet/2/427/dcrcw-176215D.pdf	\$0.12	
50	1 R8	Thick Film Resistors - SMD Thick Film Resistors - SMD 1 Watt, 4.7Kohms 5% 100ppm	CRCW080520R0FKEA	Mouse	71-CRCW0805-20-E3	https://www.mouser.com/datasheet/2/427/dcrcw-3-1762152.pdf	\$0.10	
51	1 R17	Thick Film Resistors - SMD Thick Film Resistors - SMD 1 Watt, 30Kohms 1% 100ppm	CRCW080530K0FKEA	Mouse	71-CRCW0805-30K-E3	https://www.mouser.com/datasheet/2/427/dcrcw-3-1762152.pdf	\$0.10	
52	1 R20, R57	Thick Film Resistors - SMD Thick Film Resistors - SMD 1kOhm 1%	RC0805FR-071KL	Mouse	603-RC0805FR-071KL	https://www.mouser.com/datasheet/2/447/PLU_RC_Group_51_Rohs_L_10-166068.pdf	\$0.13	
53	1 R21	Thick Film Resistors - SMD Thick Film Resistors - SMD 1 Watt, 40.2ohms 2% 100ppm	CRCW080540R2KTA	Mouse	71-CRCW0805-40.2	https://www.mouser.com/datasheet/2/427/dcrcw-176215B.pdf	\$0.16	
54	1 R28	Thick Film Resistors - SMD Thick Film Resistors - SMD 1 Watt, 63.4Kohms 1% 100ppm	CRCW080563K4FKEA	Mouse	71-CRCW0805-63.4K-E3	https://www.mouser.com/datasheet/2/427/dcrcw-3-1762152.pdf	\$0.10	
55	3 R29, R30, R31	Thick Film Resistors - SMD Thick Film Resistors - SMD 1 Watt, 4.7Kohms 1% 100ppm	CRCW08054K70FKEA	Mouse	71-CRCW0805-4K7-E3	https://www.mouser.com/datasheet/2/427/dcrcw-3-1762152.pdf	\$0.10	
56	2 R32, R34	Thick Film Resistors - SMD Thick Film Resistors - SMD 10K Ohm 1%	RC0805FR-0710KL	Mouse	603-RC0805FR-0710KL	https://www.mouser.com/datasheet/2/447/PLU_RC_Group_51_Rohs_L_10-166068.pdf	\$0.13	
57	2 R33, R36	Thick Film Resistors - SMD Thick Film Resistors - SMD 1 Watt, 100ohms 5% 200ppm	CRCW080510R0NEA	Mouse	71-CRCW080510R0NEA	https://www.mouser.com/datasheet/2/427/dcrcw-3-1762152.pdf	\$0.10	
58	2 R35, R37	Thick Film Resistors - SMD Thick Film Resistors - SMD 10K Ohm 1%	RC0805FR-0710KL	Mouse	603-RC0805FR-0710KL	https://www.mouser.com/datasheet/2/447/PLU_RC_Group_51_Rohs_L_10-166068.pdf	\$0.13	
59	1 R38	Current Sensors Resistors - SMD Current Sense Resistors - SMD 1 Watt, 0.05ohms 1%	VIS1205FR0200FEA	Mouse	71-W5L1205FR0200FEA	https://www.vishay.com/doc/30373	\$0.89	
60	1 R39	Thin Film Resistors - SMD Thin Film Resistors - SMD 1 Watt, 158Kohms 1%	CRCW1206LSBK1KEA	Mouse	71-CRCW1206-158K-E3	https://www.mouser.com/datasheet/2/427/dcrcw-3-1762152.pdf	\$0.10	
61	1 R40	Thin Film Resistors - SMD Thin Film Resistors - SMD 10Kohms 1% 206.25mm Auto - Thick Film Resistors - SMD Thick Film Resistors - SMD 1 Watt, 0.05ohms 1%	MCA12060D1002BFB500	Mouse	594-MCA12060D1002BFB5	https://www.mouser.com/datasheet/2/427/mca00pre-1762843.pdf	\$0.51	
62	3 R41, R42, R45	Thick Film Resistors - SMD Thick Film Resistors - SMD 100mJumper	CR1206-1/000ELF	Mouse	652-CR1206-1/000ELF	https://www.mouser.com/datasheet/2/5/crxxxxxx-185836.pdf	\$0.10	
63	6 R43, R44, R45, R47, R48, R49	SMD Dohm Jumper	CR1206-1/000E1F	Mouse	652-CR1206-1/000E1F	https://www.mouser.com/datasheet/2/5/crxxxxxx-185836L.pdf	\$0.10	
64	1 R50	Thin Film Resistors - SMD Thin Film Resistors - SMD 91Kohm 1% 25ppm	RT0805RBRD0793IKL	Mouse	603-RT0805RBRD0793IKL	https://www.mouser.com/datasheet/2/447/PLU_RT_1_to_01_Rohs_L_11-16606912.pdf	\$0.43	
65	1 R51	Thin Film Resistors - SMD Thin Film Resistors - SMD 1.8V 6.5K Ohm 1% 25ppm	RT0805RBRD07649KL	Mouse	603-RT0805RBRD07649KL	https://www.mouser.com/datasheet/2/447/PLU_RT_1_to_01_Rohs_L_11-16606912.pdf	\$0.43	
66	1 R52	Thick Film Resistors - SMD Thick Film Resistors - SMD 1 Watt, 1.1Mohms 1%	CRCW0805M10FKEA	Mouse	71-CRCW0805M10FKEA	https://www.mouser.com/datasheet/2/427/dcrcw-3-1762152.pdf	\$0.10	
67	1 R53	Thick Film Resistors - SMD Thick Film Resistors - SMD 10Watt 75Kohms 1% 100ppm	CRCW080575K0FKEA	Mouse	71-CRCW0805-75K-E3	https://www.mouser.com/datasheet/2/427/dcrcw-3-1762152.pdf	\$0.10	
68	1 R54	Thick Film Resistors - SMD Thick Film Resistors - SMD 10Watt 28Kohms 1% 100ppm	CRCW080528K0FKEA	Mouse	71-CRCW0805-28K-E3	https://www.mouser.com/datasheet/2/427/dcrcw-3-1762152.pdf	\$0.10	
69	1 R55	Thick Film Resistors - SMD Thick Film Resistors - SMD 0.05 2.46ohms 1% AEC-Q200	Panasonic	ERU6ENF2941V	Mouse	667-ERU6ENF2941V	https://www.mouser.com/datasheet/2/315/AOA0000C304-1140630.pdf	\$0.10
70	1 R56	Thin Film Resistors - SMD Thin Film Resistors - SMD 1.0Watt 75Kohms 1% 100ppm	Susumu	RR1220P-202-D	Mouse	754-RR1220P-202-D	https://www.mouser.com/datasheet/2/392/Asumu_RR_Data_Sheet-120638.pdf	\$0.10
71	2 R51, R52	Current Sensors Resistors - SMD Current Sense Resistors - SMD 120E 0.010ohm 1% Curv Sense AEC-Q200	Panasonic	ERU8BWFR010V	Mouse	667-ERU8BWFR010V	https://www.mouser.com/datasheet/2/315/AOA0000C313-1141758.pdf	\$0.74
72	6 SW1, SW2, SW3, SW4, SW5, SW6	Tactile Switches Tactile Switches Top Actuated w/o Bezel w/ Bezel	Omrton	B3J-1000P	Mouse	653-B3J-1000P	https://www.mouser.com/datasheet/2/397/eh-13-3615.pdf	\$0.92
73	3 TP1, TP2, TP3	Circuit Board Hardware - PCB TEST POINT BLACK	Keystone Electronics	5001	Mouse	534-5001	https://www.mouser.com/datasheet/2/215/000-50044-741181.pdf	\$0.35
74	1 U1	Supervisory Circuits Supervisory Circuits Open Drain	Microchip	MCP1117-240E/T	Mouse	579-MCP1117-240E/T	https://www.mouser.com/datasheet/2/268/21889-b-04653.pdf	\$0.47
75	1 U2	16-bit Microcontrollers - MCU 16-bit Microcontroller - MCU	Texas Instruments	MSP430FR5941HM	Mouse	595-MSP430FR5941HM	https://www.ti.com/lit/pdf/scea0164	\$8.11
76	1 U3	Translation - Voltage Levels Translation - Voltage Levels 4-Bit Bidirectional V-Level Translator	Texas Instruments	TXB0104PWR	Mouse	595-TXB0104PWR	&gt;&gt;url=https://ti.com/r/2Ht3z2_Fgpnb2Efb010	\$0.93
77	1 U4	Translation - Voltage Levels Translation - Voltage Levels 8-Bit Bidirectional V-Level Translator	Texas Instruments	TXB0108PWR	Mouse	595-TXB0108PWR	8	\$1.29

78	1 U5	Operational Amplifiers - Op Amps Operational Amplifiers - Op Amps Single 1.8V/1MHz	Microchip MCP6001T-J/OT	Mouse	579-MCP6001T-J/OT	https://www.mouser.com/datasheet/2/268/21731-740845.pdf	\$0.24
79	1 U6	Gate Drivers Gate Drivers 12V Industrial Relay Inductive Load	GN Semiconductor NUD3112LTIG	Mouse	863-NUD3112LTIG	https://www.onsemi.com/pub/Collateral/AN98116-D.PDF	\$0.44
80	1 U7	Digital Potentiometer ICs Digital Potentiometer ICs Single 78 V 2C POT	Microchip MCP4531-103E/MS	Mouse	579-MCP4531-103E/MS	https://www.mouser.com/datasheet/2/268/DS_22096a-36467.pdf	\$0.70
81	1 U8	Power Isolators Digital Isolators Low-Power Isolators DC/DC	Texas Instruments ISO1540DR	Mouse	595-ISO1540DR	https://www.ti.com/lit/pdf/synt403a	\$4.51
82	1 U9	Battery Management Battery Management 3.5V/3.6A Multi-cell Lithium-on Step-Down Battery Charger with PowerPath and DC Telemetry Current & Power Monitors & Regulators Current & Power Monitors & Regulators Vfb Out Hi-Sd	Analog Devices Inc. LTC4162EUFD-SAD#PBF	Mouse	584-4162EUFD-SAD#PBF	https://www.mouser.com/datasheet/2/609/LTC4162_S-1398197.pdf	\$7.33
83	1 U10	Non-isolated DC/DC Converters Non-isolated DC/DC Converters	Texas Instruments INA194ADBV/T	Mouse	595-INA194ADBV/T	https://www.ti.com/lit/pdf/sylo228	\$2.89
84	1 U11	Non-isolated DC/DC Converters Non-isolated DC/DC Converters	Texas Instruments LMZM22360LV5SLT	Mouse	595-LMZM22360LV5SLT	https://www.ti.com/lit/pdf/syva834	\$6.17
85	1 U12	DC/DC Converters	Texas Instruments LMZM22360LV5SLT	Mouse	595-LMZM22360LV5SLT	https://www.ti.com/lit/pdf/syjip015	\$6.17
86	1 U13	LDI/Voltage Regulators LDO Voltage Regulators 50mA 1.00V/5% Our pull/DIO Linear Reg	Texas Instruments TP574401DDNT	Mouse	595-TP574401DDNT	https://www.ti.com/lit/pdf/syjip015	\$2.81
87	1 U14	Switching Voltage Regulators Switching Voltage Regulators	Texas Instruments LM516LPWPR	Mouse	595-LM516LPWPR	https://www.mouser.com/datasheet/2/440/e_WIMA_MKS_2-001	\$4.21
88	3 C22, C23, C24	Film Capacitors Film Capacitors 1.00V 47uF 10%	WIMA MKS20034701E0KSSD	Mouse	595-MKS2-47/100/10	https://www.mouser.com/datasheet/2/440/1138871.pdf	\$0.48
89	1 R16	Thick Film Resistors - SMD Thick Film Resistors - SMD 1/16watt 47Kohms 1% 100ppm	Vishay CRW080547K0RKEA	Mouse	71-CRW080547K0RKEA	https://www.mouser.com/datasheet/2/47/dcrwa-3-1762152.pdf	\$0.10
90	1 X1	Crystals Crystals 8MHz 20pF	Fox FOXS1F/080-20	Mouse	599-FOX080-20-LF	https://www.mouser.com/datasheet/2/160/C45D-1131563.pdf	\$0.27
91	2 C41, C43	Multilayer Ceramic Capacitors MLCC - SMD/SMT Multilayer Ceramic Capacitors MLCC - SMD/SMT 1206 100pF 1000Vdc COG - 5%	Murata GRM11A5CA101JW0D	Mouse	81-LGRN31AC101JW0D	https://www.mouser.com/datasheet/2/281/GRM31AC101JW0D	\$0.52
92	1 C45	Multilayer Ceramic Capacitors MLCC - SMD/SMT 50V 0.01uf X_R 0805 10%	KEMET C0805X103K5RAC7210	Mouse	80-C0805X103K5R7210	https://www.mouser.com/datasheet/2/212/KEM_C1013_XTR_FT_Cap_SMD-1103280.pdf	\$0.35
93	1 C53	Multilayer Ceramic Capacitors MLCC - SMD/SMT 50V 0.03uf X_R 0805 10%	KEMET C0805S33K5RACTU	Mouse	80-C0805S33K5RACTU	https://www.mouser.com/datasheet/2/212/Y/KEM_C1014_XR_FT_Cap_SMD-1102761.pdf	\$0.41
94	2 C55, C56	Multilayer Ceramic Capacitors MLCC - SMD/SMT 50V 100pF CG 0805 5%	KEMET C0805C1015GACTU	Mouse	80-C0805C1015GACTU	https://www.mouser.com/datasheet/2/212/KEM_C1003_CG_S-MD-1101588.pdf	\$0.16
95	0 Y1	Crystals Crystals 32.768MHz 2.7PF -40C +95C ABRACON	ABSO166-32.768MHz-T	Mouse	815-ABSO166-32.768MHz-T	https://www.mouser.com/datasheet/2/122/ECK-34G-1064121.pdf	\$0.66
96	1 Alternative Y1	Crystals 32.768MHz 6pF -40C +95C	ECS ECS-327-6-34G-TR	Mouse	520-327-6-34G-TR	https://www.mouser.com/datasheet/2/122/ECK-34G-1064121.pdf	\$0.74

APPENDIX G: TRANSMITTER BOM

ASSEMBLY NO:		DESCRIPTION		DATE:		PREPARED BY:		VERIFIED BY:		
ITEM	QTY	REFERENCE	DESCRIPTION	MFG	MFG PN	VENDOR	VENDOR PN	Datasheet URL	NOTES	Unit Price
1	1	R42	Thick Film Resistors - SMD Thick Film Resistors - SMD 1/8watt ZEROOhm Jumper	Vishay	CRCW0805000020EA	Mouser	71-CRCW0805-0-E3	https://www.mouser.com/datasheet/7/427/dcrcwe3-1762152.pdf	\$0.10	
2	1	R8	Thick Film Resistors - SMD Thick Film Resistors - SMD 1/8watt 20ohms 3% 100ppm	Vishay	CRCW080520R0FKA	Mouser	71-CRCW0805-20-F3	https://www.mouser.com/datasheet/7/427/dcrcwf-1762152.pdf	\$0.10	
3	1	R23	Thick Film Resistors - SMD Thick Film Resistors - SMD 1/8watt 40.2ohms 3% 100ppm	Vishay	CRCW080540R2FKTA	Mouser	71-CRCW0805-40.2	https://www.mouser.com/datasheet/7/427/dcrcw-1762150.pdf	\$0.16	
4	2	R31, R32	Thick Film Resistors - SMD Thick Film Resistors - SMD 0805 47.0ohms 3% To AEC-Q200	Panasonic	ERJ-6E-N47R0V	Mouser	667-ERJ-6E-N47R0V	https://www.mouser.com/datasheet/7/47/PYu_RC_Group_51_RoHS_L_10-1664068.pdf	\$0.10	
5	8	R1, R7, R9, R10, R11, R12, R13, R14	Thick Film Resistors - SMD Thick Film Resistors - SMD 470 OHM 1%, TEST POINT BLACK	Yageo	RC0805FR-07470RL	Mouser	603-RC0805FR-07470RL	https://www.mouser.com/datasheet/7/45/6130161121-1717958.pdf	\$0.13	
6	4	TP1, TP2, TP3, TP4	Circuit Board Hardware - PCB Circuit Board Hardware - PCB Electronics	Keystone	5001	Mouser	524-5001	https://www.mouser.com/datasheet/7/215/000-5004-7411811.pdf	\$0.35	
7	1	PS	Headers & Wire Holdings Header & Wire Housing VR-PHD 2.54mm Hat 16P Single Str Gold	Wurth Elektronik	6130161121	Mouser	710-6130161121	https://www.mouser.com/datasheet/7/15/000-503V35IBL-321080.pdf	\$0.90	
8	4	D13, D14, D15, D16	ESD Suppressors /TVS Diodes ESD Suppressors / TVS Diodes	Diodes Incorporated	DESD30351B1-76	Mouser	621-DE-SD30351B1-76	https://www.mouser.com/datasheet/7/115/000-503V35IBL-D-1102033.pdf	\$0.29	
9	16	C50, C51, C52, C53	Multilayer Ceramic Capacitors MLCC - SMD/SMT Multilayer Ceramic Capacitors MLCC - SMD/SMT 50V 0.1uf X7R 0805 1.0% KEMET	Yageo	CC0805K87R7BB474	Mouser	603-CC0805K87R7BB474	https://www.mouser.com/datasheet/7/281/GQM2195C2E1R6R6IBI-to-50V-18-1669420.pdf	\$0.13	
10	1	C13	Multilayer Ceramic Capacitors MLCC - SMD/SMT Multilayer Ceramic Capacitors MLCC - SMD/SMT 50V 0.1uf X7R 10% Yageo	Yageo	CC0805K87R7BB474	Mouser	603-CC0805K87R7BB474	https://www.mouser.com/datasheet/7/281/GQM2195C2E1R6R6IBI-to-50V-18-1669420.pdf	\$0.23	
11	2	C35, C45	Multilayer Ceramic Capacitors MLCC - SMD/SMT 20volts 1.6PF 250pfits COG 0.1nF	Murata	GDM2195C2E1R6B812D	Mouser	81-GDM2295C2E1R6B82D	https://www.mouser.com/datasheet/7/212/KEM_C1006_XSR_5M-D-103219.pdf	\$0.14	
12	3	C36, C38, C46	Multilayer Ceramic Capacitors MLCC - SMD/SMT 10% Yageo	YAGEO	CD805C10KSPACTU	Mouser	80-C0805C10KSP	https://www.mouser.com/datasheet/7/47/PYu_RT_1_to_0.1_Rohs_L_11-1669422.pdf	\$0.43	
13	1	R24	Thin Film Resistors - SMD Thin Film Resistors - SMD 1/8W 10K 10% ohm, 1.3% 25ppm	Yageo	RT0805BRD07105KL	Mouser	603-RT0805BRD07105KL	https://www.mouser.com/datasheet/7/47/PYu_RT_1_to_0.1_Rohs_L_11-1669422.pdf	\$0.13	
14	6	R22	Thin Film Resistors - SMD Thick Film Resistors - SMD 10K OHM 1%, R2, R3, R4, R5, R21,	Yageo	RC0805FR-0710KL	Mouser	603-RC0805FR-0710KL	https://www.mouser.com/datasheet/7/47/PYu_RT_1_to_0.1_Rohs_L_11-1669422.pdf	\$0.10	
15	1	R29	Thin Film Resistors - SMD Thick Film Resistors - SMD 10K 5%	Bourns	CR0805-1W-103ELF	Mouser	652-CR0805-1W-103ELF	https://www.mouser.com/datasheet/7/54/Crxxxx-1858351.pdf	\$0.63	
16	6	C20, C26, C30, C31, C41, C42	Multilayer Ceramic Capacitors MLCC - SMD/SMT Multilayer Ceramic Capacitors MLCC - SMD/SMT 2.0W 10uF X5R 1.0% T: 1.6mm	TDK	C3216X5R-H106K160A8	Mouser	810-C3216X5R-H106K	https://product.tdk.com/info/en/catalog/datasheets/mlcc_commercial_general_en.pdf?ref_dlytymouse	\$0.85	
17	2	C10, C11	Multilayer Ceramic Capacitors MLCC - SMD/SMT Multilayer Ceramic Capacitors MLCC - SMD/SMT 20V 12pF COG 0805 5%	KEMET	CD805C1205GACTU	Mouser	80-C0805C1205G	https://www.mouser.com/datasheet/7/212/KEM_C1003_COG_5M-D-110588.pdf	\$0.11	
18	1	V2	Standard Clock Oscillators Standard Clock Oscillators 13.5MHz Sop16 -40C +85C	Epson	SG5032CAN 13.5MHz 0.0000004f T/G3	Mouser	732-SG5032CAN13.5fG3	https://www.mouser.com/datasheet/7/137/SG5032CAN_Env-95.1596.pdf	\$1.17	
19	1	R20	Thick Film Resistors - SMD Thick Film Resistors - SMD 1K OHM 1%	Yageo	RC0805FR-071KL	Mouser	603-RC0805FR-071KL	https://www.mouser.com/datasheet/7/47/PYu_RT_1_to_0.1_Rohs_L_11-1669422.pdf	\$0.13	
20	2	R35, R40	Thick Film Resistors - SMD Thick Film Resistors - SMD 2512 1Kohms 1% To AEC-Q200	Panasonic	ERJ-1TNE100IU	Mouser	667-ERJ-1TNE100IU	https://www.mouser.com/datasheet/7/315/A0A0000C304-119820.pdf	\$0.63	
21	2	R36, R41	Thick Film Resistors - SMD Thick Film Resistors - SMD 0805 1Kohms 5% AEC-Q200	Panasonic	ERJ-6GEV102V	Mouser	667-ERJ-6GEV102V	https://www.mouser.com/datasheet/7/315/A0A0000C304-1488782.pdf	\$0.10	

22	2 R30, R37	Thick Film Resistors - SMD Thick Film Resistors - SMD 2512 1Mohm 1% tol ECO200	Panasonic	EB1-1TYF105J	Mouser	657-ER-1-TYF105U	https://www.mouser.com/datasheet/2/315/AOA000C301-1488782.pdf	\$0.46
23	3 R23, R34, R39 Q200	Thick Film Resistors - SMD 0805 1.0Mohm 0.5W 1% To AEC-C	Panasonic	ERI-P06F1004AV	Mouser	657-ER-P06F1004AV	https://www.mouser.com/datasheet/2/315/AOA000C331-11418742.pdf	\$0.18
24	4 C1, C3, C5, C7	Multilayer Ceramic Capacitors MLCC - SMD/SMT Multilayer Ceramic Capacitors MLCC - SMD/SMT 1.0nF 10V X7R 10%	Yageo	CC0805KKX7R6BB105	Mouser	603-CC0805KKX7R6BB105	https://www.mouser.com/datasheet/4/47/JUPY-SPHC_X7R_6.3V-to-S0V_18-1154002.pdf	\$0.25
25	1 C12	Multilayer Ceramic Capacitors MLCC - SMD/SMT Multilayer Ceramic Capacitors MLCC - SMD/SMT 50V 2200pf X8R 0805 5%	KE-MET	CD805C222J5HACTU	Mouser	80-C0805C222J5H	https://www.mouser.com/datasheet/2/112/KEM_C1007_388_JLT-RA_150C_SMD-102703.pdf	\$0.69
26	3 C16, C17, C18	Multilayer Ceramic Capacitors MLCC - SMD/SMT Multilayer Ceramic Capacitors MLCC - SMD/SMT 1210 1.0nF 2.2uF X7R Headers & Wire Holdings Headers & Wire Holdings 3P VERT	TDK	C3225XVR2A225K230AB	Mouser	810-C3225XVR2A225K	https://product.tdk.com/info/en/catalog/datasheets/mlcc_commcriti_mivitgate_en.pdf?ref_distr=moouser	\$0.70
27	4 P1, P2, P4, P6	Headers & Wire Holdings Headers & Wire Holdings 3P VERT	Molex	22-28-4030	Mouser	538-22-28-4030	https://www.mouser.com/datasheet/2/776/002224030_PCB_HEA-DERS-228162.pdf	\$0.16
28	1 R27	Thin Film Resistors - SMD Thin Film Resistors - SMD 1/8W 28.7K ohm 1% 100ppm	Yageo	RT0805FR0728R7L	Mouser	603-RT0805FR0728R7L	https://www.mouser.com/datasheet/2/47/PYU_RT_1_to_0.01_R-oh5_L-11-1669912.pdf	\$0.12
29	1 R26	Thin Film Resistors - SMD Thin Film Resistors - SMD 1/8W 3.4K ohm 1% 25ppm	Yageo	RT0805BRD073K4L	Mouser	603-RT0805BRD073K4L	https://www.mouser.com/datasheet/2/47/PYU_RT_1_to_0.01_R-oh5_L-11-1669912.pdf	\$0.43
30	1 R19	Thick Film Resistors - SMD Thick Film Resistors - SMD 1/B watt 300Kohms 1% 100ppm	Vishay	CRCW080530K0KEA	Mouser	71-CRCW080530K0E3	https://www.mouser.com/datasheet/2/47/dcrcw3-1762152.pdf	\$0.10
31	0 Y1	Crystals Crystals 32.768kHz 5pF -40C +85C	ABRACON	AB507-166-32.768RH2-T	Mouser	815-AB50716632.768H2T	https://www.mouser.com/datasheet/2/122/ECC-34G-1064121.pdf	\$0.66
32	1 Alternate Y1	Crystals Crystals 32.768kHz 5pF -40C +85C	ECS	ECS-32-6-3-4G-TR	Mouser	520-32-6-3-4G-T	https://www.mouser.com/datasheet/2/45/PYU_RT_1747714331-1722995.pdf	\$0.74
33	1 L1	Fixed Inductors Fixed Inductors WE-PD 330uH 710mA DC=750uHrms AECQ200	Wurth Elektronik	744771331	Mouser	710-7447714331	https://www.wuerth-elektronik.de/de/DocumentDelivery/DDEController/Actions/scrchtrn&docName=641215&DocType=CustomerDrawing&DocLang=English&Par.Ctrxt=3-641215_5&DocFormat=pdf	\$2.17
34	1 L2	Headers & Wire Holdings Headers & Wire Holdings FRICION LCK HDP Sp Straight Post Gold	TE Connectivity	345412155	Mouser	571-3-641215-5	https://www.te.com/commerce/DocumentDelivery/DocController/Actions/scrchtrn&docName=641215&DocType=CustomerDrawing&DocLang=English&Par.Ctrxt=3-641215_5&DocFormat=pdf	\$1.45
35	1 R25	Thin Film Resistors - SMD 365Kohms .1% 25ppm	Vishay	TNPW0805365KBEEN	Mouser	71-TNPW0805365KBEEN	https://www.vishay.com/doc/28771	
36	1 C22	Multilayer Ceramic Capacitors MLCC - SMD/SMT Multilayer Ceramic Capacitors MLCC - SMD/SMT 50V 36pF COG 0805 5%	KE-MET	CD805C360J5GACTU	Mouser	80-C0805C360J5G	https://www.mouser.com/datasheet/2/122/KEM_C1003_COG_5M-D-1101588.pdf	\$0.29
37	2 C8, C9	Multilayer Ceramic Capacitors MLCC - SMD/SMT Multilayer Ceramic Capacitors MLCC - SMD/SMT 50V 36pF COG 0805 5%	KE-MET	CD805C390J5GACTU	Mouser	80-C0805C390J5G	https://www.mouser.com/datasheet/2/112/KEM_C1003_COG_5M-D-1101588.pdf	\$0.24
38	4 R6, R15, R17, R18	Thick Film Resistors - SMD Thick Film Resistors - SMD 1/B watt 4.7 Kohms 5% 200ppm	Vishay	CRCW08054670INTA	Mouser	71-CRCW08054670	https://www.mouser.com/datasheet/2/47/dcrcw3-1762150.pdf	\$0.12
39	1 R16	Thick Film Resistors - SMD Thick Film Resistors - SMD 1/B watt 470nhm 1% 100ppm	Vishay	CRCW080547K0KEA	Mouser	71-CRCW080547K-E3	https://www.mouser.com/datasheet/2/47/dcrcw3-1762152.pdf	\$0.10
40	1 C24	Multilayer Ceramic Capacitors MLCC - SMD/SMT Multilayer Ceramic Capacitors MLCC - SMD/SMT 50V 0.04uf COG 0805 5%	KE-MET	CD805C473J5GACTU	Mouser	80-C0805C473J5G	https://product.tdk.com/info/en/catalog/datasheets/mlcc_comcriti_general_en.pdf?ref_distr=moouser	\$1.05
41	2 C21, C27	Multilayer Ceramic Capacitors MLCC - SMD/SMT Multilayer Ceramic Capacitors MLCC - SMD/SMT 1206 2.5uFDC 47uF 20%	TDK	C3216XSR1E7BM160AC	Mouser	810-C3216XSR1E7BM	https://www.mouser.com/datasheet/2/83/murata_03052018_GR_M_Series_3-1310166.pdf	
42	1 C23	Multilayer Ceramic Capacitors MLCC - SMD/SMT 0.068uF 500vols COG 1%	Murata	GRM2195C1H62PFA01D	Mouser	811-GRM2195C1H62PFA01D	https://www.mouser.com/datasheet/2/15/AOA000C307-1149632.pdf	
43	1 R28	Thin Film Resistors - SMD 0805 732Kohm 0.1% 25ppm	Panasonic	ERA-GAEBA723V	Mouser	657-ERA-GAEBA723V	https://www.mouser.com/datasheet/2/160/CSD-1131563.pdf	\$0.27
44	1 X1	Crystals Crystals 8MHz 20pf	Fox	F0XSDLF080-20	Mouser	559-F0XSDLF080-20-LF	https://www.mouser.com/datasheet/2/160/CSD-1131563.pdf	

45	6 SW1, SW2, SW3, SW4 SW5, SW6	Tactil Switches Tactile Switches Top Actuated w/o cross w/o ground	Omrion	B3U-1000P	Mouser	653-B3U-1000P	https://www.mouser.com/datasheet/2/307/en-b3u-3615.pdf	\$0.92
46	2 D20, D21	Schottky Diodes & Rectifiers Schottky Diodes & Rectifiers Silicon Schottky Diode	Infineon	BA514DWE622HT5A1	Mouser	726-BA514DWE622HT5A	https://www.mouser.com/datasheet/2/106/infinion-BA514DWE622HT5A1.pdf	\$0.48
47	2 C28, C39	Trimmer / Variable Capacitors Trimmer / Variable Capacitors TRIMMER CAPACITOR	Vishay	BFC280332659	Mouser	594-222-808-2659	https://www.vishay.com/doc?28528	\$7.21
48	4 C32, C34, C43, C44	Multilayer Ceramic Capacitors MLCC - SMD/SMT Multilayer Ceramic Capacitors MCC - SMD/SMT 1.00pf-3kV 100% 5%	Vishay	VH1812A101XGAT	Mouser	77-VH1812A101XGAT	https://www.mouser.com/datasheet/2/427/vjcommercialseries-176445.pdf	\$0.76
49	1 C15	Aluminum Organic Polymer Capacitors Aluminum Organic Polymer Capacitors 500volts 68nF 65°C 20mohm	Panasonic	SOSPF68M	Mouser	667-SOSPF68M	https://www.mouser.com/datasheet/2/315/AABB000C77-947360.pdf	\$2.65
50	6 D14, D11, D12, D17, D18	ESD Suppressors / TVS Diodes ESD Suppressors / TVS Diodes Low Cap BiTS Opt. 3.3V 3.8V br 25kV	Diodes Incorporated	DESD351BL-TB	Mouser	621-DESD351BL-TB	https://www.mouser.com/datasheet/2/115/ESD351BL-321080.pdf	\$0.29
51	1 R38	Thick Film Resistors - SMD Thick Film Resistors - SMD 0805 47.0ohms 2% Tol AlfcQ200	Panasonic	EPR46EN647R0V	Mouser	657-ER46EN647R0V	https://www.mouser.com/datasheet/2/115/AOA000C304-1149620.pdf	\$0.10
52	1 Q1	N-Channel 200V 8.5A Ta Surface Mount Diode	EPIC	EPIC2019	Digitkey	917-1087-2-RD	https://www.digitkey.com/epic/documents/documents/datasheets/EPC2019_datasheet.pdf	3.54
53	1 Q2	N-Channel 200V 48A Ta Surface Mount Diode	EPIC	EPIC2034C	Digitkey	917-1214-2-ND	https://www.digitkey.com/epic/documents/documents/datasheets/EPC2034C_data_sheet.pdf	7.32
54	2 L4, L5	Fixed Inductors Fixed Inductors 47uH 20%	Vishay	IHL-P4020DZER470W11	Mouser	71-HLP4020DZER470W11	https://www.vishay.com/doc?24251	\$2.58
55	1 J1	DC Power Connectors DC Power Connectors 4P JACK SKT SHIELDED SNAP AND LOCK	Kycon	KPJ4-5-S	Mouser	806-KPJ4-5-S	https://www.snapeda.com/part/KPJ4-5-S#Kycon/view-part/tref/mouser	\$2.23
56	1 U11	Gate Driver Gate Drivers Tiny 7A MOSFET Gate Driver Non-Isolated DC/DC Converters	Teas Instruments	LMS512M07/NOPB	Mouser	926-LMS512M07/NOPB	https://www.ti.com/lit/pdf/sna9806	\$1.31
57	1 U9	Non-Isolated DC/DC Converters Non-Isolated DC/DC Converters	Teas Instruments	LWZN23600V03SLIR	Mouser	595-LWZN23600V03SLIR	https://www.ti.com/lit/pdf/sna9807a	\$4.52
58	1 U10	Non-Isolated DC/DC Converters Non-Isolated DC/DC Converters	Teas Instruments	LWZN23600V05SLIR	Mouser	595-LWZN23600V05SLIR	https://www.ti.com/lit/pdf/sna9807a	\$4.52
59	1 U1	Supervision Circuits Supervisory Circuits Open Drain Digital Potentiometer IC Digital Potentiometer (5 Seg) 7V Microchip	Microchip	MCP111T-240E/TT	Mouser	579-MCP111T-240E/TT	https://www.ti.com/lit/pdf/sna9806	\$0.47
60	1 U7	12C POT Operational Amplifiers - Op Amps Operational Amplifiers - Op Amps Single 1.8V 1MHz	Microchip	MCP4531-103E/MS	Mouser	579-MCP4531-103E/MS	https://www.ti.com/lit/pdf/sna9806	\$0.70
61	1 U5	Operational Amplifiers - Op Amps Operational Amplifiers - Op Amps Single 1.8V 1MHz	Microchip	MCP6001T-J/OT	Mouser	579-MCP6001T-J/OT	https://www.ti.com/lit/pdf/sna9805	\$0.24
62	2 L2, L3	Ferrite Beads Ferrite Beads 600 ohms 25% HIGH CURRENT Bourns	Bourns	MH3261-601Y	Mouser	652-MH3261-601Y	https://www.ti.com/lit/pdf/sna9805	\$0.10
63	2 F2, F3	Resettable Fuses - PPTC Resettable Fuses - PPTC 5A 13.2V 40A Imax	Microchip	MICROSMID050F-2	Mouser	650-MICROSMID050F-2	https://www.ti.com/lit/pdf/sna9805	\$0.47
64	1 U2	16-bit Microcontrollers - MCU 16-bit Microcontrollers - MCU	Teas Instruments	MSPA30FR59401PM	Mouser	595-MSPA30FR59401PM	https://www.ti.com/lit/pdf/sna9822	\$8.11
65	1 U6	Gate Drivers Gate Drivers 12V Industrial Relay Inductive Load ON Semiconductor	ON Semiconductor	NUD312LT1G	Mouser	853-NUD312LT1G	http://www.onsemi.com/pub/Collateral/AN0816-D.PDF	\$0.44
66	1 F1	Resettable Fuses - PPTC Resettable Fuses - PPTC Radial Lead 2.5A 27V 40A Imax	RXF250		Mouser	650-RXF250	https://www.ti.com/lit/pdf/sna9805	\$0.63
67	2 P7, P9	Headers & Wire Housings Headers & Wire Housings VR-PHD 2.54mm SMT GP Hd Dual Srt.	Würth Elektronik	61000612121	Mouser	710-61000612121	https://www.ti.com/lit/pdf/sna9805	\$0.93
68	1 D19	Schottky Diodes & Rectifiers Schottky Diodes & Rectifiers Schottky Diode Amp 100 Volt	Vishay	SS3H10-E3/5/T	Mouser	625-SS3H10-E3	https://www.ti.com/lit/pdf/sna9805	\$0.60
69	1 U8	Switching Voltage Regulators Switching Voltage Regulators 3.5-60V 2.5MHz Step Down Converter	Teas Instruments	TP554260SGQR	Mouser	595-TP554260SGQR	https://www.ti.com/lit/pdf/sna9805	\$3.50
70	1 U3	Translation - Voltage Levels Translation - Voltage Levels 4-Bit Bi-directional V-level Translator	Teas Instruments	TXB0104PWR	Mouser	595-TXB0104PWR	https://www.ti.com/general/docs/supporinfo/tso2disid-24286otd041	\$0.93
71	1 U4	Translation - Voltage Levels Translation - Voltage levels 8-Bit Bi-directional V-level Translator	Teas Instruments	TXB0108PWR	Mouser	595-TXB0108PWR	https://www.ti.com/general/docs/supporinfo/tso2disid-24286otd041	\$1.29

72	1	L1A	Fixed Inductors Fixed Inductors 330uH Smd 10% 1.7A 360mOhms AECQ22	Colcraft	MGS1210-334KED	Mouser	994-MGS1210-334KED	https://www.mouser.com/datasheet/2/597/mgs1210-270677.pdf	\$2.26
73	1	L1B	Fixed Inductors Fixed Inductors WEPD 330uH 1.5A DC-R430mOhms AECQ200	Wurth Elektronik	7447709331	Mouser	710-7447709331	https://www.mouser.com/datasheet/2/445/7447709331-1722838.pdf	\$2.41
74	1	L1C	Fixed Inductors Fixed Inductors PA4320 12x12mm 33uH 1.7A 340mOhms	Pulse	PA4320.33ANLT	Mouser	673-PA4320.33ANLT	https://www.mouser.com/datasheet/2/336/P787-1526943.pdf	\$2.57
75	8	D1, D2, D5, D6, D7, D8, D9, D10	Standard LEDs - SMD Standard LEDs - SMD Red Diffused 625nm 3.0mcd	Broadcom Limited	HBM5-C150	Mouser	630-HM5-C150	https://www.mouser.com/datasheet/2/678/bv02-055ten-ds-hm5-c0xx-05mar2012-1827673.pdf	\$0.41
76	1	M01	Bluetooth Modules (802.15.1) Bluetooth Modules (802.15.1) Bluetooth Low Energy BLE Module, Shielded, Antenna, ASCII Interface, 12x22mm	Microchip	RN4470-I/RM140	Mouser	579-RN4470-I/RM140	https://www.mouser.com/datasheet/2/668/RN4470-71-Bluetooth-Low-Energy-Module-Data-Sheet-D-165854.pdf	\$7.38
77	1	P3	Headers & Wire Housings, Headers & Wire Housings, VR-PhDI 1.27mm Hdpr 14P Dual Str Gold	Wurth Elektronik	62201421121	Mouser	710-62201421121	https://www.mouser.com/datasheet/2/445/62201421121-1718302.pdf	\$1.48

APPENDIX H: WIRELESS POWER TRANSFER MODULE BOM

ITEM	QTY	REFERENCE	DESCRIPTION	MFG	MFG P/N	VENDOR	VENDOR P/N	Datasheet URL	NOTES	Unit Price
1	1	RECEIVER	Desktop AC Adapters 65W 48V/out	TDK-Lambda	D162PWA480D	Mouse	967-D162PWA480D	https://www.mouser.com/datasheet/2/400/dt62-801-e-182570.pdf		\$53.00
2	1	RECEIVER / TRANSMITTER	Electrical Enclosures IP68/NEMA GP Plastic Enclosure 5.88" x 4.36" x 2.19" Opaque	Bud Industries	PU-16537	Mouse	967-D162PWA480D	https://www.mouser.com/catalog/specsheets/Bud_PU-20Series_NEMA_6PWP68_Pc_Enclosure.pdf	Custom made	\$25.30
3	1	RECEIVER	Printed Circuit Board	JLC PCB		JLC PCB				\$6.68
4	1	TRANSMITTER	Printed Circuit Board	JLC PCB		JLC PCB				\$6.69
5	0.1	COIL RECEIVER	Hook-up Wire 14AWG 19/27 PTFE Spool 304.8 m	Alpha Wire	5859 R0005	Mouse	602-5859-100-03	https://www.mouser.com/datasheet/2/14/AW_Product_Specification-1873756.pdf		\$1.98
6	0.1	COIL TRANSMITTER	Hook-up Wire 14AWG 19/27 PTFE Spool 304.8 m	Alpha Wire	5859 R0005	Mouse	602-5859-100-03	https://www.mouser.com/datasheet/2/14/AW_Product_Specification-83736.pdf		\$1.98
7	4	COIL RECEIVER / TRANSMITTER	Terminals SOLUS DIN 05-1.0 TE Connectivity		105291	Mouse	571-165291			\$0.45
8	0.67	COIL RECEIVER	Super-Conductive 101 Copper Tubes/Copper Tubing 1/8" 5ft spool	Mcmaster-Carr	8965K22	Mcmaster-Carr	8965K22	https://www.mcmaster.com/tubing/pdf/1_8/material-copper/		\$6.94
9	0.67	COIL TRANSMITTER	Super-Conductive 101 Copper Tubes/Copper Tubing 1/8" 5ft spool	Mcmaster-Carr	8965K22	Mcmaster-Carr	8965K22	https://www.mcmaster.com/tubing/pdf/1_8/material-copper/		\$6.94
10	1	1 Receiver	RRCSMBus Cable	RRCSMBus	Cable	Mouse	328-RRCSMBUSCABLE	https://www.mouser.com/datasheet/2/826/DS_SM_Bus_Battery_Cable_B-1360935.pdf		\$22.35
11	2	COIL RECEIVER / TRANSMITTER	Enclosures, Boxes, & Cases SENSOR CUBE WHITE	New Age Enclosures	789-S1A-40012	Mouse	789-S1A-40412	https://www.mouser.com/datasheet/2/230/NewAgeEnclosures_12092019_40012_cube_11_0-1673104.pdf	Coil enclosure	\$5.70

APPENDIX I: DIMENSIONAL COIL DRAWING

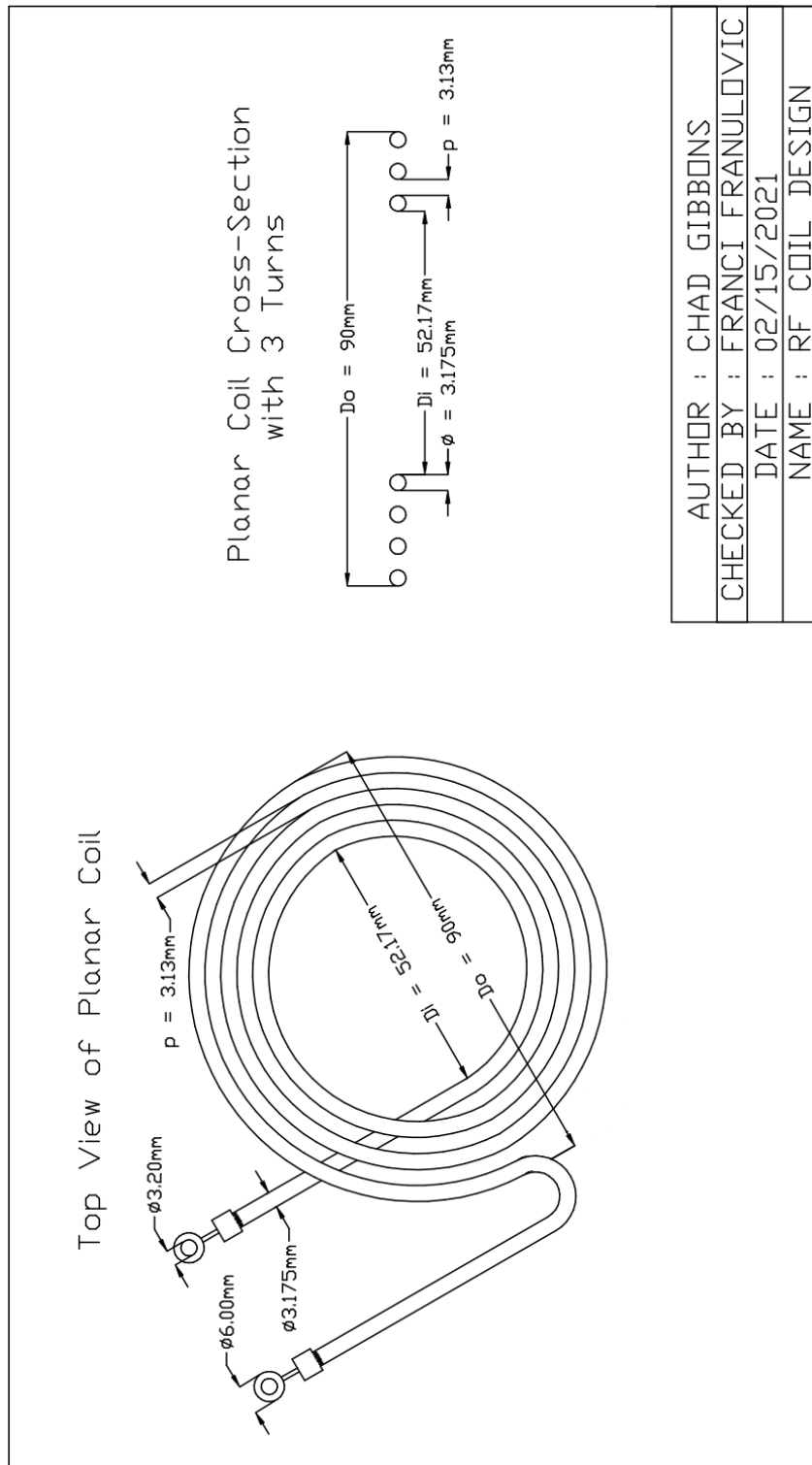


Figure 38: Dimensional Coil Drawing

APPENDIX J: GUI WIREFRAME DIAGRAM

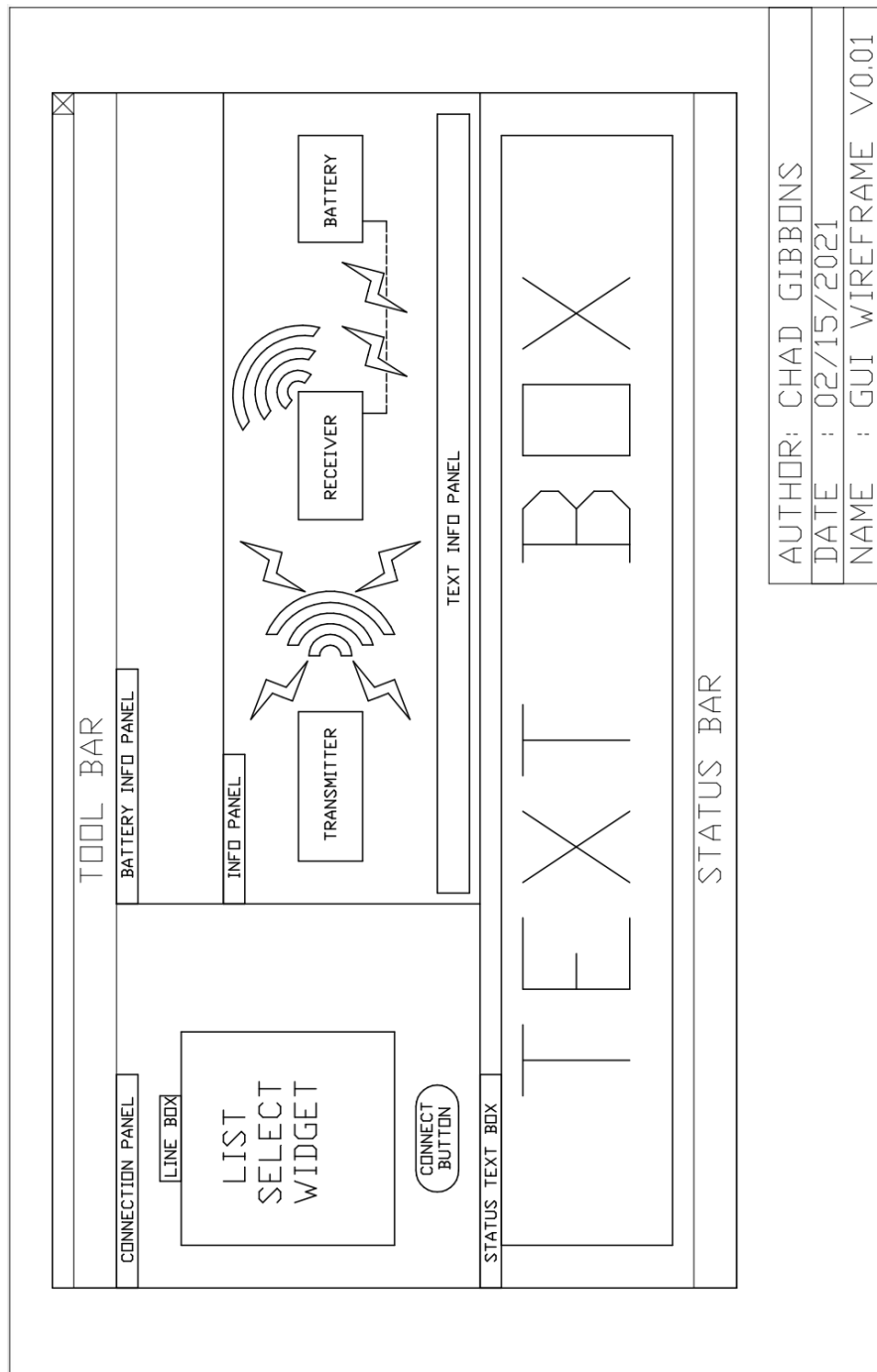


Figure 39: GUI Wireframe Diagram

APPENDIX K: EXPERIMENTAL DATA COLLECTION SHEETS

1. Transmitter Subsystem Data

Transmitter Subsystem Data

Test Description	Test Results
30V power supply voltage nominal 30V +/-2% Measured (TP1)	_____ V Pass / Fail
3.3V regulator (U11) test point TP2 nominal voltage 3.3V tolerance +/- 1.5%	_____ V Pass / Fail
5V regulator (U11) test point TP3 nominal voltage 5V tolerance +/- 1.5%	_____ V Pass / Fail
TXCO Voltage and Frequency Test	____ V _{pp} & ____ MHz Pass / Fail
Coil Driver (U11) Output Test	____ V _{pp} Pass / Fail
Voltage V _{DS} Test of Class E Amplifier GaN FET	_____ V Pass / Fail
Peak to Peak Voltage Load Test	_____ V Pass / Fail
Transmitter Power Output Test	_____ W Pass / Fail
Firmware Upload JTAG Test	Pass / Fail

This process is repeated for distances of 5 cm, 4 cm, 3 cm, 2 cm, 1 cm, and 0 cm.

2. Receiver Regulators Subsystem Data

Receiver Regulators Subsystem Data

Test Description	Test Results
DC voltage across coil terminals (J2 & J4)	_____ V Pass / Fail
5V regulator (U11) test point TP3 nominal voltage 5V tolerance +/- 1.5%	_____ V Pass / Fail
3.3V regulator (U11) test point TP2 nominal voltage 3.3V tolerance +/- 1.5%	_____ V Pass / Fail
Firmware Upload JTAG Test	Pass / Fail

3. Receiver Rectifier Subsystem Data

Receiver Rectifier Subsystem Data

Test Description	Test Results
Transmitter RF Output Test	_____ W
Coil Placement Distance	_____ cm
Load Voltage (Test Load: ____ Ω)	_____ V Pass / Fail
Load Power	_____ W Pass / Fail
Efficiency	_____ % Pass / Fail

This process is repeated for distances of 5 cm, 4 cm, 3 cm, 2 cm, 1 cm, and 0 cm.

4. Charger Subsystem Data

Charger Subsystem Data

Test Description	Test Results
Set Bench Power Supply Current Limit: 1 A Voltage Limit: 20V	_____ V Supplied
Number of Cells Attached	_____ Cells
Verify Charge Current Target Current : 3.2 A	_____ A
Peak Charge Current	_____ mA Pass / Fail
Query Battery Cell of SMBus	Response : _____ Pass / Fail

5. SMBus Subsystem Test Data

SMBus Subsystem Test Data

Test Description	Test Results
Verify Interface Functionality SMBus Read/Write	Pass / Fail
Verify Interface Functionality SMBus Read/Write with MSP430	Pass / Fail
Verify Interface Functionality SMBus LTC4162	Pass / Fail
Target Charge Current SMBus RRC Smart Battery	Pass / Fail
Input Current Limit Target SMBus Read	Pass / Fail

6. Coil Subsystem Test Data

Coil Subsystem Test Data

Test Description	Test Results
Complex Impedance @ 13.56 MHz	_____ + j _____ Ω
Inductance	_____ μH Pass / Fail
Quality Factor Estimation	_____ Pass / Fail